PRECAMBRIAN GEOLOGY OF THE TAOS RANGE, TAOS COUNTY, NEW MEXICO

by

Timothy P. McCrink

Submitted in Partial Fulfillment
of the Requirements for the Degree of
Master of Science in Geology

New Mexico Institute of Mining and Technology

Socorro, New Mexico

ABSTRACT

Proterozoic metavolcanic rocks in the Taos Range, northern New Mexico, have been complexly intruded prior to, during and after metamorphism to the lower amphibolite facies. Metavolcanic rocks comprise a bimodal mafic-felsic assemblage in the Gold Hill area, and a primarily mafic assemblage in the Wheeler Peak-Lake Fork Peak area. The intrusive complex contains amphibolites, hornblendite, tonalites and granite.

The supracrustal rocks appear to have been deformed by two major folding events and are now found with vertical to nearly vertical layering. In the case of the Gold Hill area this layering is the original bedding, and some stratigraphic relationships suggest these rocks are younger to the north. No such stratigraphic relationships are found in the Wheeler Peak-Lake Fork Peak areas. The relationship between the Gold Hill and the Wheeler Peak-Lake Fork Peak supracrustal rocks is not known.

Mineral assemblages in the mafic supracrustal and intrusive rocks indicate a metamorphic grade corresponding to the medium pressure range of the lower amphibolite facies. Retrograde minerals are common in all the rocks studied.

Chemical analyses confirms the compositional bimodality of the Gold Hill supracrustal rocks, and despite the high degree of alteration in the mafic rocks this is beleived to

be an original feature. Field, petrographic and chemical analyses of the rocks in the Wheeler Peak-Lake Fork Peak areas suggest a mafic volcaniclastic sedimentary origin for the majority of these rocks. The intrusive rocks, with the possible exception of granite, are pre- to syntectonic and roughly define a calc-alkaline trend.

Two tectonic regimes are interpreted from the rocks of the Taos Range. The first is an extensional environment producing bimodal volcanics and diabase intrusives. The second is a compressional environment accompanied by the intrusion of mafic to intermediate composition dikes and plutons, and later, granitic plutons.

ACKNOWLEDGMENTS

I would like to acknowledge and thank the following people, without whose help this project would never have succeded. Dr. Kent Condie, whose insight, enthusiasm and support made this project possible. Dr. James Robertson, who made the thin section photographs possible, provided many thought provoking conversations, and critically read this paper. Dr. Antonius Budding, who helped with the petrography and critically read this manuscript. Jack Reed of the U.S.G.S., and John Jenkins, for their support in the field, and Ernie Blake for allowing access to the Taos Ski Area. The staff of the Sandia National Laboratory Reactor, Phillip Allen and Gary Anderson, for making the Neutron Activation Analysis possible. Kathleen B. Faris and Jacques Renault, for their help with the X-Ray Fluorescence Analysis, and Mark Leo for making the typing of this paper as painless as possible. Finally, I would like to thank my wife, Marie Taaffe McCrink, for her endless support and encouragement throughout this project.

TABLE OF CONTENTS

FIGURES

TABLES

INTRODUCTION

The Taos Range is situated in the Sangre de Cristo Mountains of Taos County, northern New Mexico (Figure 1). Three separate Proterozoic supracrustal areas were studied within the vicinity of Twining, roughly 30 km by road from Taos. Since the best exposure of Proterozoic rock is found on the high ridges, and the foliation trend is roughly northeasterly, this study concentrated on three north-south ridges in the high peaks area of the Taos Range. These areas are located on the Red River and Wheeler Peak 7.5-min quadrangles and are outlined in Figures 2 and 3. The areas are here referred to as the Gold Hill, the Lake Fork Peak and the Wheeler Peak sections, after the most prominent peak found in each.

Although Proterozoic metavolcanic and intrusive rock types were studied, special emphasis is placed on the metavolcanics and related metasediments. The major objectives of this study are to:

1) map, describe and to chemically classify the major Proterozoic rock types;
2) determine the original stratigraghic relationships of the metavolcanics;
3) determine the genetic relationships, if any, between the metavolcanics and the intrusive rocks;

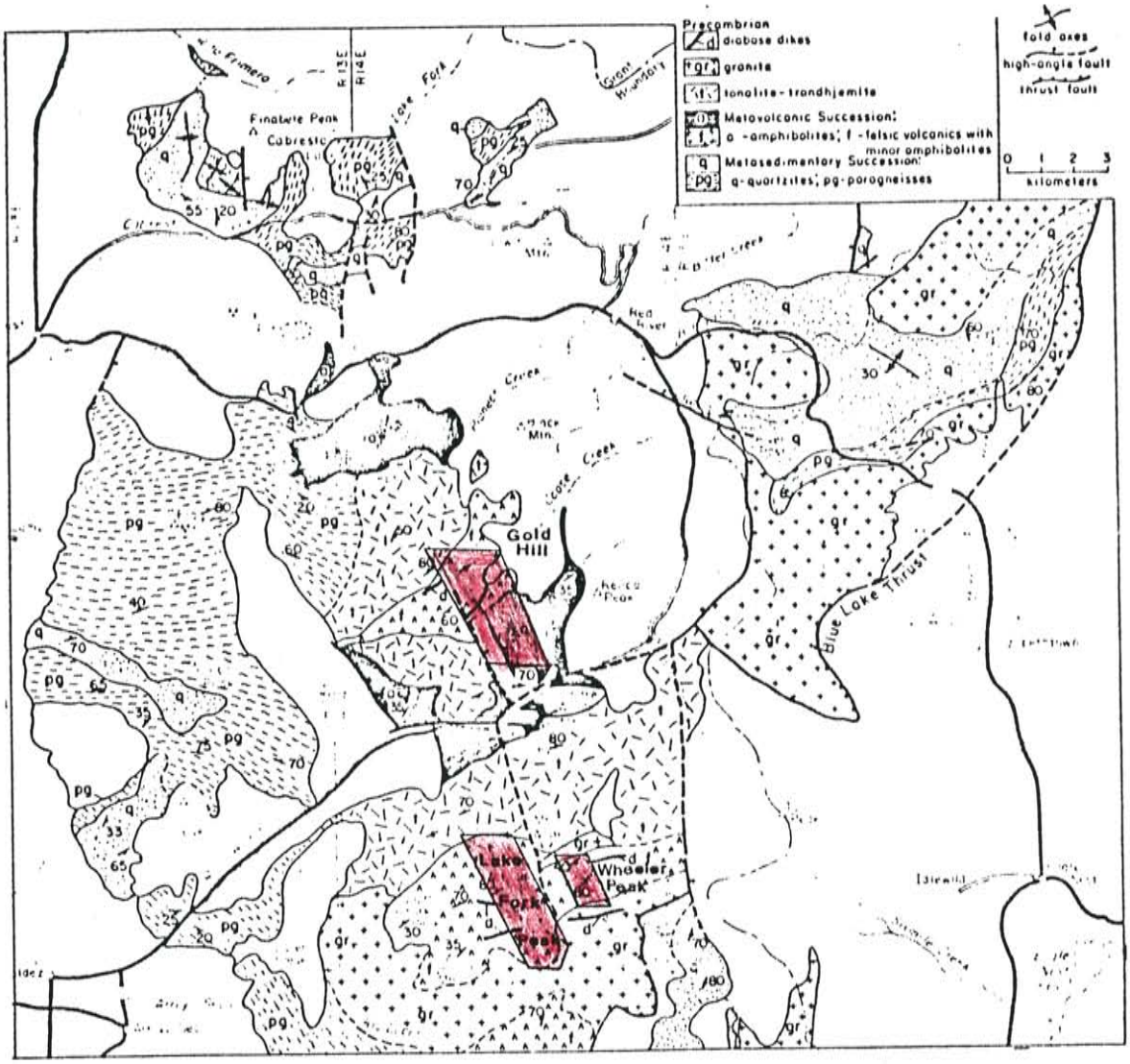

Figure 1. Location map of the measured sections showing the geology of the Taos Range. (Modified after Condie, 1979)

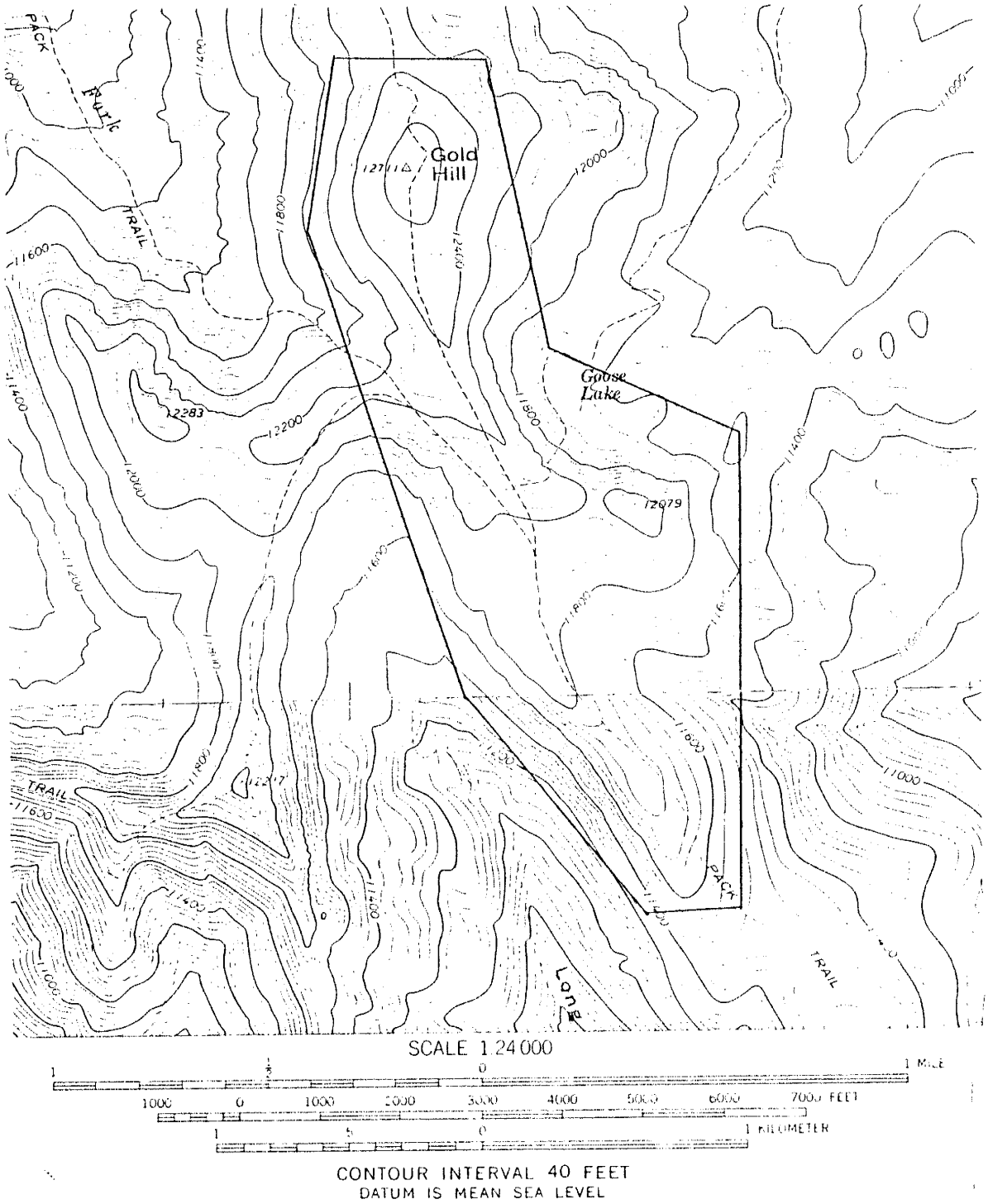

Figure 2. Location map of the Gold Hill measured section.

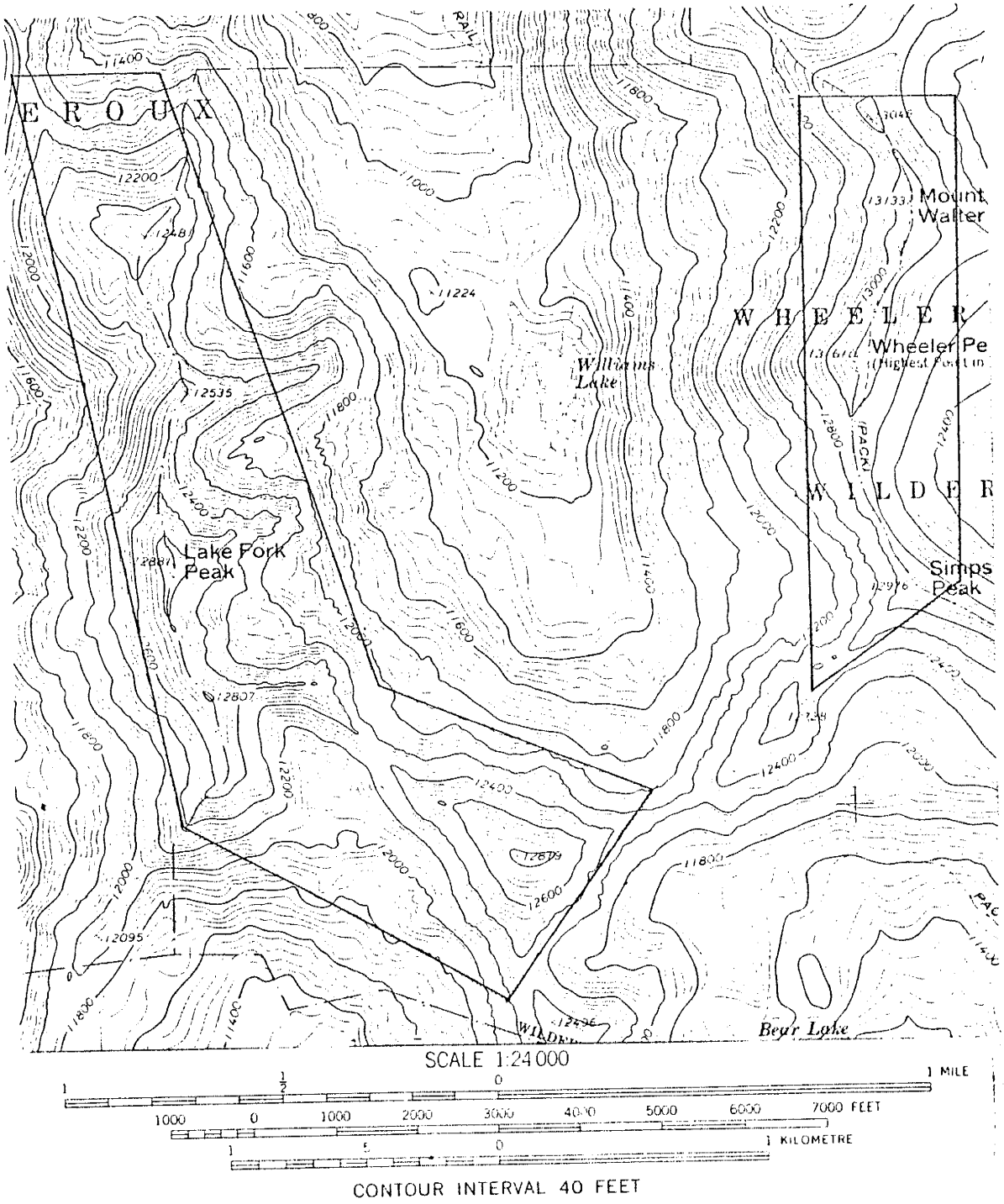

Figure 3. Location map of the Lake Fork Peak and Wheeler Peak measured sections.

5) determine the regional metamorphic grade of the Proterozoic rocks;

4) suggest a depositional and tectonic environment represented by the Proterozoic rocks.

The first major geologic investigation of the Taos Range was the reconnaissance mapping of Gruner (1920). Although this author mapped mostly to the south of the areas of this study, he did recognize the important Precambrian rock types. Mapping in the northern and western parts of the Range was done by McKinlay (1956; 1957) who was able to subdivide the metamorphic lithologies and recognize remnant sedimentary structures. Schilling (1960) described the mineral deposits of the area in some detail. Clark and Read (1972) included the areas of this study in their mapping of Eagle Nest Region. These authors, using lithologic descriptions similar to McKinlay, outlined two periods of metamorphism in the Precambrian of the Taos Range: an early regional metamorphism and a later contact metamorphism related to the intrusion of granitic stocks. Between 1976 and 1979 detailed mapping of the Precambrian was carried out by Dr. Kent C. Condie (1979) and by his students in the New Mexico Tech field geology courses in 1977 and 1978. The U.S. Geological Survey is currently mapping the Sangre de Cristo Mountains on a regional scale to determine potential

mineral deposits and to designate areas to be approved as wilderness (Reed et al, 1981).

Field work for this project was carried out in a seven week period during the summer of 1980. During this time, strip maps of the individual sections were made at a scale of 1:12,000 on enlarged U.S.G.S. quadrangle maps. Due to the rugged nature of the area, the sections were measured using a 30 meter measuring line, although pace traverses were employed when possible. An altimeter accurate to within plus or minus 20 feet was utilized on a limited basis.

Ninety-eight thin sections were examined petrograghically using a Vickers polarizing microscope. Plagioclase compositions were determined by the Michel-Levy method as described in Kerr (1959) and thin sections of the felsic rock types were stained to aid in the identification of alkali feldspar. Detailed descriptions of forty samples were made and these same samples were analyzed for major and trace elements using both instrumental neutron activation (INAA) and x-ray fluorescence analysis (XRF). Analytical procedures for these methods are discussed in Appendices C, D, and E. From the major element geochemistry CIPW norms were calculated on the New Mexico Tech DEC20 computer system. All the Proterozoic rocks of the Taos Range have undergone at least one metamorphic event and rock names should be prefixed by the term "meta-". In the style

popular among some Precambrian geologists, this prefix will be used sparingly throughout this text. Also, because the rocks found in the Wheeler Peak and Lake Fork Peak sections are the similar, they will be collectively referred to as the Wheeler Peak sections.

GEOLOGIC SETTING

Precambrian basement rocks in the southwestern U.S.A. show decreasing ages from north to south. Archean crust is in fault contact with Proterozoic crust in southern Wyoming along the Nash Fork-Mullen Creek shear zone. South from this shear zone to west Texas, Condie (1981) has recognized three major Proterozoic age provinces in supracrustal rocks. These provinces are 1,800 to 1,750 m.y., 1,720 to 1,650 m.y., and 1,200 to 1,100 m.y. (Figure 4). The supracrustal rocks in the Taos Range lie in the 1,800 to 1,750 m.y. age province.

Besides the Taos Range, seven other major Proterozoic supracrustal belts of this age province are known to crop out in northern New Mexico and southern Colorado. From north to south these belts are the Big Thompson Canyon, Salida, Dubois, Irving, Tusas, Picuris, and the Pecos. In Arizona the Yavapi Series and rocks of the Grand Canyon are also within the 1,800 to 1,750 m.y. age province.

In the Big Thompson Canyon belt, Braddock (1966) recognized two deformational and two metamorphic episodes in metasedimentary rocks. Quartz diorite was emplaced during the older deformation. Tonalite (Mount Olympus Granite) and granodiorite (Sherman Granite) were intruded after the second deformation, and still later, quartz monzonite was intruded.

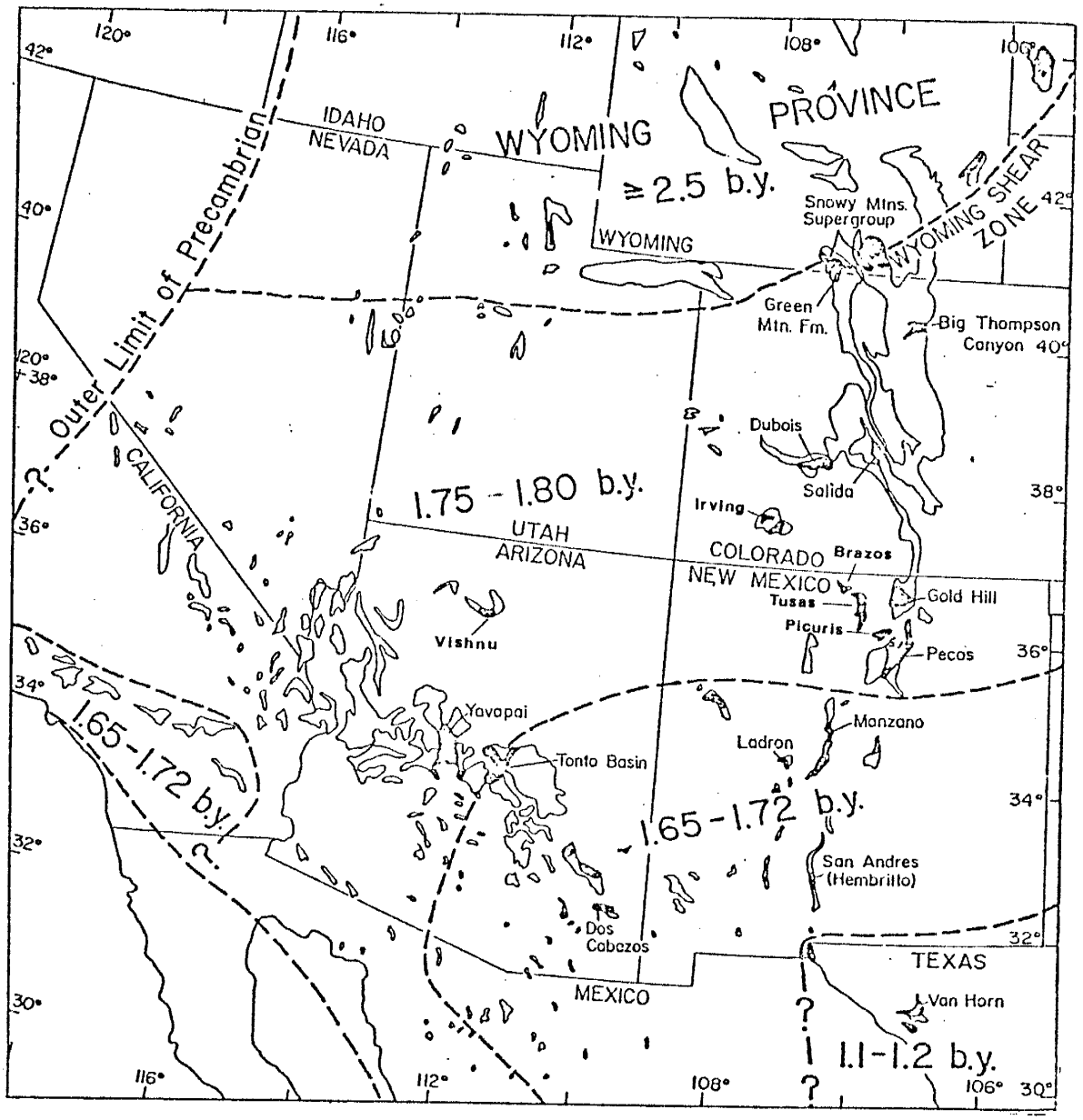

Figure 4. Major Precambrian age provinces of the Southwestern United States. Proterozoic supracrustal successions in the 1.75 to 1.80 b.y. age province are discussed in the text. (Modified after Condie, 1982)

The Salida belt is composed of bimodal volcanics (basalts and dacites to rhyodacites), volcaniclastic sediments, and quartzites grading into pelitic rocks (Boardman, 1976). These rocks were metamorphosed to the middle amphibolite facies. Intrusion of quartz monzonite dated at 1,650 to 1,700 m.y. followed the regional metamorphism.

Condie and Nuter (1981) report bimodal volcanics (basalts and rhyolites to quartz latites) and volcaniclastic sediments in the Dubois Belt. These rocks have been metamorphosed to the middle or upper amphibolite facies. Late syntectonic to post-tectonic granite and granodiorite-tonalite have been dated at 1,650 to 1,700 m.y.

A complex history for the Irving Greenstone belt is outlined by Barker (1969). It includes deposition of conglomerates, which are overlain by volcanics of basaltic, intermediate and acidic compositions. These volcanics are interbedded with conglomerates, graywackes, quartzites, sandstones, siltstones, and clays. This sequence is overlain by the bimodal Twilight Gneiss. After intense folding, metamorphism, and post-metamorphic granitic intrusions (dated at 1,720 m.y.), another cycle of erosion, deposition of sediments, and folding and metamorphism occurred. Post-tectonic granitic intrusion ended approximately 1,400 m.y. ago.

Detailed work in the Tusas area by Kent (1980) and

Gibson (1981) indicates that the supracrustal rocks are composed of bimodal volcanics (basaltic and rhyolitic), volcaniclastic sediments, arkoses, minor conglomerates, and quartzites. These rocks have undergone multiple periods of deformation and have been metamorphosed to the lower greenschist facies. They have also been intruded by syntectonic granodiorites and late syntectonic to post-tectonic granites.

In the Picuris Mountains, southeast of the Taos Range, Nielsen and Scott (1979) report mainly quartzites, phyllites, slates, conglomerates, and other metasediments. The upper unit of the Vadito Formation, however, is composed of amphibolite. This amphibolite is interpreted to be basaltic flows and volcaniclastic sediments by these authors.

The Precambrian rocks of the Picuris Mountains are believed to be correlative with those in the Truchas Peak area (Grambling, 1979). In particular, the Vadito Formation of the Truchas Peak area is found to contain a bimodal igneous suite. Both the Picuris and Truchas Peak areas have undergone at least two deformational episodes and metamorphism to the middle amphibolite facies (Nielsen and Scott, 1979; Grambling, 1979; Holdaway, 1978).

In the Pecos greenstone belt, Robertson and Moench (1979) and Robertson (1981) report quartzite overlain by bimodal volcanics. The volcanics are overlain by

volcaniclastic sediments, shales, sandstones, and iron formation. These authors recognized at least two periods of deformation and metamorphism to the greenschist and amphibolite facies. Two suites of intrusive rocks are recognized: (1) amphibolite, tonalite, and trondhjemite; and (2) granite to tonalite.

Rocks of similar age in Arizona inclide the Vishnu Complex of the Grand Canyon and the Yavapi Series of central Arizona. The Vishnu Complex is composed of sandstones, shales, impure carbonate sediments, and basic volcanic rocks (Brown etal, 1979). These rocks have been subjected to two major and one minor metamorphic-deformational event, as well as syntectonic to post-tectonic plutonic intrusions.

In the Yavapi Series, 1,700 to 1,800 m.y. basalts, andesites and rhyolites, and minor associated sediments are reported by Anderson and Silver (1976). Granodiorites and a quartz diorite intrude these volcanics and sediments.

In summary, Proterozoic supracrustal rocks to the south, west, and north of the Taos Range are characterized by bimodal volcanics, volcaniclastic sediments, quartzites, quartzo-feldspathic sandstones, siltstones, comglomerates, and sometimes iron formation. Far to the north and west, the Big Thompson Canyon and Vishnu Complex are dominated by sedimentary units. The Proterozoic rocks of the Needles Mountains and the Yavapi Series contain the volcanic rock suites including those of intermediate composition. Lastly,

all supracrustal belts have been intruded by numerous plutonic rocks prior to, during, and after metamorphism. The compositions of the plutonic rocks are highly variable and include granite, quartz-monzonite, granodiorite, tonalite, and trondhjemite.

GEOLOGY OF THE TAOS RANGE

PHANEROZOIC

TERTIARY

The only Phanerozoic rocks encountered in the measured sections are several types of Tertiary igneous dikes. Andesite, quartz latite, rhyolite and diabase dikes are found in all sections. They are commonly only a few meters thick although they can be as much as 500 meters long where the exposure is good. Andesite, quartz latite and rhyolite dikes were not distinguished from each other when encountered in the measured sections. For a more detailed study of these tertiary dikes and their extrusive equivalents the reader is referred to Clark and Read (1972).

The diabase dikes are distinguished from the other tertiary dikes on the geologic maps (Figures 5A and 5b) because of their possibly older age. Clark and Read (1972) note that unmetamorphosed diabase dikes are found to intrude all the Proterozoic rocks but not the overlying Mississppian sediments. On the basis of this relationship Clark and Read state that diabase dikes throughout the Taos Range are probably of very late Precambrian age (p. 26). However, a spatial relationship exists between many smaller diabase dikes and the other intermediate to silicic Tertiary dikes in that they are often found side by side or in parallel intrusions. This suggests that many of the diabases may be of Tertiary age. Thicker, more prominent diabase dikes

are not usually associated with other Tertiary dikes and do not always show the northwest alignment of the Tertiary intrusives. Therefore, it is suggested that there may be two ages of diabase intrusives. The first would be post metamorphic (1,250 m.y.; Gresens, 1975) and pre-Mississippian, and the second would be Tertiary. It should be stressed that the diabase dikes were not studied in detail and that the above suggestion of two diabase intrusve events is a speculation based on limited field relationships. These disbase dikes will be referred to as post metamorphic diabase to avoid confusion with older metadiabase discussed below.

PROTEROZOIC

SUPRACRUSTAL ROCKS

INTRODUCTION

The rocks studied in the Gold Hill, Wheeler Peak, and Lake Fork Peak measured sections include both supracrustal and intrusive rocks. The supracrustal rocks in the Gold Hill section comprise a compositionally bimodal volcanic and volcaniclastic sediment suite. Supracrustal rocks in the Lake Fork Peak and the Wheeler Peak sections are believed to be primarily mafic volcaniclastic sediments. However, these rocks are more sheared and folded than the Gold Hill supracrustals and thus their origin is more speculative. The intrusive rocks include metadiabase, hornblendite, coarse-grained amphibolite, and two types of tonalitic rocks, intruded prior to and during the main metamorphic event. Late syntectonic granite plutons are the last intrusive rocks of Proterozoic age to intrude the Taos Range with the possible exception of the post metamorphic diabase.

A problem that faces Precambrian researchers is whether to refer to metamophosed rocks by their metamorphic names or by the name of their protolith based on the results of the study. In the case of this study, the majority of the rocks encountered are completely recrystallized and are therefore referred to by the appropriate metamorphic name. In the case of the felsic volcanic rocks of the Gold Hill section,

the tonalitic rocks, and the granitic rocks, enough textural and geochemical evidence is present to warrant the use of the original rock name instead of the often tedious metamorphic terms. As mentioned in the Introduction, rocks in the Lake Fork Peak and Wheeler Peak sections are extremely similar and will be collectively referred to as the Wheeler Peak sections.

FELSIC VOLCANIC ROCKS

Felsic volcanic rocks occur only in the northern part of the Gold Hill section and comprise approximately 1/4 of the total thickness of that section. This rock type extends from the 12,079 ft. hill south of Goose Lake in the central part of the section, to the top of Gold Hill in the north (refer to map, Figure 5A). To the south, the felsic volcanics become interbedded with mafic schists and related layered gneisses. On the top of Gold Hill the felsic volcanics are truncated by a long, east-west trending hornblendite dike which forms the northern contact. The felsic rocks are cut by numerous amphibolite dikes and sills of variable thickness. These amphibolites stand out well in contrast to the light colored felsic volcanics but most are too small to show on the map. Roughly 200m south of Gold Hill the felsic rocks are intruded by a well foliated tonalite and this tonalite is also found north of Gold Hill. A younger, less foliated tonalite intrudes felsic volcanics as well as all of the above rocks on the west side of Gold Hill (Figure 5A). Only one post metamorphic diabase dike is found in this section and it intrudes felsic volcanics just southwest of the Gold Hill summit.

The felsic volcanic rocks are generally massive to moderately well bedded and the foliation, which trends northeast and is nearly vertical, is defined by the

alignment of biotite. Where bedding can be distinguished, it is discerned by changes in the type and abundance of phenocrysts and the presence or absence of biotite-rich lenses. In general, these changes are gradational rather than sharp and bedding is only well developed where the felsic volcanics are interlayered with the layered gneiss. Other than this bedding, there is a lack of any well preserved volcanic and/or sedimentary structures and textures, such as cross-bedding, graded-bedding or eutaxitic texture. This may be the result of metamorphism.

The felsic volcanic rocks are light green to gray and porphyritic, with subhedral and euhedral phenocrysts comprising 20 to 40% of the rock. The one exception is sample R-245 which contains no phenocrysts. The phenocryst assemblage, in decreasing order of abundance, is alkali feldspar (mostly microcline), quartz, plagioclase, +/- biotite, +/- quartz-muscovite intergrowths (mineral modes are given in Table 1). The size of the phenocrysts ranges from 1 to 6mm long with stubby 2 x 4mm crystals being most common.

Plagioclase is the dominant feldspar in the northern part of the Gold Hill section, and alkali feldspar becomes dominant to the south. Alkali feldspar phenocrysts are subhedral to euhedral and show carlsbad, albite, and microcline grid-iron twinning. Although microcline is the common alkali feldspar, the crystal shapes suggest that they

TABLE 1
MINERAL PERCENTAGES
FELSIC VOLCANICS

	MINS	R-59	R-105	R-124	R-196	R-200	R-222	R-245
PHENOS	QTZ	18	5	5	4	2	2	-
	KF	7	5	-	26	10	18	-
	PL	-	10	25	-	-	-	-
	BI	-	7	-	15	15	-	-
	MUSC	5	3	-	-	-	-	-
MATRIX	Q+F	65	50	63	30	50	50	20
	BI	3	15	5	-	10	5	20
	SER	2	5	2	15	8	20	60
	CARB	-	-	-	10	-	5	-
	EP	-	-	-	-	5	-	-

	SCHIST			GNEISS						
MINS	LC-1	LC-2	LF5	LF-1	LF-37	W-25	LF-16	R-88	R-207	R-169
BI	30	25	-	40	10	10	7	25	5	-
HBL	-	15	-	-	30	35	45	-	7	55
QTZ	-	-	55	-	15	7	-	-	55	15
Q+F	30	25	-	35	-	-	35	60	-	-
CARB	20	25	2	-	-	-	3	-	-	-
EP	5	10	18	25	3	5	5	2	-	-
PL	15	-	-	-	40	40	-	-	-	-
SER	-	-	25	-	-	1	-	5	3	-
OPQ	-	-	-	-	2	2	5	8	-	10
GAR	-	-	-	-	-	-	-	-	30	-
CHL	-	-	-	-	-	-	-	-	-	15

For mineral abbreviations see Table 2.

were originally sanidine. Plagioclase phenocrysts are subhedral with albite twinning and relict oscillatory zoning (Plates 1 and 2). Feldspars are variably sericitized and locally replaced by carbonate. Quartz phenocrysts are dominantly round and composed of interlocking quartz grains, although some samples contain subhedral to euhedral, optically continuous crystals (Plate 3). Quartz-muscovite grains are round and have equal amounts of both minerals and occasionally some plagioclase (Plates 3 and 4). Biotite occurs as irregular-shaped glomerophenocrysts and may or may not be altered to chlorite. For a detailed petrographic description of each sample refer to Appendix B.

In hand specimens of the felsic volcanics, the crystals are oriented randomly, and often broken feldspars are observed. Thin sections show relict zoning and imperfect twinning in feldspars which are common igneous textures. Formerly euhedral crystals have granulated grain boundries but the original crystalline shape can often be observed in the staining of alkali feldspar. For these above reasons it is beleived that the larger minerals are original crystals and not porphyroblasts produced by metamorphism.

The remaining 60 to 80% of the felsic volcanic rock is composed of extremely fine groundmass in which the minerals rarely exceed 0.5mm in diameter. This groundmass is composed of quartz, plagioclase, subordinate microcline, and variable amounts of biotite and sericite which show parallel

alignment. All minerals in the groundmass are anhedral. This fine-grained material most likely represents recrystallized glassy material. Approximately one third of the felsic rocks contain biotite and muscovite-rich lenses ranging from 2 to 20cm long (Plate 5). These fine-grained lenses occur where the felsic volcanics are crystal-rich. Although it cannot be proven with certanty, it is suggested that these lenses may be relict pumice or lithic fragments.

The presence of original phenocrysts and possible pumice fragments are suggestive of a volcanic origin for these rocks. The phenocryst assemblage is quite similar to phenocryst assemblages reported for rhyolites of orogenic and bimodal volcanic associations (Ewart, 1979) and the Bishop Tuff of California (Hildreth, 1979). However, since most phenocrysts have granulated grain boundries and volcanic and/or sedimenary textures have been destroyed during metamorphism, a volcaniclastic origin cannot be eliminated. The quartz-muscovite grains may have originally been lithic fragments, but even this can be interpreted as evidence for either a sedimentary or volcanic origin, or both.

At the south end of the Gold Hill measured section, a highly silicified breccia is found (Figure 5A). This massive rock does not extend far in any direction, although it becomes increasingly foliated and grades into a quartz-muscovite schist to the east, south, and west. The

silicified rock contains dominantly cryptocrystalline quartz, in which numerous angular quartz fragments, some up to 5cm long, are found. The fragments are white, clear, and light brown in color and all three can be found together. Also found are fragments which are white, very angular, 0.5 to 1.0cm in length, and resemble volcanic glass shards. Silicification must have occurred in localized areas prior to metamorphism.

The silicified and schistose rocks from this locality have not been studied in detail. However, it is believed that these rocks probably originated as felsic pyroclastic and epiclastic deposits. This interpretation is based on the textures preserved in the silicified area, and the generally felsic composition of the schistose area.

MAFIC SCHISTS OF THE GOLD HILL SECTION

Like the felsic volcanics, mafic schists only occur in the Gold Hill Section and make up roughly 1/3 of the section (Figure 5A). The largest mass of mafic schist extends from the 11,690 ft. contour on the rim of Long Canyon in the south, almost to the 12,079 foot knoll, south of Goose Lake, in the north (Figure 5A). Two, possibly three, smaller mafic schist units are interbedded with felsic volcanics and become increasingly thinner to the north. Associated with each schist unit is a proportional thickness of layered gneiss (see below). These layered gneisses are always found on the north side of each mafic schist unit and the gneisses then become interbedded with felsic volcanics. The fact that the layered gneisses are always on the north side of the mafic schist units argues against repetition of the section caused by folding in the Gold Hill section. Felsic volcanics or layered gneiss, related to a mafic schist unit to the south, can occur on the south side of a mafic schist unit.

There are several features in the mafic schists which suggest an original stratigraphic top to the north. The northernmost mafic schist unit contains light colored inclusions near its southern contact with felsic volcanics. These inclusions are believed to be clasts of the felsic rocks. Just southeast of the 12,079 ft. hill, south of

Goose Lake (Figure 5A), the layered gneiss appears to have been deposited on an erosion surface in the mafic schist. This possible erosion surface resembles scour and fill troughs approximately 0.5m wide and 6.0cm deep. Also, the color index of the layered gneiss at the contact decreases from that of the mafic schist (~60), to a much lighter color (~40) in about 2m to the north. The mafic schists are intruded by several amphibolite dikes but the mineralogic similarities between the two rock types make the amphibolites difficult to distinguish in the field.

The mafic schists are fine-grained, medium to dark green and massive. Schistosity increases toward the south. The minerals present are biotite, carbonate, hornblende, very fine quartz and feldspar, albitized plagioclase (An6-8), and radiating masses of chalcedony and epidote (Table 1). Most minerals are anhedral and grain sizes range from 0.1 to 2.0mm. The mafic schists show extensive alteration in both hand specimen and thin section. Carbonate and epidote veining is readily visible in the field. Thin sections indicate that besides the obviously secondary carbonate, chalcedony and epidote, biotite is chloritized and the remaining minerals are completely recrystallized.

In many places, most notably at the 11,800 ft. contour on the east rim of Long Canyon, horizons containing elongate and irregularly shaped, dark green fragments are found

(Plates 6 and 7). These fragments range from 1 to 20cm long and average 3 to 4 cm. The fragments are composed of intergrown 0.1 to 0.3mm amphibole crystals. Although this amphibole is too fine-grained to determine with confidence, it is thought to be ferro-actinolite. Within each fragment are round to slightly elongate amygdules and euhedral plagioclase phenocrysts (Plate 8). The amygdules are filled with granular quartz, feldspar, calcite, and epidote, and range from 1 to 6mm in diameter. The untwinned phenocrysts are about the same size as the amygdules, but are less common.

Several features of the above mafic fragments are important to the understanding of their origin:

1) fragments are only found in certain horizons
2) fragments show variable shape and size
3) vesicles within the fragments may or may not be present
4) vesicles, if present, are best preserved in the center of the fragment
5) the vesicles are spherical to slightly elongate

The presence of ironstones nearby (dicussed below) indicates the presence of water at the time of deposition, yet no pillow structures are preserved in the mafic schists. It has been suggested that the fragment-bearing horizons

may be mafic laharic breccias (Klich and Robertson, in progress). A simpler hypothesis is that the fragments are volcanic bombs erupted subareally and dropped into shallow water. In an aqueous environment the vesicles would be allowed to fill with secondary minerals which preserved the vesicular shape through metamorphism.

The remainder of the mafic schists are also most likely volcaniclastic sediments, although the degree of alteration casts some doubt on the original composition. If the mafic schists are volcaniclastic sediments, the high mafic content and the locally fragmental nature necessitate a nearby mafic volcanic source.

LAYERED GNEISSES OF THE GOLD HILL SECTION

Gold Hill layered gneisses are found only on the north side of the mafic schist units and comprise less than 1/4 of the Gold Hill section (Figure 5A). As mentioned previously, their thickness is proportional to the relative thickness of the schist units. The largest unit of mafic schist has the largest associated layered gneiss sequence while the smallest schist unit has the smallest. Thus, the thickness of the layered gneisses decreases towards the north with the mafic schists. Two thirds of each gneiss sequence is composed of a fine to coarsely layered, biotite-hornblende gneiss, and the foliation is parallel to the original bedding planes in the rock (Plate 9).

On the north side of each layered gneiss sequence, the remaining 1/3 is composed of garnet and magnetite-bearing layers which are interbedded with the previously mentioned biotite-hornblende gneiss. The garnet-bearing gneiss then grades into minor finely laminated ironstone further north. A generalized sketch of this relationship is given in Figure 6.

This general sequence occurs on both large and small scales, depending upon the size of the layered gneiss accumulation. For example, the largest accumulation to the south has a total thickness of 274m and the alternating garnet-rich and garnet-poor layers are 0.5 to 1.0m thick.

Figure 6.
Idealized Relationship of the Mafic Schist to the Layered Gneiss and Ironstone in the Gold Hill Section.

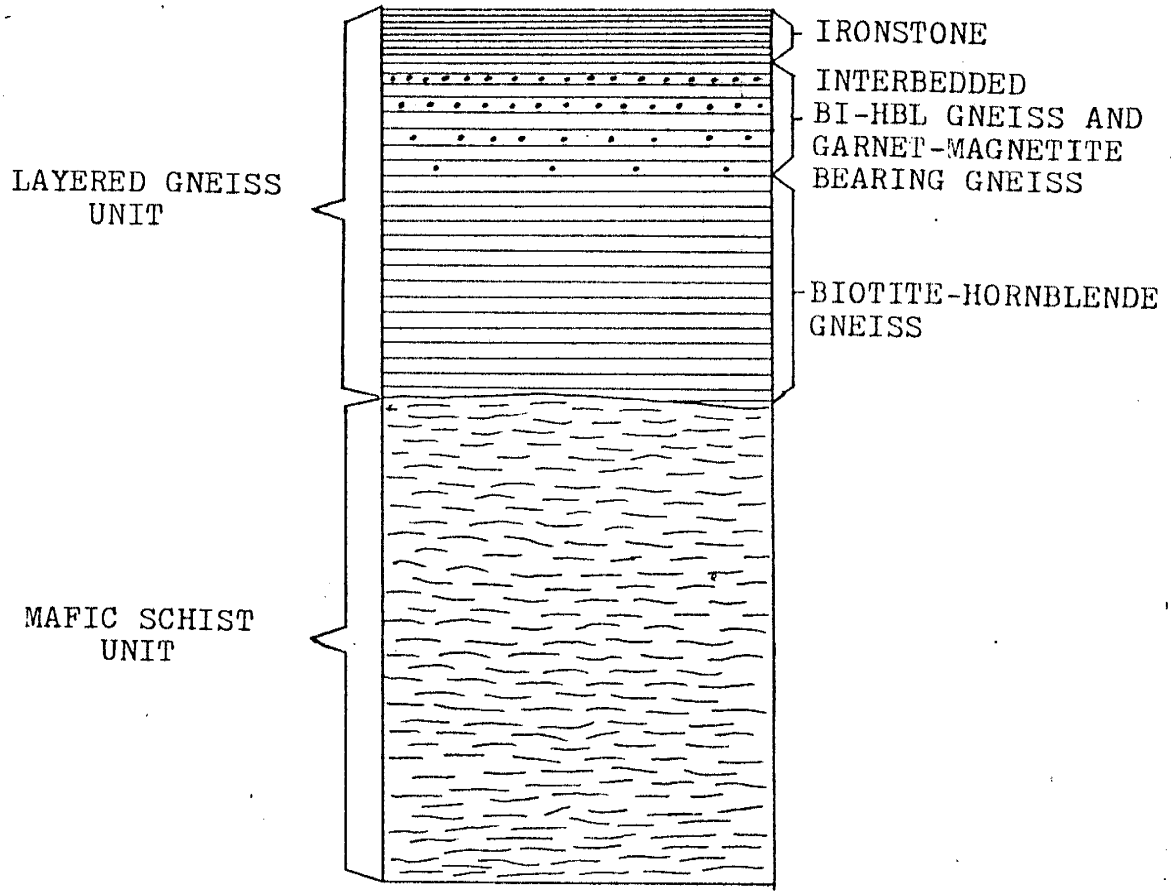

The smallest unit to the north, however, is only 38m thick and the garnet layers are only 8 to 10cm thick. The only intrusive rocks found to cut the layered gneisses are several amphibolite dikes.

Biotite-hornblende gneiss is composed of brown biotite, hornblende, quartz, feldspar, sericite, epidote and hematite (sample R-88; Table 1). These minerals are rarely larger than 0.5mm. Laminations are mostly biotite and hornblende alternating with the leucocratic minerals and range from 0.5 to 10cm thick. The garnet-bearing gneiss is similar to the above rock but contains poikiloblastic red garnets, and variable amounts of magnetite (sample R-207; Table 1). Inclusions in the garnets are small (0.5mm), round quartz grains. Garnets are elongate along the foliation and in some garnet-bearing layers the garnets show a small increase in size from north to south. Where subhedral to euhedral magnetite octahedra are present, garnet appears to be an alteration product of the magnetite, and where magnetite is very abundant (greater than 10%) both garnet and magnetite are surrounded by radiating coronas of tremolite-actinolite (Plate 10). The other minerals present in the garnet-bearing rocks are quartz, biotite, sericite, and minor iron alteration on the tremolite-actinolite.

Ironstone stands out in the field due to the oxidation of magnetite to hematite on weathered surfaces, but individual units rarely exceed several meters in thickness.

The term "ironstone" is here used instead of "iron formation" because this rock does not form a mappable unit (Kimberly, 1978). The ironstones are finely laminated with quartz layers alternating with mafic layers and these mafic layers are slightly magnetic. Thin sections reveal that the layers are composed of hornblende and chlorite (5 to 10mm thick), quartz (1 to 3mm thick), and tremolite-actinolite and hornblende (0.5 to 1.0mm thick; Plate 11). The ore minerals, magnetite and hematite, range from 0.01 to 0.5mm and are scattered evenly through the mafic layers but absent from the quartz layers (sample R-169; Table 1). The quartz layers are themselves banded, being composed of layers of different grain size, any single band containing fairly uniform grains of quartz. Due to their association with volcanic rocks and limited thickness, the ironstones most closely resemble the Algoma type iron formations of Gross (1968) and the Shallow-Volcanic-Platform-Iron-Formation (SVOP-IF) of Kimberly (1978).

Despite the lack of well developed sedimentary structures other than the fine bedding in the layered gneisses of the Gold Hill section, the possible scour and fill in the mafic schist and the presence of ironstone within each sequence support a sedimentary origin. The source for these sediments is most likely the enclosing volcanic/volcaniclastic rocks. According to Kimberly (1978; p.217), the generalized paleo-environment for SVOP-IF is

interpreted to be "... a volcano largely eroded or collapsed down to wave base or built up to shallow water depths, with a platform around a small island or a shallow rim protecting a lagoon". In conclusion, it appears that the layered gneisses are sediments derived from the mafic and felsic volcanics, probably in a shallow marine environment.

HORNBLENDE-BIOTITE GNEISS OF THE WHEELER PEAK SECTIONS

A strongly foliated hornblende-biotite gneiss comprises at least 80% of the Wheeler Peak sections (this includes the Wheeler Peak and Lake Fork Peak sections; Figure 5B). The remainder is interbedded quartz-sericite schist and/or quartz-biotite gneiss and minor quartzite. Unlike the layered gneisses of the Gold Hill section, there are no garnet-rich layers or ironstones in the Wheeler Peak sections and the relationships between the Gold Hill and Wheeler Peak sections, if any, are not known. The Wheeler Peak hornblende-biotite gneiss is intruded by large hornblendite dikes on Fairveiw Mountain (Kachina Peak) and Mount Walter (Figure 5B) and by numerous small (~1x10m) discordant hornblendite dikes throughout the southern sections. Dikes of amphibolite, tonalite and granite also intrude the hornblende-biotite gneiss, and granitic bodies of variable size form the north and south boundaries of the Wheeler Peak sections.

The hornblende-biotite gneiss is composed of hornblende, quartz, plagioclase (An42-50), biotite, epidote, sericite, carbonate and opaque minerals (hematite and pyrite). The minerals average 0.1 to 0.5mm in size, are anhedral, and the rock is granoblastic. The compositional layering ranges from 0.5cm to more than 1m but is only locally as well developed as in the layered gneiss of Gold

Hill. Hornblende, quartz, plagioclase and biotite modal percentages are highly variable throughout the Wheeler Peak sections and in general the more mafic the rock the more poorly laminated it is.

The quartz-sericite schist and quartz-biotite gneiss are interbedded with the hornblende-biotite gneiss in several places but are only minor in total volume. These rocks are very fine-grained and composed of quartz, feldspar (too fine to be determined), epidote, biotite, sericite and carbonate (samples LF-5 and LF-16; Table 1). They are finely laminated with bands 0.1 to 1.0mm thick and exhibit granoblastic textures. The only true quartzite occurs at the north end of the Lake Fork Peak section as two small beds about 20 to 30cm thick. It is a purple to redish brown, medium grained quartzite composed chiefly of irregular, 1 to 2 mm quartz grains with sutured boundries and undulose extinction. The only other minerals are magnetite and garnet (sample LF-6; Table 1). Magnetite blebs are within the quartz grains and shattered looking garnets form thin layers and are responsible for the red color of the rock. The garnets in this quartzite are not associated with the magnetite and are not poikiloblastic like the garnets in the Gold Hill layered gneiss.

Since these rocks in the Wheeler Peak sections are more sheared and deformed, the origin of the hornblende-biotite gneiss is a problem. There are no well preserved primary

textures to indicate a sedimentary, volcanic, or combined volcanic-sedimentary origin. Also, there is some evidence that the compositional layering may be the result of isoclinal folding rather than sedimentary bedding (see Structure below). The general high mafic content of the gneiss may possibly suggest a mafic volcanic source. The quartzite and quartz-sericite schist do not show any apparent similarities with the Gold Hill felsic volcanics and are most likely sedimentary.

INTRUSIVE ROCKS

AMPHIBOLITE OF THE GOLD HILL SECTION

Intrusive amphibolites of the Gold Hill Section occur as dikes and sills 1 to 20m thick and cut all the supracrustal rocks. The majority of the dikes and sills are too small to show on the map. They are cut by hornblendite and two types of tonalite on the west side of Gold Hill (Figure 5A). The amphibolites are concordant or nearly concordant with the foliation of the supracrustal succesion. Because of this nearly concordant nature, it is often difficult to distinguish intrusive amphibolite from the small mafic schist units. Several features are helpful in the field to distinguish the two rock types. Mafic schist units contain horizons with elongate, dark green fragments and have a layered gneiss sequence on their north side. The mafic schists are also fine grained and alteration is quite obvious in hand specimen. Although some of the smaller amphibolites are fine grained, the minerals are typically coarser than in the mafic schists. The amphibolites are rarely as altered as the schists, and lastly, the intrusive amphibolites locally exhibit discordant contacts. It is not known how many intrusive events are represented by the amphibolites since none of the dikes are found to cut each other.

The amphibolites are fine to medium-grained, dark gray to black and aphanitic. The smaller dikes and sills are

finer grained than the larger ones. The minerals comprising the amphibolites are blue-green to green hornblende, saussuritized plagioclase (An47-58), brown biotite, and minor amounts of epidote, sphene and hematite. Most samples contain up to 5% quartz and one, R-78, contains 15% (Table 2). In one thin section, R-114, hornblende pseudomorphs after pyroxene were observed with ragged Fe-rich hornblende outlines (Plate 12). Minerals in the amphibolites are anhedral and grain sizes are 1 to 3mm for most of the major minerals and less than 1mm for biotite and the minor minerals. In most of the dikes and sills the primary igneous textures have been destroyed by metamorphic recrystallization. The relict hornblende pseudomorphs after pyroxene in R-114 however, indicate that these dikes and sills were intruded as diabase prior to metamorphism.

TABLE 2
MINERAL PERCENTAGES
AMPHIBOLITES

MINS	R-78	R-91	R-224	LF-32	LF-44	LF-47	W-30
HBL	40	50	45	40	70	70	30
PL	35	30	38	30	10	15	35
BI	5	7	10	10	TR	5	25
QTZ	15	8	5	-	-	-	5
EP	TR	5	TR	20	15	8	5
OPQ	TR	TR	2	TR	-	-	TR
SP	TR	-	TR	TR	3	1	TR
AP	-	-	-	TR	2	1	TR

HORNBLENDITES

MINERALS	R-1	R-23	W-13
HBL	95	75	80
PL	-	10	10
EP	-	15	10
AP	2	TR	-
SP	-	TR	-
OPQ	3	TR	TR

Mineral abbreviations: QTZ = Quartz; KF = Potassium Feldspar; PL = Plagioclase; BI = Biotite; MUSC = Muscovite; Q+F = Very fine grained Quartz and Feldspar; SER = Sericite; CARB = Carbonate; EP = Epidote; HBL = Hornblende; OPQ = Opaque Minerals; GAR = Garnet; CHL = Chlorite; SP = Sphene; AP = Apatite; AL = Allanite; TR = Trace Amounts; - = Not Present.

AMPHIBOLITE OF THE WHEELER PEAK SECTIONS

A group of extremely inhomogeneous intrusive amphibolites occur in the southern sections. These amphibolites occur south of Lake Fork Peak and north of Mount Walter and may extend completely across Lake Fork Canyon in a northeasterly direction (Figure 5B). North of Mount Walter this rock type occurs as a single 60 meter wide dike, while south of Lake Fork Peak it occurs as numerous dikes of variable thickness intruding the country rock.

This intrusive rock cuts deformed hornblendite north of Mount Walter and is itself cut by granitic dikes. If the hornblendite is the same age in both the Gold Hill and the Wheeler Peak sections, the amphibolites of Wheeler Peak are younger than the intrusive amphibolites of Gold Hill. They are older than the granites and the post metamorphic diabase dikes, but no meaningful age relationships are found with the tonalite. However, where tonalite dikes intrude the Wheeler peak sections they are strongly deformed whereas the amphibolites are not. This may indicate that the tonalites may be older.

The Wheeler Peak amphibolites are medium to coarse-grained and poorly foliated. These amphibolites are composed of blue-green hornblende, brown biotite, variably sericitized plagioclase (An69), quartz, epidote and trace amounts of apatite, sphene and hematite. Close to the

intrusive contacts, the amphibolites are medium to coarse-grained with roughly equal amounts of hornblende and plagioclase (see samples W-30 and LF-32 in Table 2). The rocks near the central areas of the dikes have much more hornblende and exhibit cumulus textures (Plates 13 and 14; see samples LF-44 and LF-47 in Table 2).

The center of some of these amphibolite dikes contain an extremely coarse mafic pegmatite. In this pegmatite, randomly oriented hornblende crystals surrounded by plagioclase, have possible pyroxene cross-sections and may reach 15cm long and 2cm in diameter. Plagioclase comprises up to half of this pegmatitic zone. It is believed that this is an original textural feature of the rock and that some of the hornblendes are pseudomorphs after clinopyroxene.

The relict textures, change in grain size (coarser toward the center) and change in plagioclase abundance are all evidence for a zoned mafic intrusive. The zoning most likely occurred due to the migration of the felsic material to the pegmatitic area leaving behind cumulus mafic minerals. These amphibolites were probably intruded at depth and cooled slow enough to allow zoning to occur. The poorly foliated nature of the amphibolites suggests that the dikes were intruded during the late stages of metamorphism.

HORNBLENDITE

Hornblendite intrusives are found on the top and west side of Gold Hill, on the top of Fairview Mountain, on Mount Walter, and as numerous small dikes and sills throughout the Wheeler Peak sections. The larger bodies, which are up to 100m wide and 500m long, are coarse-grained and unfoliated while the smaller (2 meters or less) dikes and sills show more effects of metamorphism. On the top and west side of Gold Hill, hornblendite dikes cut both felsic volcanics and intrusive amphibolite. The same dikes are intruded by a tonalite pluton on the west side of Gold Hill (Figure 5A). In the Wheeler Peak sections, the hornblendite cuts only hornblende-biotite gneiss. Hornblendite is cut by the amphibolite of Wheeler Peak and by granitic dikes throughout the southern sections. Tonalite does not cut hornblendite in the Wheeler Peak sections but the former is beleived to be younger on the basis of the Gold Hill relationships.

The large undeformed hornblendite bodies contain 90-95% blue-green, interlocking hornblende crystals which are 2 to 7mm in diameter and have inclusions of apatite, opaque minerals (hematite), and chlorite after biotite (Table 2). Some of the hornblendites, such as the one on Fairview Mountain (Kachina Peak), contain up to 10% saussuritized plagioclase. The hematite occurs as thin bands along cleavage traces and may be relict schiller structure of

original orthopyroxene (Plates 15a and 15b).

The smaller intrusives are characterized by randomly oriented, large (2 to 7mm) hornblende porphyroblasts in a fine-grained amphibole matrix. These hornblendite dikes contain 50 to 75%, anhedral to subhedral hornblende porphyroblasts in a matrix (1mm or less) of hornblende, highly saussuritized plagioclase, and minor epidote. The porphyroblasts are randomly oriented but the matrix minerals show parallel alignment.

Many hornblendite intrusives are found to have originally been pyroxenites that have undergone amphibolite facies metamorphism (Nockolds et al, 1978). The presence of possible relict schiller structure and the fact that hornblende is found to pseudomorph pyroxene in other mafic intrusive rocks in the Gold Hill section, support a similar origin for the hornblendites of the Taos Range.

TONALITE

Two types of tonalite are encountered in the Taos Range. Type 1 tonalite is older than type 2 and they are mineralogically distinct from each other. Type 1 tonalite is a single, early pluton which cuts the felsic volcanics, amphibolite dikes and hornblendite in the Gold Hill section. The main body of the type 1 tonalite occurs to the west of the Gold Hill Section. South of Gold Hill, this tonalite intrudes the country rock as large dikes up to 75m thick (Figure 5A). These dikes show a decrease in thickness to the south and occur as numerous small dikelets, 2 to 5cm thick in the felsic volcanics. The type 2 tonalite is found throughout the Taos Range, mainly as large plutons. West of Gold Hill, a pluton of type 2 tonalite intrudes type 1 tonalite as well as felsic volcanics, amphibolite and hornblendite (Figure 5A). In the Wheeler Peak Sections the type 2 tonalite occurs as occasional dikes, 1 to 10m thick, related to the large intrusives nearby.

Type 1 tonalite is a strongly foliated, crystal rich rock characterized by prominent blue quartz eyes and abundant plagioclase (An61). The other major minerals are partially chloritized biotite and minor epidote (Table 3). Minerals range from 1 to 7mm, the texture is porphyroblastic, and sutured and granulated grain boundries are common. A possibly related intrusive occurs to the

TABLE 3
MINERAL PERCENTAGES
TONALITES

	TYPE 1		TYPE 2						
MINS	R-81	R-103	R-19	R-22	R-25	R-43	R-54	R-42	LF-14
PL	50	55	45	55	50	40	30	50	50
QTZ	35	30	15	15	10	10	25	10	15
BI	15	15	30	15	25	15	5	25	20
HBL	-	-	-	10	8	30	40	-	-
EP	TR	TR	3	6	6	2	TR	6	5
KF	-	-	7	-	TR	-	-	4	2
SP	-	-	TR	3	1	1	-	1	2
AP	-	-	-	1	TR	2	-	1	3
OPQ	-	-	TR	TR	TR	-	-	-	1
AL	-	-	-	-	-	-	-	3	2

GRANITE

MINERAL	R-18	R-46	LF-3
KF	55	30	30
QTZ	15	25	25
PL	10	25	14
BI	10	15	20
EP	2	1	10
SP	5	4	-
OPQ	3	TR	-
AL	-	-	1

For mineral abbreviations see Table 2.

north of Gold Hill. This rock is typically very fine-grained and only locally contains minor amounts of blue quartz phenocrysts. On the east and west sides of Gold Hill this rock intrudes hornblendite. Although not studied in detail, this rock appears to be composed of quartz, plagioclase and highly variable amounts of biotite.

Type 2 tonalite is well foliated to locally massive and in smaller dikes and in areas of strong deformation it takes on a porphyroblastic appearance similar to the type 1 tonalite. The most distinct feature that separates the type 2 from the type 1 tonalite is the high mafic content of the type 2 tonalite. Mafic minerals comprise 25 to 40% of the type 2 compared to 15% in the type 1 tonalite (Table 3).

The massive (undeformed) variety of the type 2 tonalite contains plagioclase (An56), hornblende, biotite, quartz, epidote, sphene and apatite. One sample, R-19, which is from the East Fork of the Red River, contains up to 7% alkali feldspar which has been introduced through small veinlets related to granitic dikes nearby (Table 3). The minerals in this massive tonalite are anhedral and range from 0.5 to 7.0mm in diameter. The more deformed variety contains the same basic mineral assemblage but has more biotite, less quartz, and minor amounts of microcline and allanite. The microcline and allanite are interpreted as being introduced during metamorphism since these minerals are not found in the massive variety. The texture is

porphyroblastic for the deformed variety; the porphyroblasts of quartz and plagioclase are 1.0 to 4.0mm, and the remaining minerals average 0.5mm. Both varieties of the type 2 tonalite show sutured and granulated grain boundries.

One sample, R-54, needs to be discussed in more detail. As shown in Table 3, this rock contains more hornblende and less plagioclase than the other type 2 tonalites. R-54 is a sample of the massive variety type 2 tonalite from the west side of Gold Hill near the contact with amphibolite, felsic volcanics, and hornblendite (Figure 5A). Xenoliths up to 1m long are found here and the high mafic content in this case is due to assimilation of the country rock.

GRANITE

Large granitic plutons of Precambrian age are found throughout the Taos Range. The Wheeler Peak sections are surrounded by granite bodies of different sizes and one altered granitic body occurs on the mesa north of Gold Hill. Granitic dikes ranging from 0.5 to 25m cut all rock types in the Wheeler Peak sections but no granite dikes are found in the Gold Hill section. Although the large plutons are largely unfoliated, the smaller dikes are strongly foliated.

In the field the plutons are composed of massive, coarse-grained, pink granites. The minerals in the plutons are alkali feldspar, quartz, biotite (altered to chlorite), plagioclase, sphene, hematite, and epidote in decreasing abundance (Table 3). Subhedral alkali feldspar exhibits microperthitic structure and, although the plutons are rarely foliated, most minerals show metamorphic textures. The rock is coarse grained with minerals ranging from 0.5 to 7.0mm. Sample LF-3 represents a small (1.5m) dike from the north side of Fairview Mountain. In this dike, 1.0 to 6.0mm, round alkali feldspar porphyroblasts are set in a 0.1 to 1.0mm, strongly foliated matrix of quartz, biotite, plagioclase, epidote, and allanite. Although not all the granitic dikes are as strongly deformed as this one, it shows that Precambrian granites were intruded prior to the end of metamorphism in the Taos Range.

STRUCTURAL GEOLOGY

FOLIATION

The Proterozoic rocks of the Taos Range are mostly foliated although the large granite and type 2 tonalite plutons are poorly to moderately well foliated. In the Gold Hill (GH) section the dominant foliation trend ranges from N40-56E although it can be quite variable. In the north part of the section, north of the the two major faults (Figure 5A), the foliation dips are vertical or dip steeply to the southeast. South of the NE trending fault the foliation dips steep to the northwest. On the east side of Long Canyon the foliation trends are generally the same as to the north and foliation dips are moderate to steep, dipping towards the southeast. North of the NE trending fault in Long Canyon, the foliation dip angles are very small and this is probably due to the close proximity to both the NE and NW trending faults. Minor foliation dip reversals are common in the GH section and are the result of small dislocations and minor shear zones.

Foliations in the Wheeler Peak (WP) sections are even more variable than in the GH section and range from N40-80E. Foliation typically dips steeply to the northwest or is vertical. Near granite intrusives, which form the boundaries of the WP sections, the foliations generally conform to the contact trend.

LINEATION

Linear structures are rarely encountered in the measured sections. In the GH section lineations are not found. South of this section, however, along the east rim of Long Canyon fine crenulations in the plane of the foliation are found in quartz-muscovite schist in the float. In the WP sections lineations are found as hornblende porphyroblasts elongate along the plane of foliation in some small hornblendite dikes. These lineations are only found where the hornblendite dikes are near fault related shear zones.

FAULTS

There are two major faults in the Gold Hill section. The earlier fault is located in the topographic low points along the ridge south of Goose Lake and along the east rim of Long Canyon, and it trends in a northeasterly direction. The second fault offsets the first and runs at almost right angles to it from the head of Long Canyon, south across the meadow separating Long Canyon from Goose Lake (Figure 5A). It is difficult to estimate either the direction or amount of displacement along the first fault. If, however, the mafic schist units east and west of the fault south of Goose Lake are displaced members of the same unit, the maximum offset is roughly 400m and at least part of the motion was right lateral stike slip.

The amount of horizontal movement is easier to estimate for the second fault by extrapolating the trend of the first fault and the contact between mafic schist and layered gneiss. The horizontal displacement across this fault is between 275 and 340m with a right lateral offset. A very rough estimate of the offset of the southern contact of the type 2 tonalite in Placer Creek was made in the field and the displacement is approximately the same. This fact argues against the horizontal movement being due to rotation, since the amount of displacement is expected to change with distance from the axis of rotation. However, it does not rule out dip-slip motion.

Only one major fault occurs in the WP sections. This fault is located between Lake Fork Peak and Fairview Mountain (Figure 5B). An estimate of direction of movement is based on the lineations in hornblendite dikes and indicates that the northern block moved down and to the west in a dip-slip motion. The amount of movement cannot be determined due to limited exposure and the similarity of rock types. Small shear zones, less than one meter thick, are found occasionally through the WP sections and on the north side of Fairview Mountain some small brecciation cuts across the fine laminations of the hornblende-biotite gneiss (Plate 16). Minor offsets are suspected south of Wheeler Peak based on changes in foliation trends.

According to Clark and Read (1972) much of the faulting

in the Taos Range occured during the Cenozoic, and they suggest that faulting at this time may have occurred along previous lines of weakness. Two general types of faults are encountered in the measured sections: faults that are associated with wide shear zones which tend to mask the actual displacement; and, poorly exposed faults which are recognized mainly by changes in foliation trends or displacement of rock units. It is beleived that the first type of fault is of Proterozoic age, mainly due to the presence of linear structures in hornblendite dikes near some of these faults. They may have been reactivated during the Cenozoic. The second type is probably much younger, since one, located southeast of Lake Fork Peak offsets a Tertiary dike.

FOLDS

As pointed out in the petrographic discussion, the consistant relationship of layered gneiss on the north side of mafic schist units in the GH section argues against any major folding and repetition of bedding in that section. This does not eliminate the possibility that the entire Gold Hill section may be the limb of a fold, or that the section is repeated due to thrusting prior to metamorphism. There is intrabed folding found in two of the layered gneiss sequences (Plate 17). This folding is attributed to minor movement along bedding planes during metamorphism.

Although folding is not a very prominent feature of the WP sections, it is more pronounced than in the GH section. At the north end of the Lake Fork Peak section, tight isoclinal folding of the hornblende-biotite gneiss has resulted in the shearing and tranpostion of the fold noses away from the fold limbs (Plate 18). The largest observable fold wavelenths are only tens of centimeters across and amplitudes could not be measured. This same type of folding occurs northeast of Lucero Peak at the southern end of the Lake Fork Peak section. The presence of the isoclinal folding suggests that at least some of the compositional layering in the WP sections is the result of this folding of the original rock.

The folding history of the Proterozoic in the Taos Range is difficult to determine in the measured sections. However, other studies in the Taos Range and in the Picuris Range to the southeast are able to document Precambrian folding with more success.

Condie (1980) was able to show two periods of folding in the Precambrian of the Taos Range. The dominant folds have wavelengths from ten to hundreds of meters, trend N10-30E, and plunge to the northeast. The second set, probably older, have small amplitudes and wavelengths, trend northwest to west, and plunge steeply to the southeast. The scale of this project did not permit the documentation of these folds.

At the south end of the Lake Fork Peak section, from approximately the top of Lucero Peak to the granite contact, the hornblende-biotite gneiss is folded into tight chevron folds with a wavelength of 5 to 10cm. These chevron folds reflect the forceful emplacement of this granite pluton and is the last recorded folding event in the measured sections.

METAMORPHISM

The Proterozoic rocks of the Gold Hill and Wheeler Peak sections have undergone at least one period of regional metamorphism to the lower amphibolite facies. Contact metamorphism near large plutons caused local deformation of the supracrustal rocks but has not significantly changed the mineral assemblages. Determinations of the stable metamorphic mineral assemblages are made difficult by the fact that the rock types studied do not lend themselves to the formation of aluminum-silicate index minerals. In addition, all Proterozoic rocks show evidence of retrograde metamorphism.

The best mineralogic indicators of metamorphic grade are found in the mafic rocks. Those considered here are the intrusive amphibolites of the Gold Hill and Wheeler Peak sections, the hornblende-biotite gneiss of the Wheeler Peak sections, and the mafic schists of the Gold Hill section. The intrusive amphibolites of the Gold Hill section are characterized by the following mineral assemblage:

hornblende + andesine-labradorite + quartz + biotite.

The Wheeler Peak amphibolites are similar with the assemblage:

hornblende + biotite + labradorite + sphene + apatite.

As for the mafic supracrustal rocks, the hornblende-biotite gneiss of the Wheeler Peak section contains:

hornblende + quartz + andesine + biotite.

The mafic schists of the Gold Hill section have a distinct assemblage composed of:

biotite + amphibole (ferro-actinolite?) + albite + quartz

This last assemblage is characteristic of the greenschist facies (Miyashiro, 1973). However, due to the extreme alteration of the mafic schists, it is not advisable to use them for the determination of stable metamorphic mineral assemblages. Therefore, the mafic schists will not be considered in the following discussion.

Hornblende in the mafic rocks is typically blue-green to green in color, and brown hornblende is rare. Blue-green to green hornblende is indicative of lower metamorphic temperatures corresponding to the lower amphibolite facies (Miyashiro, 1973).

Plagioclase compositions are quite calcic, with anorthite ranging from 42 to 69% . An anorthite content of 30% is taken to mark the change from greenshist to amphibolite facies, since after 30% anorthite, the rate of compositional variation becomes very rapid (Ramberg, 1952; referenced in Miyashiro, 1973). The presence of epidote in the mafic rocks is apparently the result of retrograde metamorphism.

Almandine of metamorphic origin is absent from the rocks of the measured sections. The formation of this mineral may or may not occur depending on the Fe2+/Mg ratio,

the amount of rock pressure, and the oxidation state of the rocks (Miyashiro, 1973). Therefore, the absence of this mineral is not critical to the determination of the metamorphic grade. The only garnets encountered are in the Gold Hill layered gneisses and in the small quartzites located at the very north end of the Lake Fork Peak section. The former occurence is a post deformation mineral probably formed by late crystallizing intergranular liquids (Spry, 1969; p.271). In the latter occurence, garnets are deformed and thus, pre-tectonic (Spry, 1969; p.252).

The ACF values for the mafic rocks are plotted in Figure 7. Because the total iron content of the analyses is in the form of Fe2O3, part of this amount was allocated for the amount of magnetite in each sample. The remaining iron oxide was recalculated as FeO and added to the Mgo to determine the F value. On the ACF diagram the mafic samples lie on or near the hornblende-anorthite join.

The above mineralogy is consistent with a regional metamorphic grade corresponding to the medium pressure range of the lower amphibolite facies as described by Miyashiro (1973). Figure 8 is a pressure-temperature diagram showing low, medium, and high pressure metamorphic zones along with a tentative scheme of metamorphic facies. This diagram is compiled from similar diagrams in Miyashiro (1973; p. 420) and Turner (1981; p. 72). Using this diagram, the

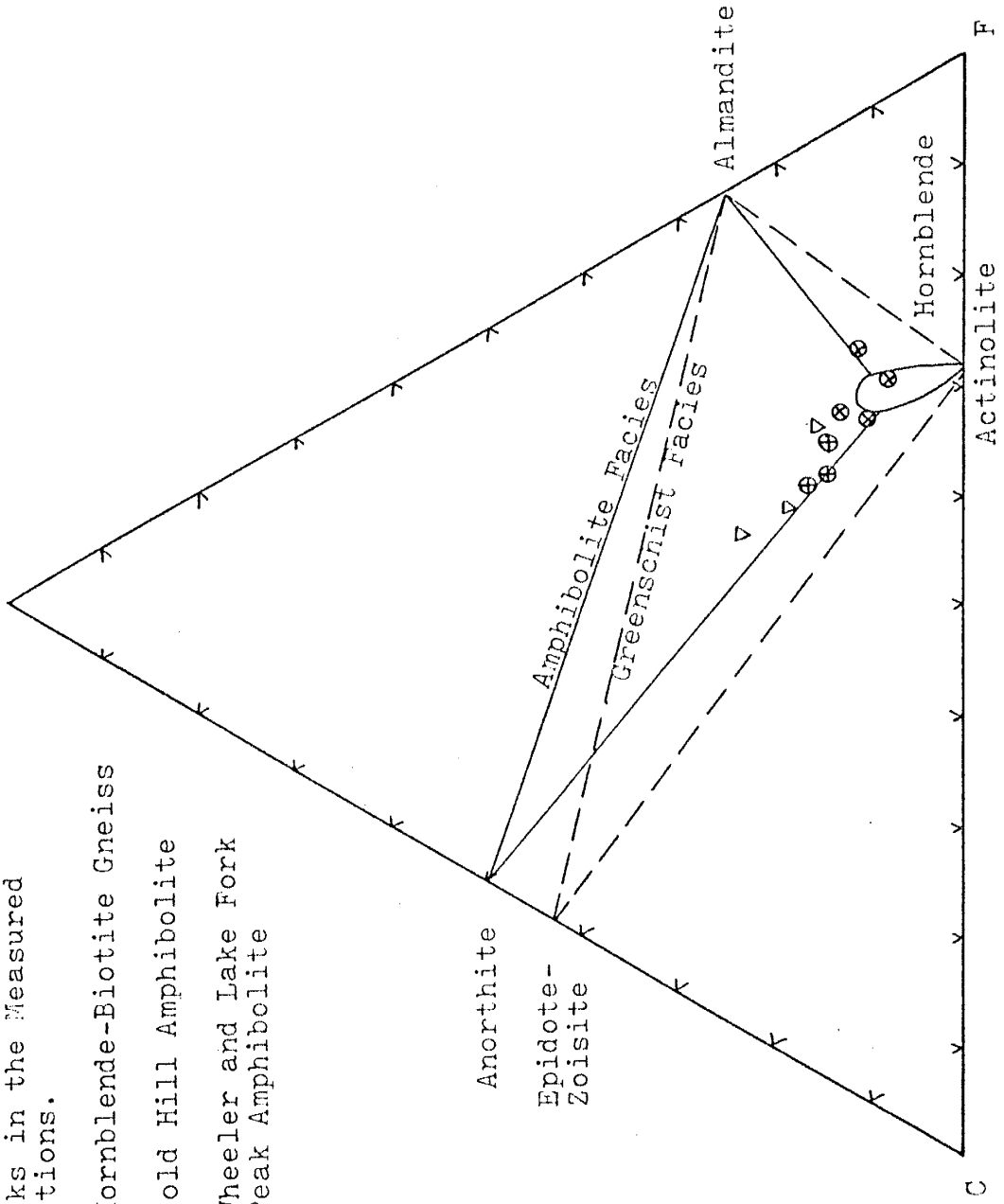

Figure 7.
ACF Diagram of the Mafic Rocks in the Measured Sections.

▽ Hornblende-Biotite Gneiss

⊕ Gold Hill Amphibolite

⊗ Wheeler and Lake Fork Peak Amphibolite

Figure 8.
Pressure-Temperature
Diagram of Metamorphic
Facies and Facies Series

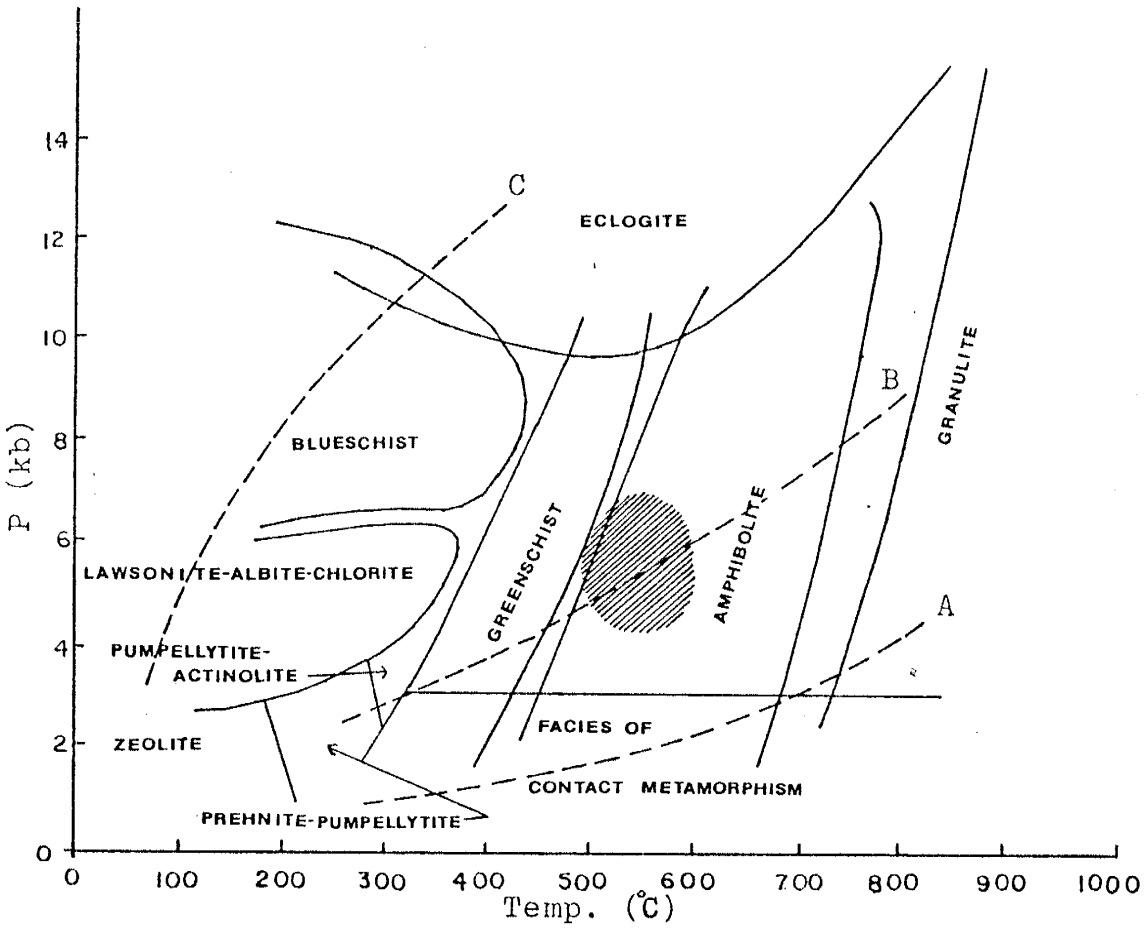

Facies Series:
A=Low-Pressure Metamorphism
B=Medium-Pressure Metamorphism
C=High-Pressure Metamorphism
(Modified after Miyashiro, 1973, and Turner, 1981)

▨ =Estimated Metamorphic Grade of the Proterozoic Rocks in the Taos Range.

metamorphic mineral assemblage corresponds to a temperature between 500 and 600 C, and 4 to 7 Kb pressure.

Retrograde metamorphic minerals are pervasive throughout the measured sections. Retrograde minerals include chlorite after biotite, tremolite-actinolite after hornblende and as coronas around garnet and magnetite, sericitization of feldspar, and the partial breakdown of plagioclase to albite and epidote (saussuritization).

The first major metamorphic event is believed to have occurred relatively soon after the deposition of the supracrustal rocks (1,700 m.y.; Callender et al, 1976; Condie, 1981), and the Proterozoic rocks of the Taos Range may have undergone more than one metamorphic event. According to Gresens (1975), K/Ar and Rb/Sr studies of the Precambrian in north-central New Mexico indicate that there are at least three metamorphic events which post date the initial metamorphism. These are: (1) 1,425 m.y. tectonic and metamorphic event accompanied by pegmatite emplacement; (2) 1,350 m.y. thermal event; and (3) 1,250 m.y. tectonic and hydrothermal event. The effects of these later metamorphic events on the rocks in the Taos Range are not clear.

GEOCHEMISTRY

INTRODUCTION

Thirty-seven samples of both supracrustal and intrusive rocks from the measured sections have been analyzed for major and trace element concentrations by X-ray fluorescence (XRF) and instrumental neutron activation methods (INAA). Major element oxides (except Na2O, MnO and P2O5), and Rb, Sr and Zr were determined by XRF using methods modified after Norrish and Hutton (1969). Na2O, trace elements and REE were determined by INAA using methods modified after Gordon et al (1968). Analytical errors associated with these methods are 1 to 3% for the major elements and 10% or less for the trace elements. The sample preparaton and other pertinent information on the analytical procedures are given in Appendices C, D, and E.

With few exceptions, the intrusive rocks appear to be relatively unaltered. The supracrustal rocks, however, appear to have undergone varying degrees of alteration. In particular, the mafic schists contain large amounts of secondary carbonate and the felsic volcanics are also locally carbonized. It is difficult to exactly monitor which elements have been moved around. To get an idea of how mobile the alkali elements (K2O, Na2O, and CaO) have been, the samples have plotted on an An-Or-Ab diagram after Irvine and Baragar (1971)(Figure 9). From this diagram, we can see that for the majority of the supracrustal rocks, the

alkalis have been very mobile and in the mafic schists they have been extremely mobile.

If these rocks started out as volcaniclastic sediments as the petrography would indicate, alteration may have occurred during reworking and depositional processes. In addition, the presence of ironstones interbedded with these volcanic rocks indicates shallow marine waters which may also have changed the original chemistry of the rocks.

Despite the obvious alteration of some of the supracrustal rocks it is assumed that they originated as volcanic material based on relict textures found in the Gold Hill section. For this reason the supracrustal rocks are classified using only igneous and volcanic rock diagrams.

FELSIC VOLCANICS

Felsic volcanic samples are chosen to represent as many textural variations as possible the from the Gold Hill section. The analyses for these samples are given in Table 4 and are listed in order from north to south through the Gold Hill (GH) section.

The composition of all the felsic volcanics are quite similar. They are characterized by high SiO2 (69 to 77%), high CaO (1.3 to 4.6%), and extremely low MgO (0.0 to 0.9%). For the most part, Na2O and K2O values are dependant on the phenocryst assemblage for each sample. Samples R-105 and R-124 contain mostly plagioclase phenocrysts and have higher Na2O than K2O. Samples R-196 through R-245 contain mostly alkali feldspar phenocrysts and subsequently have K2O values greater than Na2O. The only exception to this is R-59 which has mostly quartz phenocrysts and a high alkali feldspar content in the groundmass.

Following Irvine and Baragar's (1971) method for classifying volcanic rocks, all samples fall in the subalkaline and tholeiitic fields (Figures 10,11, and 12A). A Jensen cation plot (Jensen, 1976) of the felsic volcanic rocks places them in the rhyolite field of the tholeiitic trend (Figure 13A). This particular graph also emphasizes the MgO-poor nature of the felsic volcanics. The low to absent MgO is most likely an alteration effect. On Church's

(1975) volcanic classification scheme (Figure 14), the felsic volcanics fall in and near the rhyolite and dacite fields. The fact that a number of the felsic samples lie outside the fields of the Na2O + K2O side of this diagram indicates that some alkali elements have probably been added to these samples. On the Al2O3/SiO2 side, sample R-196 is above the rhyolite field due to a secondary vein composed of carbonate and biotite. R-245 is a sample from a felsic unit interlayered with layered gneiss. This sample has the highest Fe2O3T and MgO of all the felsic volcanics and this accounts for the shift into the trachytic field. Sample R-200 has so little Al2O3 (9.6%) that it does not even plot on this side of the diagrams. These diagrams by Church show a rough increase in iron and calcium in the felsic volcanics from north to south.

Using the classification diagrams for volcanic rocks proposed by Winchester and Floyd (1977), which use Zr/TiO2 ratios versus SiO2, all but two samples, R-196 and R-245, lie in the rhyolite field. These two samples lie in the rhyodacite-dacite field (Figure 15).

Scandium concentrations have been used in other Proterozoic terrains in New Mexico as a rough index of original rock type (Robertson, pers. comm.). Sc is relatively immobile during alteration processes (Condie et al, 1977) and typically shows an increase with increasing mafic content. Figure 16 is a Sc vs SiO2 diagram. The

felsic volcanics have Sc values under 10ppm, and from this diagram it can be seen that they show an increase in Sc values from north to south.

For the sake of comparisons, analyses of Proterozoic rhyolite from the Tusas Mountains, northern New Mexico (Gibson, 1981), and Tertiary rhyolite of the Bishop Tuff, California (Hildreth, 1979), have been added to table 4. In relation to the Proterozoic Tusas rhyolite, the felsic volcanics of the Gold Hill section generally have more CaO and less MgO, Na2O and K2O. No trace element data were reported for the Tusas rhyolites. The Bishop Tuff is also similar to the felsic volcanics in major element chemistry but has higher MgO and K2O, and lower FeO* (Total iron reported as FeO) and CaO. As for the trace elements, the felsic volcanics have higher Sc, Co, Sr, Ba and Ta, lower Rb, U and Th, and roughly the same Zr, Cs and Hf as the Bishop Tuff.

The rare earth element (REE) patterns for the felsic volcanic rocks are very similar in profile and magnitude, which may be indicative of a common source. All show a light REE (LREE) enrichment, chondritic heavy REE (HREE) and a small to moderate negative Eu anomaly (Figure 19). The REE patterns of the felsic volcanics are quite similar to the REE patterns for the Bishop Tuff (Hildreth, 1979; p. 60) with the exception that the latter has greater negative Eu anomalies. The felsic volcanic REE patterns are also

similar to the Archean rhyolites of the Marda calc-alkaline suite (Taylor and Hallberg, 1977).

Other modern analogues, at least for the major elements, are the rhyolites of orogenic and bimodal associations reported by Ewart (1979). The similarities between the phenocryst assemblages of the felsic volcanics and these modern analogues has already been pointed out in the petrographic dicussion. These similarities, when coupled with the major and trace element chemistry offer strong evidence that the felsic volcanics were originally rhyolitic to dacitic volcaniclastic sediments prior to metamorphism.

MAFIC SCHISTS OF THE GOLD HILL SECTION

Analyses of two samples of mafic schist were obtained from atomic absorption methods by Ingrid Klich, who analyzed these rocks for a New Mexico Tech independant study project (Klich, pers. commun.). The data for these samples, LC-1 and LC-2, are in Table 5. Thin sections of the mafic schist reveal a high content of secondary carbonate (see Table 1), and the major element chemistry reflects this alteration.

When compared to the intrusive amphibolites and the hornblende-biotite gneiss, the mafic schists are similar in major element chemistry except for extremely high CaO (13 to 16%), extremely low SiO2 (40 to 41%) and high CO2 and H2O lost on ignition. This implies that CaO has been added at the expense of SiO2. This particular alteration does not remove the compositional bimodality of the supracrustal rocks. Instead, it produces an artificial trimodality on those diagrams which utilize SiO2. The bimodal relationship remains on diagrams that do not use SiO2.

The loss of SiO2 is shown by Figure 10 where LC-1 and LC-2 lie in the alkaline series field due to the low SiO2. On Figures 11 and 12A, the mafic schist samples lie in the tholeiitic and calc-alkaline fields, respectively. Figure 12A is the more reliable plot since the normative plagioclase composition of Figure 11 is dependant upon the CaO composition in the rock.

A Jensen cation plot, which is not dependant on either CaO or SiO2, places LC-1 on the line between high magnesian tholeiitic basalt and calc-alkaline basalt (Figure 13A). LC-2 lies well in the calc-alkaline basalt field near the hornblende-biotite gneiss samples. The compositional bimdality of the supracrustal rocks is very evident on this diagram. Using Church's volcanic classification (Figure 14), LC-1 and LC-2 can be classified as basalts but this scheme uses CaO in both diagrams and SiO2 in one. However, if CaO and SiO2 values similar to the other mafic rocks are substituted for LC-1 and LC-2, these samples still fall in the basaltic fields.

Zr data are not available for the mafic schist samples and thus could not be plotted on the Zr/TiO2 vs SiO2 diagram of Winchester and Floyd. The validity of this diagram for classifying the mafic schist samples, however, is questionable considering the amount of carbonization (Hynes, 1980). Sc values are slightly higher, but in the same range as the amphibolites and hornblende-biotite gneiss (Figure 16). Both samples show island-arc affinities on a Ti vs Cr plot (Figure 17; Pearce, 1975). As for the other trace elements, LC-1 and LC-2 have more Cr and less Co, Ba, U and Th than either the amphibolites or the hornblende-biotite gneiss.

The REE patterns for the mafic schists are LREE enriched and HREE depleted, and both samples show a positive

Eu anomaly (Figure 20). According to Condie, et al (1977) trace element and REE data are reliable for up to 10% carbonization and 60% epidotization. The mafic schists have been subject to much more than 10% carbonization and classifications based on trace elements are likely to be faulty.

Since there are only limited trace element data for the mafic schists and these data may be questionable due to the addition of carbonate, any geochemical classification must be based on the available major element data. If only SiO2 has been affected by the addition of CaO, as the results suggest, then it is possible that the mafic schists originally had a basaltic composition with possible calc-alkaline affinities. The Sc values support the major element data.

LAYERED GNEISS OF THE GOLD HILL SECTION

R-207 is the only sample representing the layered gneiss of the GH section and the data are given in table 5. This sample is one of the garnet-bearing gneisses and is from a small gneiss unit near the Goose Lake trail (Figure 26A). R-207 has high SiO2 (68.3%) and Fe2O3T (13.0%), and low MgO (0.79%), Al2O3 (9.1%) and Na2O (0.34%). These characteristics reflect the abundance of quartz and iron-garnet in the rock.

Geochemically, this particular sample is not like any of the other rock types studied. Field relations suggest a combined felsic volcanic and mafic schist source for the layered gneisses and therefore, R-207 should plot somewhere between these two on the diagrams. On most of the diagrams which use major elements, however, R-207 plots away from the projected line between the felsic volcanics and the mafic schists. Every time Fe2O3T is used as an end member of a major element diagram (Figures 12A, 13A and 14), R-207 is shifted strongly toward the Fe2O3T end of the diagram. It is suggested that R-207 does not plot between the felsic volcanics and mafic schists on the major element diagrams because iron was added to this sample soon after deposition by chemical precipitation out of a solution.

The trace element diagrams are applied with more success to this sample. On the Zr/TiO2 vs SiO2 diagram

(Figure 15) R-207 lies in the rhyodacite-dacite field between the felsic volcanics and the amphibolites (the mafic schists could not be plotted on this diagram). The Sc vs SiO2 diagram places R-207 between the felsic volcanics and the mafic schists. This is what is expected if the layered gneisses are sediments derived from a mafic and felsic source as the field relations indicate. The REE pattern is also supportive of the trace element plots (Figure 21). R-207 shows a LREE enrichment similar to the felsic volcanics, a HREE depletion like the mafic schists and no Eu anomaly.

HORNBLENDE-BIOTITE GNEISS OF THE WHEELER PEAK SECTIONS

Four supracrustal samples were chosen to represent the rocks of the WP sections. Two, LF-1 and LF-37, are poorly layered, mafic-rich samples. One sample, W-25 is slightly less mafic but still poorly layered. Only one sample has been chosen to represent the leucocratic rocks of the WP sections since they are limited in total volume. This sample, LF-5, is from one of the few small quartz-sericite schist units at the north end of the Lake Fork Peak section. It has been chosen in an attempt to compare these schists with the felsic volcanics of the GH section. The geochemical data for the hornblende-biotite gneiss and quartz-sericite schist are given in Table 5.

The major element composition for the hornblende-biotite gneiss samples is similar in many respects to that of the GH intrusive amphibolites, and in some respects to the mafic schists. In comparison to the WP amphibolites, the hornblende-biotite gneiss samples have higher SiO_2 and Al_2O_3, lower TiO_2 and MgO, and variable amounts of the other major oxides. LF-5 is similar to the felsic volcanics in its high SiO_2 (74.2%) and low TiO_2 (0.27%) and MgO (0.45%). This sample differs, however, from the felsic volcanics in that it has lower Al_2O_3 and higher CaO.

The hornblende-biotite gneiss samples lie near the GH amphibolites in the subalkaline field of Figure 10 and in

the calc-alkaline field of Figure 12A. On Figure 11, LF-37 and W-25 are in the calc-alkaline field and LF-1 is just into the tholeiitic field. The Jensen cation plot (Figure 13A) shows W-25 and LF37 to be calc-alkaline basalts and LF-1 to be a high iron tholeiitic basalt. On Church's volcanic classification scheme LF-1 and LF-37 are basalts and W-25 lies in the andesitic field (Figure 14). W-25 is in the andesite field of Church's diagrams since it contains less iron and magnesium than the others. LF-1 plots in slightly different positions than the other two samples on the majority of these diagrams because it has more TiO2, Fe2O3T and K2O, and less Al2O3 and Na2O. The high Fe2O3T in LF-1 can be attributed to the high epidote content. The high K2O may possibly be the result of potassium metasomatism since LF-1 is in close proximity to granitic dikes.

Using the Zr/TiO2 vs SiO2 diagram (Figure 15), LF-1 and LF-37 lie in the subalkaline basalt field. Zr data are not available for W-25 but this sample would probably lie in the andesite field because of its large SiO2 value. All three hornblende-biotite gneiss samples have about the same Sc values, but again, because of the high amount of SiO2 in W-25 this sample does not plot with LF-1 and LF-37 on the Sc vs SiO2 diagram (Figure 16). These Sc values are lower than those for the GH amphibolites, the mafic schists and the non-cumulus amphibolites from the WP sections. Samples W-25

and LF-37 show island-arc affinities on Figure 17. Compared to the GH amphibolites, the hornblende-biotite gneiss samples have higher Rb and Sr, lower Co, Zr and Th, and similar values for the other trace elements. Compared to the mafic schists the gneisses have higher Co, Ba and U, and lower Cr and Th.

REE patterns for LF-37 and W-25 are moderately LREE enriched and HREE depleted with a small Eu anomaly (Figure 22). These patterns are somewhat similar to the patterns for the mafic schists and the GH amphibolite sample R-91. The quartz-sericite schist sample, LF-5, consistantly plots near the felsic volcanics in the tholeiitic and rhyolitic fields of all the classificaton diagrams discussed (Figures 10-16). The REE pattern is quite different, however, in that this sample has depleted LREE and an enrichment in all the REE (Figure 21). This difference in REE patterns between LF-5 and the felsic volcanics indicates that, despite the major element similarities, LF-5 was probably a quartz-rich sediment rather than a felsic volcanic.

In conclusion, the limited data suggest that the hornblende-biotite gneisses of the WP sections have a generally basaltic composition and may have originally been basalts and/or basaltic tuffs. The chemical similarities between these samples and the mafic schists (except SiO2 and CaO) supports a similar origin for both. More analyses are need before a more conclusive answer can be obtained.

INTRUSIVE ROCKS

AMPHIBOLITE OF GOLD HILL SECTION

Samples of intrusive amphibolite from Gold Hill are representative of the numerous dikes and sills throughout the measured section. The geochemical data for the three samples analyzed are given in Table 6, along with the WP amphibolites and some modern diabases. The GH amphibolites are relatively SiO2-rich when compared to the WP amphibolites. The relatively high SiO2 content is the reason why two of the GH samples, R-78 and R-224, are quartz normative. R-91 is olivine normative partially because of the lower SiO2 but mainly because of the higher MgO. The higher MgO in R-91 reflects the higher modal hornblende in this sample compared to the other two samples (Table 2). Overall, the amphibolites of the GH section compare well with the major element data for the modern tholeiitic diabases.

All three samples plot in the subalkaline field of Figure 10. In Figure 11 all three lie in the tholeiitic field but only R-78 plots in the tholeiitic field of Figure 12B. On the Jensen cation plot (Figure 13B) R-78 and R-224 fall in the high iron tholeiitic basalt field and R-91, due to its high MgO content, falls in the high magnesium tholeiitic basalt field. On the Na2O+K2O side of Church's diagrams (Figure 14) all three samples lie in the basalt field. On the Al2O3/SiO2 side R-78 and R-224 lie outside

the basalt field due to their relatively high SiO2 content. The Zr/TiO2 vs SiO2 diagram shows the Gold Hill amphibolites to be subalkaline basalts and andesites (Figure 15). Once again the SiO2 content of R-78 and R-224 is responsible for the shift into the andesitic field.

Sc values for the GH amphibolites are all within 4ppm of each other and on Figure 16 they form a tight grouping slightly above the WP amphibolites and the hornblende-biotite gneiss. The mafic schists and the cumulus zones of the WP amphibolite are similar to the GH amphibolites in Sc values. The GH amphibolites may show island-arc affinities on the Ti vs Cr diagram (Figure 17). Comparison of the trace elements in the GH amphibolites indicates R-91 has slightly higher Cr, Ni, Sr, Ba and Cs, and slightly lower Rb, Zr, Hf, Ta, U and Th than R-78 and R-224, which are similar to each other. Most of the trace elements in the GH amphibolites exhibit lower values than the WP amphibolites (the non-cumulus samples only), with the exception of Hf and Ta which are higher, and Zr, which is roughly the same. The REE patterns are somewhat similar, but once again R-91 is slightly different than the other two. R-78 and R-224 have slightly enriched LREE, small negative Eu anomalies, and chondritic HREE. R-91 has a slightly positive Eu anomaly and more depleted HREE (Figure 23).

As mentioned previously, the composition of the GH amphibolites is similar to the composition of modern diabase

dikes. The petrography is also supportive of a diabasic origin for the GH amphibolites. One of the characteristics of diabase dike swarms is uniform chemical analyses over large areas (Carmichael et al, 1974). If the differences found in the major and trace element composition for R-91 are not the result of alteration, perhaps it records two diabase intrusive events prior to metamorphism.

AMPHIBOLITE OF THE WHEELER PEAK SECTIONS

As mentioned in previous sections, the intrusive amphibolite dikes of the WP sections show many of the characteristics of zoned mafic intrusives. To study this geochemically, two samples from near contacts and two samples from near the centers of dikes (except for the extremely coarse mafic pegmatite) have been chosen for analysis. Samples W-30 and LF-32 are medium-grained samples from near contacts and, LF-44 and LF-47 are coarse-grained samples from near central areas. This is not, however, a complete study of the zonation, since samples of the very coarse mafic pegmatite have not been analyzed. Data for these amphibolites are in Table 6.

Compared to the GH amphibolites, the amphibolites of the WP sections have lower SiO2 and higher Al2O3, MgO, Na2O and K2O. LF-47 is an exception in that it has lower TiO2, Al2O3 and K2O and higher CaO than the GH amphibolites. These features are attributed to the higher modal amounts of hornblende in this sample. None of the WP amphibolites are quartz normative and all have Ne in the norm.

Unlike the intrusive amphibolites of the GH section, the WP amphibolite is slightly more alkaline in nature. All but one, LF-47, lie in the alkaline field of Figure 10. On the AFM diagram and the Al2O3 vs Normative Plagioclase Composition plot (Figures 12B and 11) there is a correlation

between sample location within the dike and whether the sample falls in the calc-alkali or tholeiitic field. Samples W-30 and LF-32, which are from near contacts, are close to or well within the calc-alkaline field. LF-44 and LF-47, which are samples from the central areas show tholeiitic trends and even ultramafic characteristics. This ultramafic character is seen again in the Jensen cation plot (Figure 13B) where the latter two samples lie in the basaltic komatiite field. W-30 and LF-32 plot as high-Mg tholeiites. Only LF-47 lies outside the basaltic field of Figure 14, but LF-44 and LF-47 both show a shift toward ultramafic compositions.

The Sc vs SiO2 plot (Figure 16) allows one to see through the apparent ultramafic character of LF-44 and LF-47. These samples plot with the rest of the amphibolites, almost 20ppm lower in Sc than the hornblendites. Using the Zr/TiO2 vs SiO2 diagram (Figure 15) all samples lie in the subalkaline basalt field. From these two diagrams it is evident that Sc shows a slight increase from the contacts to the center but the Zr/TiO2 ratio does not. These samples appear to show ocean floor basalt affinities (Figure 17). The other trace elements, Rb, Sr, Zr, Cs, Ba and Th show a decrease from contact to center, Cr and Ni show an increase, and the remaining trace elements seem to be unaffected. In comparison with the older intrusive amphibolite of Gold Hill, this rock

generally has slightly higher concentrations of the trace elements.

The REE patterns show much variation between samples (Figure 24). Sample W-30 shows LREE enrichment and HREE depletion, and may have a slight positive Eu anomaly. LF-44 has slightly depleted LREE, depleted HREE and a large positive Eu anomaly. LF-47 has chondritic LREE, a nearly chondritic HREE distribution and a small positive Eu anomaly. Unfortunately, sample LF-32 does not give sufficient REE data. It would appear from these REE patterns that LREE are concentrated near the contact and the HREE were transported with the later crystallizing liquid.

The samples collected from near the contacts appear to be representative of the major element composition of the rock. On this basis, the WP amphibolites can be considered as high magnesium tholeiite basalts after Jensen's classification. Whether or not these rocks represent a segment of a calc-alkaline suite depends upon whether the magma responsible for the WP amphibolites is also responsible for the type 2 tonalite and the later granite.

HORNBLENDITE

Since hornblendite dikes are found both undeformed and highly schistose in the measured sections, both types are considered for this study. The data are in Table 7, along with reported chemical analyses of hornblendites from the Rio Brazos, northern New Mexico (Barker etal, 1976), and from the Vishnu Group and Granite Park Mafic Body in the Grand Canyon (Clark, 1979). Samples R-1 and R-23 are from large undeformed hornblendite intrusive bodies in Deer Creek, north of Gold Hill, and from Fairview Mountain, respectively. Sample W-13 is from a small strongly deformed dike south of Wheeler Peak.

The samples analyzed are characterized by low SiO2 (45.3 to 48.2%), Al2O3 (5.1 to 8.3%), Na2O (0.51 to 1.3%), and K2O (0.4 to 0.39%), and high Fe2O3T (11.2 to 16.6%), MgO (14.5 to 18.2%), and CaO (13.3 to 14.6%), relative to the amphibolites. The major element geochemistry of the hornblendites apparently reflects the amount of plagioclase in each sample. Samples R-23 and W-13, which contain minor plagioclase, have greater Al2O3 and less Fe2O3T than R-1, which has no plagioclase. The hornblendites of the Taos Range resemble the hornblendites of the Grand Canyon in major element compositions. In comparison with the hornblendites of the Rio Brazos, the Taos hornblendites have more TiO2, Fe2O3T, MgO and Na2O, and less Al2O3. Although

not given here, the hornblendites of the Taos Range are also similar to the composition of several pyroxenites given in Nockolds (1954). The CIPW norms for the hornblendites show 41 to 53% normative diopside and 14 to 25% normative olivine.

According to Irvine and Baragar's classification scheme these rocks are classified as mafic tholeiites (Figures 10 and 12B). Samples R-1 and R-23 are too Al_2O_3-poor to plot on Figure 11. On a Jensen cation plot these three hornblendite samples fall in the basaltic komatiite field (Figure 13B). Only W-13 plots on Church's volcanic classification diagrams (Figure 14) since R-1 and R-23 are too rich in Fe_2O_3T, MgO, and CaO. W-13 appears to have lost some of each of these oxides upon deformation. On the Zr/TiO_2 vs SiO_2 diagram (Figure 15) the hornblendites all lie in the subalkaline basalt field. The combined effects of slightly lower TiO_2, and higher SiO_2 and Zr are responsible for W-13 plotting near the intrusive amphibolites of the WP sections.

On the Sc vs SiO_2 diagram (Figure 16), the hornblendite samples show a marked increase in Sc values over the amphibolites, however the deformed sample, W-13, does have about 5ppm less Sc. The hornblendites have much more Co, Cr, and Ni, slightly less Rb, Sr, Zr, Hf, Ta, and Th, and the same U content when compared to the intrusive amphibolites of Gold Hill and Wheeler Peak. The REE

concentrations appear relatively unaffected by deformation since both deformed and undeformed samples have similar patterns. They show chondritic to slightly enriched LREE, variable Eu anomalies, and depleted HREE (Figure 25).

No suggestions are made in the literature on the protoliths of the hornblendites of the Rio Brazos and the Grand Canyon (Barker, 1976; Clark, 1979). However, The similarities of the Taos Range hornblendites to younger pyroxenites (Nockolds, 1954) along with the high diopside and olivine in the norm calculation are suggestive that they were originally pyroxenites.

TONALITE

For the tonalites of the Taos Range, two samples of type 1 and six samples of type 2 have been selected for this geochemical study. Two of the six type 2 tonalites are a the strongly deformed (porphyroblastic) variety and the remaining four are massive. These samples represent tonalites encountered in the measured sections as well tonalite plutons throughout the Taos Range. The data for the tonalites are given in Table 8.

The minerology suggests that the two types of tonalite are chemically distinct. From table 8 it is immediately apparent that the type 1 tonalite has much higher SiO2 (68 to 71% vs 55 to 61%), slightly higher Na2O (4.6 to 6.3% vs 4.1 to 4.7%), and lower values for the other major oxides than the type 2 tonalite.

In plotting type 1 tonalites, R-81 and R-103 lie near the granites and felsic volcanics in the subalkaline field of Figure 10. In Figure 11 these samples show calc-alkaline trends while in Figure 12B they show tholeiitic trends. When plotted on the Jensen cation plot R-81 and R-103 lie in the tholeiitic rhyolite field near the felsic volcanics (Figure 13B). The type 1 tonalites are also similar to the felsic volcanics on the Sc vs SiO2 diagram (Figure 16). Using other volcanic rock classification schemes, the type 1 tonalites fall in the dacite fields of Church's diagrams

(Figure 14), and in the rhyodacite-dacite field of the Zr/TiO2 diagram (Figure 15). Since dacite is the extrusive equivalent of tonalite these volcanic diagrams are useful in classifying the type 1 tonalite.

On the Ab-Or-An graph of Barker (1979), R-81 and R-103 lie in the trondhjemite field (Figure 18). However, according to the definition of trondhjemite (Barker, 1979; p. 1) the type 1 tonalite has too little Al2O3, much too little MgO and too much Fe2O3T. Also, the high anorthite content of the plagioclase (61) and the high color index (caused by the biotite present) prohibit the use of the term trondhjemite.

The type 2 tonalites also lie in the subalkaline field of Figure 10, although the samples are closer to the alkali series line than the type 1 tonalite. On Figures 11 and 12B the type 2 rocks show a distinct calc-alkaline trend. This calc-alkaline trend is also evident on the Jensen cation plot where the deformed samples R-42 and LF-14 lie in the dacite field and the massive samples lie in the andesitic fields (Figure 13B). The same rock names are obtained using Church's classification (Figure 14) although on the Zr/TiO2 diagram all the type 2 tonalites fall in or near the trachyandesite field (Figure 15). The intrusive equivalent of an andesite is a diorite (Travis, 1955). This suggests that the type 2 tonalites are actually diorites. However, since quartz comprises more than 20% of the light colored

minerals and plagioclase comprises 90 to 100% of the feldspar (where the samples have not had alkali feldspar introduced; see Table 3), these rocks are tonalites (Streckeisen, 1973). The Ab-Or-An plot of Barker (1979) also indicates that they are tonalites (Figure 18). R-19, which has been subject to potassium metasomatism, is shifted toward the Or end but still lies in the tonalite field. The deformed samples, which also contain alkali feldspar, are shifted to the granodiorite field. The most appropriate name for the type 2 tonalite, based on the geochemistry, is a mafic tonalite. Plagioclase diorite is probably also correct and may be preferred by some researchers.

On the Sc vs SiO2 diagram (Figure 16) the massive samples which have not had potassium feldspar intrduced (R-22, R-25 and R-43), all have equal amounts of Sc. R-19, a massive sample which has had potassium feldspar introduced, shows a decrease in Sc. The deformed and metasomatized samples, R-42 and LF-14, show an even greater decrease. This may be an original feature of the rocks or may somehow be related to the metasomatism.

A comparison of the trace elements in the two types of tonalite indicates that type 1 has lower Co, Cr, Rb, Sr and Zr, roughly the same Ba, Cs, U and Th, and the same to slightly higher Ta. The deformed variety of the type 2 tonalite generally has higher values of the trace elements than the massive variety, with the exception of Co, Sr and

Ta which are the same or slightly lower. Ce is enriched in R-42 due to the presence of allanite. Ba is significantly enriched in the deformed variety. This is believed to be the result of the addition of alkali feldspar, since R-19, which also has had alkali feldspar added, is enriched relative to the other massive samples.

The REE patterns for the type 1 tonalite show slightly enriched LREE, a small to large positive Eu anomaly, and a relatively flat HREE pattern (Figure 27). With the exception of the positive Eu anomaly, the type 1 tonalite has a similar REE pattern compared to the felsic volcanics. Perhaps this suggests that the type 1 tonalite is a hypabyssal intrusive of the same magma that produced the felsic volcanics.

Besides altering the major element compositions, potassium metasomatism apparently also affects the REE patterns of the type 2 tonalite (Figure 28). The massive samples with no potassium feldspar show only moderate LREE enrichment, slight HREE depletion, and minor Eu anomalies. With the introduction of potassium feldspar into the massive variety (R-19), a moderate positive Eu anomaly and HREE depletion is found. The deformed samples, R-42 and LF-14, which also contain secondary potassium feldspar, have highly venriched LREE, a pronounced positive Eu anomaly, and strongly depleted HREE.

R-54 has been ignored in the above discussion because

is chemically distinct from the rest of the type 2 nalites. This sample has extremely low SiO2 (50%) and K2O .67%), and very high Al2O3 (20.8%), MgO (6.21%), and CaO 0.7%) relative to the other type 2 tonalites. For these asons R-54 resembles the amphibolites on most of the major d trace element diagrams. The trace element values are ther similar to the mafic rocks or somewhere between mafic id type 2 tonalite values. The REE pattern for R-54 is .so distinct in that it has a negative Eu anomaly (Figure 3). The best explanation for these features is that this ock has been contaminated by assimilation of the country ock where the sample was taken. The presence of large enoliths in the field and high hornblende content in thin ection support this conclusion.

GRANITE

Three Proterozoic granitic samples were collected from a variety of environments. Sample R-18 is from a large dike intruding type 2 tonalite in the East Fork of the Red River. This same dike is responsible for the potassium metasomatism found in the tonalite sample R-19 (precise locations for these samples are given in Appendix C). R-46 was taken from the large granite pluton south of Wheeler Peak. Sample LF-3 is from a relatively small (1m), highly foliated dike at the north end of the Lake Fork Peak section. The data for these granites are in Table 7.

The major element compositions are typical for granites although MgO concentrations in these samples are quite low (Nockolds, 1954). Also, Na2O is rather high in in all samples and in R-46 and LF-3 this oxide even exceeds K2O values. This is best explained by albitization of the original plagioclase.

When plotted on Irvine and Baragar's graphs (Figures 10, 11 and 12B) these samples plot as subalkaline rocks with a calc-alkaline affinity. All samples fall in the granitic field of the Ab-Or-An plot (Figure 18). On the Sc vs SiO2 diagram (Figure 16) all lie in the same general area as the felsic volcanics of Gold Hill. LF-3, which is from a highly deformed dike, shows lower Sc than the other granites.

Most of the trace elements show a wide variation in

concentration between samples. This might be expected in a slow cooling magma where these elements would be allowed to migrate freely through the melt. The most immobile trace elements appear to be Sc, Ta, U, Th, and possibly Co.

With the exception of R-46, the granite REE patterns are highly fractionated, showing a systematic enrichment from HREE to LREE and a minor negative Eu anomaly (Figure 26). These three granites were probably derived from the same source. R-46, however, has a flat HREE pattern which cuts across two of the other granite patterns. This indicates that either the HREE were not fractionated in this particular intrusive or this rock belongs to a separate intrusive event.

TABLE 4
CHEMICAL ANALYSES FOR THE FELSIC VOLCANICS

	R-59	R-105	R-124	R-196	R-200	R-222	R-245	BMR	BT
SiO2	76.6	75.4	76.0	71.6	76.7	73.9	69.4	76.5	75.5
TiO2	0.12	0.11	0.08	0.25	0.20	0.20	0.38	0.32	0.21
Al2O3	12.3	13.1	12.2	12.4	9.57	12.2	14.3	12.2	13.0
Fe2O3T	1.45	2.45	2.00	3.23	3.18	2.80	4.18	1.44	1.10
MgO	0.00	0.00	0.00	0.54	0.00	0.00	0.95	0.12	0.25
CaO	1.25	1.66	2.46	4.55	3.97	3.43	3.73	0.12	0.95
Na2O	2.66	4.08	4.24	1.97	2.07	2.43	1.21	3.36	3.35
K2O	4.42	2.73	1.44	3.05	2.44	3.41	3.70	5.15	5.55
Total	98.79	99.54	98.43	97.63	98.08	98.25	97.81	99.21	99.91
Na/k	0.60	1.50	2.94	0.65	0.85	0.71	0.33	0.65	0.60
Sc	3.2	6.0	3.5	8.2	8.4	8.1	8.8		1.8
Co	17	26	15	13	27	15	23		1.0
Rb	66	34	26	50	46	54	69		95
Sr	158	148	157	127	147	148	144		110
Ba	1340	1510	905	548	790	992	1060		465
Zr	130	125	120	93	136	137	122		140
Cs	4.1	-	-	-	3.6	0.9	1.9		1.9
Hf	4.7	5.3	3.2	2.8	3.9	3.9	4.6		3.7
Ta	3.8	4.3	3.2	2.3	4.5	2.4	3.3		0.85
U	3.7	2.9	3.0	2.0	3.8	2.8	2.5		2.6
Th	8.9	7.1	8.9	4.1	6.1	6.1	6.2		13
La	39	33	36	23	31	25	28		61
Ce	66	68	62	48	52	57	54		98
Nd	31	27	27	19	25	23	-		28
Sm	5.7	4.9	4.6	4.2	4.5	4.9	4.4		3.0
Eu	0.77	0.44	0.71	1.4	1.1	1.0	1.3		0.38
Tb	0.71	0.79	0.70	0.95	0.89	0.99	-		0.27
Yb	3.4	3.8	3.0	3.9	4.5	3.8	3.8		1.1
Lu	0.51	0.58	0.44	0.69	0.78	0.75	0.71		0.15
				CIPW NORMS					
Q	42	30	41	39	49	40	38	37	
C	0.88	0.42	-	-	-	-	-	0.90	
Or	27	16	8.7	19	15	21	22	31	
Ab	23	35	37	17	18	21	11	29	
An	6.3	8.3	10	16	9.8	13	19	0.6	
Di	-	-	2.0	5.7	4.7	4.1	-	0.3	
Hy	1.1	2.0	0.6	1.0	-	-	5.6	-	
Wo	-	-	0.94	2.8	4.3	2.0	-	-	
Mt	0.66	1.1	0.92	1.5	1.5	1.3	1.9	-	
Il	0.23	0.21	0.16	0.49	0.39	0.39	0.74	0.1	

Total Iron as Fe2O3; Mg# = (Mg/Mg+Fe)x100
BMR = Burned Mountain Rhyolite (Gibson, 1981)
BT = Bishop Tuff (Hildreth, 1979)

TABLE 5
CHEMICAL ANALYSES FOR THE:
LAYERED GNEISS QUARTZ-SERICITE SCHIST
MAFIC SCHIST HORNBLENDE-BIOTITE GNEISS

	LC-1	LC-2	R-207	LF-1	LF-37	W-25	LF-5
SiO2	40.3	41.1	68.3	52.6	52.1	58 1	74.2
TiO2	0.59	0.63	0.42	1.21	0.93	0.61	0.27
Al2O3	15.0	16.6	9.09	14.6	16.7	16.4	9.01
Fe2O3T	10.5	8.57	13.0	12.4	10.6	7.74	3.48
MgO	6.00	4.30	0.79	5.82	5.71	4.44	0.45
CaO	13.1	16.0	4.49	7.26	8.92	7.22	5.92
Na2O	3.28	4.35	0.34	2.00	4.00	3.73	1.90
K2O	1.87	0.55	2.69	3.46	0.82	0.93	2.01
MnO	0.12	0.16					
P2O5	0.17	0.18					
LOI	11.4	7.19					
Total	100.19	99.63	99.07	99.23	99.65	99.10	97.23
Mg#	-	-	-	48	52	53	-
Na/K	-	-	0.13	-	-	-	0.95
Sc	38	39	10	28	28	23	6.8
Co	23	31	42	40	38	34	30
Cr	85	100	22	-	29	37	-
Rb			65	94	19	27	30
Sr			151	458	417		153
Ba	393	164	646	949	231	-	239
Zr			221	91	94		167
Cs	-	-	5.1	4.8	1.2	-	0.46
Hf	-	-	6.6	3.4	2.1	2.9	6.1
Ta	-	-	3.9	2.0	1.1	1.9	5.1
U	-	0.35	4.3	0.80	0.48	-	2.6
Th	0.79	0.73	8.7	0.69	0.68	1.4	1.4
La	9.95	6.97	35	-	12	7.0	9.1
Ce	25	33	80	-	30	19	39
Sm	2.2	2.4	6.6	3.5	4.1	3.2	10.4
Eu	0.99	2.6	2.1	-	1.5	1.3	2.5
Tb	-	-	1.2	-	0.61	0.52	1.6
Yb	-	-	3.4	2.3	2.0	1.7	13
Lu	0.23	0.20	0.60	0.41	0.31	0.24	0.83
			CIPW NORMS				
Q	-	-	41	1.6	-	11	47
Or	11.8	3.5	16	21	4.9	5.6	12
Ab	-	5.6	2.9	17	34	32	17
An	23	26	16	21	26	26	10
Di	36	25	6.2	13	16	8.7	7.6
Hy	-	-	12	20	8.0	12.9	-
Ol	-	-	-	-	6.4	-	-
Wo	19	24	-	6.52	8.04	4.47	-
Ne	17	19	-	-	-	-	-
Mt	-	-	4.4	4.2	3.6	3.5	1.6
Il	0.28	0.37	0.81	2.3	1.8	1.2	0.53

TABLE 6
CHEMICAL ANALYSES FOR THE AMPHIBOLITES

	R-78	R-91	R-224	MD	W-30	LF-32	LF-44	LF-47
SiO2	54.3	51.4	54.7	52.7	50.5	46.9	46.8	47.7
TiO2	1.46	0.63	1.03	1.14	1.26	1.37	1.40	0.86
Al2O3	12.9	14.9	14.4	14.2	15.1	15.2	13.5	10.9
Fe2O3T	13.8	10.7	11.6	13.9	10.7	11.9	10.3	9.98
MgO	4.70	7.35	4.93	5.53	8.44	10.0	13.6	15.1
CaO	7.48	9.81	8.13	9.86	7.94	9.67	9.04	10.9
Na2O	2.71	3.57	3.35	2.51	3.51	4.47	2.65	2.24
K2O	1.57	0.95	1.32	0.64	1.94	1.38	1.36	0.81
Total	98.85	99.25	99.44	100.4	99.38	100.8	98.61	98.39
Mg#	41	58	46		61	63	72	75
Sc	34	36	38		26	28	35	34
Co	40	43	45	52	50	64	57	67
Cr	21	41	26	94	52	23	86	416
Ni	-	33	-	34	33	158	151	197
Rb	29	20	21	22	75	48	69	28
Sr	339	433	363	178	775	791	603	352
Ba	459	496	309		755	462	245	214
Zr	122	74	136	94	127	87	96	72
Cs	-	1.6	-		7.9	5.3	1.6	-
Hf	3.3	-	2.5		1.9	2.0	3.1	2.0
Ta	1.7	1.1	1.6		1.4	0.71	0.88	0.85
U	0.72	0.55	1.0		1.3	0.50	0.57	0.51
Th	2.1	1.3	1.7		4.0	-	1.2	0.89
La	17	13	14		32	9.7	7.5	8.5
Ce	42	25	36		63	-	18	22
Nd	21	-	28		-	-	-	-
Sm	5.4	3.4	4.7		6.5	5.2	4.7	4.6
Eu	1.2	1.5	1.6		1.8	2.1	2.3	2.0
Tb	0.73	0.74	0.91		0.57	-	0.66	1.2
Yb	3.0	1.8	3.7		1.1	-	1.1	3.8
Lu	0.54	0.27	0.61		0.16	-	0.17	-
			CIPW NORMS					
Q	8.0	-	4.8	6.2	-	-	-	-
Or	9.5	5.7	7.9	3.8	12	8.2	8.2	4.9
Ab	23	31	29	21	29	12	17	17
An	19	22	21	26	20	17	21	18
Di	16	22	17	19	16	25	20	30
Hy	17	3.7	15	16	-	-	-	-
Ol	-	11	-	-	17	17	25	24
Wo	8.0	11	8.5	-	8.3	12.8	10.2	15.7
Ne	-	-	-	-	0.82	14	3.3	1.5
Mt	4.7	3.6	3.9	6.0	3.6	4.0	3.5	3.4
Il	2.8	1.2	2.0	2.2	2.4	2.6	2.7	1.7

MD = Modern Tholeiitic Diabase (Carmichael et al, 1974)

TABLE 7
CHEMICAL ANALYSES FOR:

	HORNBLENDITE				GRANITE			
	R-1	R-23	W-13	RB	GC	R-18	R-46	LF-3
SiO2	46.0	45.3	48.2	47.1	46.3	71.8	70.8	71.5
TiO2	0.89	0.85	0.75	0.33	0.88	0.42	0.15	0.26
Al2O3	5.12	6.40	8.25	10.4	9.44	14.8	15.9	15.4
Fe2O3T	16.6	11.7	11.2	11.7	13.5	2.27	1.83	2.05
MgO	14.5	18.2	14.7	13.6	14.2	0.00	0.00	0.03
CaO	14.5	14.6	13.3	13.3	12.7	0.53	2.04	1.94
Na2O	1.19	0.51	1.27	0.44	1.13	4.14	4.35	4.00
K2O	0.04	0.20	0.39	0.19	0.34	5.91	3.73	3.82
Total	98.82	97.76	98.02	97.06	98.33	99.86	98.76	98.93
Mg#	63	75	72			-	-	-
Na/K	-	-	-	-	-	0.70	1.17	1.05
Sc	57	58	53			6.7	9.2	2.7
Co	85	68	59			27	8.8	27
Cr	520	885	369			-	-	-
Ni	162	-	66		704	-	-	-
Rb	4.2	8.0	18	3.5	-	41	80	96
Sr	131	122	184	268	37	80	309	422
Ba	-	-	-	46		425	969	1300
Zr	37	37	60		39	440	130	180
Cs	-	-	-			-	-	3.1
Hf	-	-	-			12	4.2	5.1
Ta	0.45	1.2	1.7			4.8	3.8	4.4
U	0.72	-	0.52			1.0	3.1	1.7
Th	0.77	-	1.3			6.4	5.2	9.0
La	6.6	3.4	6.1			155	35	30
Ce	16	8.8	15		7	300	66	58
Nd	-	-	-			243	-	-
Sm	2.3	2.3	2.8			25	6.6	3.4
Eu	0.71	1.5	1.1			5.5	2.0	1.1
Tb	-	-	0.49			2.1	1.5	0.56
Yb	1.7	1.3	1.1			4.9	6.6	1.2
Lu	0.32	0.20	0.17			0.68	1.02	0.13
CIPW NORMS								
Q	-	-	-			23	27	29
C	-	-	-			0.63	1.0	1.2
Or	0.24	1.26	2.4			35	22	23
Ab	10	4.5	11			35	37	34
An	8.7	15	16			2.6	10	9.7
Di	53	48	41			-	-	-
Hy	0.53	1.5	10			1.3	1.4	1.5
Ol	20	25	14			-	-	-
Mt	5.7	4.0	3.9			1.0	0.84	0.94
Il	1.7	1.7	1.5			0.8	1.4	0.3

RB = Rio Brazos Hornblendite (Barker et al, 1976)
GC = Grand Canyon Hornblendite (Clark, 1980)

TABLE 8
CHEMICAL ANALYSES FOR THE TONALITES

	TYPE 1		TYPE 2						
	R-81	R-103	R-19	R-22	R-25	R-43	R-54	R-42	LF-14
SiO2	70.9	67.7	60.1	58.9	59.3	55.2	50.1	61.3	59.3
TiO2	0.25	0.23	0.63	0.59	0.63	0.83	0.57	0.79	0.80
Al2O3	13.8	16.3	17.2	18.4	17.3	18.3	20.8	17.9	20.0
Fe2O3T	4.29	4.73	6.57	6.34	6.67	8.09	6.69	5.94	5.27
MgO	0.20	0.12	2.89	3.03	3.05	3.64	6.21	2.16	2.73
CaO	3.46	3.81	5.09	6.11	6.38	7.80	10.7	4.07	3.74
Na2O	4.56	6.33	4.12	4.72	4.32	4.55	3.63	4.43	4.68
K2O	1.24	1.07	2.39	1.53	1.68	1.40	0.67	2.68	2.89
Total	98.71	100.27	98.99	99.62	99.33	99.80	99.32	99.22	99.36
Na/K	3.68	5.92	1.76	3.08	2.57	3.25	5.42	1.65	1.62
Sc	12	16	12	17	17	17	24	6.8	5.3
Co	18	25	26	26	29	31	33	29	21
Cr	-	-	-	15	3.6	9.8	64	20	12
Rb	24	18	69	52	50	36	19	70	98
Sr	346	421	806	1021	954	907	543	727	777
Ba	920	535	973	664	567	452	2415	2100	535
Zr	110	109	202	185	142	227	97	382	370
Cs	3.9	-	-	2.1	2.4	2.7	3.1	-	5.6
Hf	2.6	3.9	5.0	3.5	2.0	5.2	2.3	7.7	8.4
Ta	2.0	4.1	2.6	1.9	1.5	2.5	1.5	2.5	1.8
U	2.0	1.5	1.4	1.6	2.0	0.9	0.48	1.9	2.5
Th	3.8	2.9	3.5	3.3	3.1	1.3	0.81	9.1	4.2
La	20	9.2	28	18	19	19	13	53	25
Ce	40	2.6	48	44	39	52	23	100	43
Sm	4.6	3.8	5.2	5.0	5.3	6.7	2.9	4.8	3.8
Eu	1.6	2.6	2.2	1.5	1.8	2.2	0.63	1.6	2.1
Tb	0.71	0.85	0.84	-	-	0.97	0.49	0.38	0.36
Yb	2.5	3.2	1.4	2.6	1.9	3.0	1.7	-	-
Lu	0.37	0.54	0.20	0.41	0.31	0.50	0.30	0.11	0.13
				CIPW NORMS					
Q	32	18	11	7.2	9.3	1.5	-	12	7.5
C	-	-	-	-	-	-	-	0.32	2.4
Or	7.5	6.3	14	9.1	10	8.3	4.0	16	17
Ab	39	54	35	40	37	39	30	38	40
An	14	13	22	25	23	26	39	20	19
Di	3.2	5.3	3.2	4.8	7.3	11	12	-	-
Hy	2.3	1.3	11	10	9.1	9.6	-	9.4	10
Ol	-	-	-	-	-	-	11	-	-
Wo	1.6	2.5	1.6	2.5	3.7	5.6	-	-	-
Ne	-	-	-	-	-	-	0.82	-	-
Mt	2.0	2.1	3.0	2.9	3.0	3.7	3.1	2.7	2.4
Il	0.48	0.44	1.2	1.1	1.2	1.6	1.1	1.5	1.5

KEY TO GEOCHEMICAL DIAGRAM SYMBOLS

▲ FELSIC VOLCANICS

▼ MAFIC SCHISTS

▽ HORNBLENDE-BIOTITE GNEISS

△ QUARTZ-SERICITE SCHIST

⊕ AMPHIBOLITE OF THE GOLD HILL SECTION

⊗ AMPHIBOLITE OF THE WHEELER AND LAKE FORK PEAK SECTIONS

● HORNBLENDITE

◪ TYPE 1 TONALITE

◩ TYPE 2 TONALITE

GRANITE

Figure 9.
An-Or-Ab diagram showing K-poor, "common", and K-rich volcanic rocks. (After Irvine and Baragar, 1971)

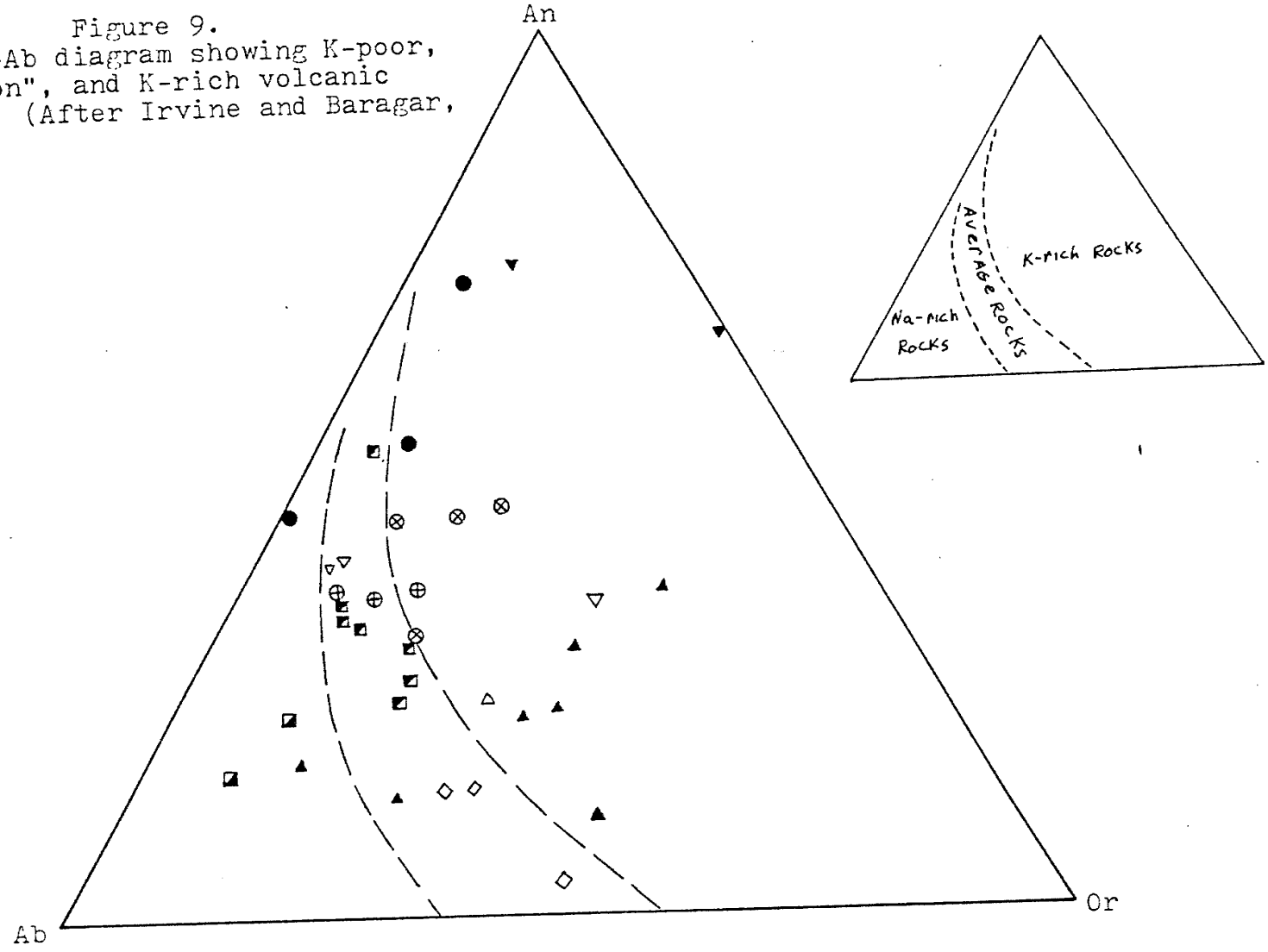

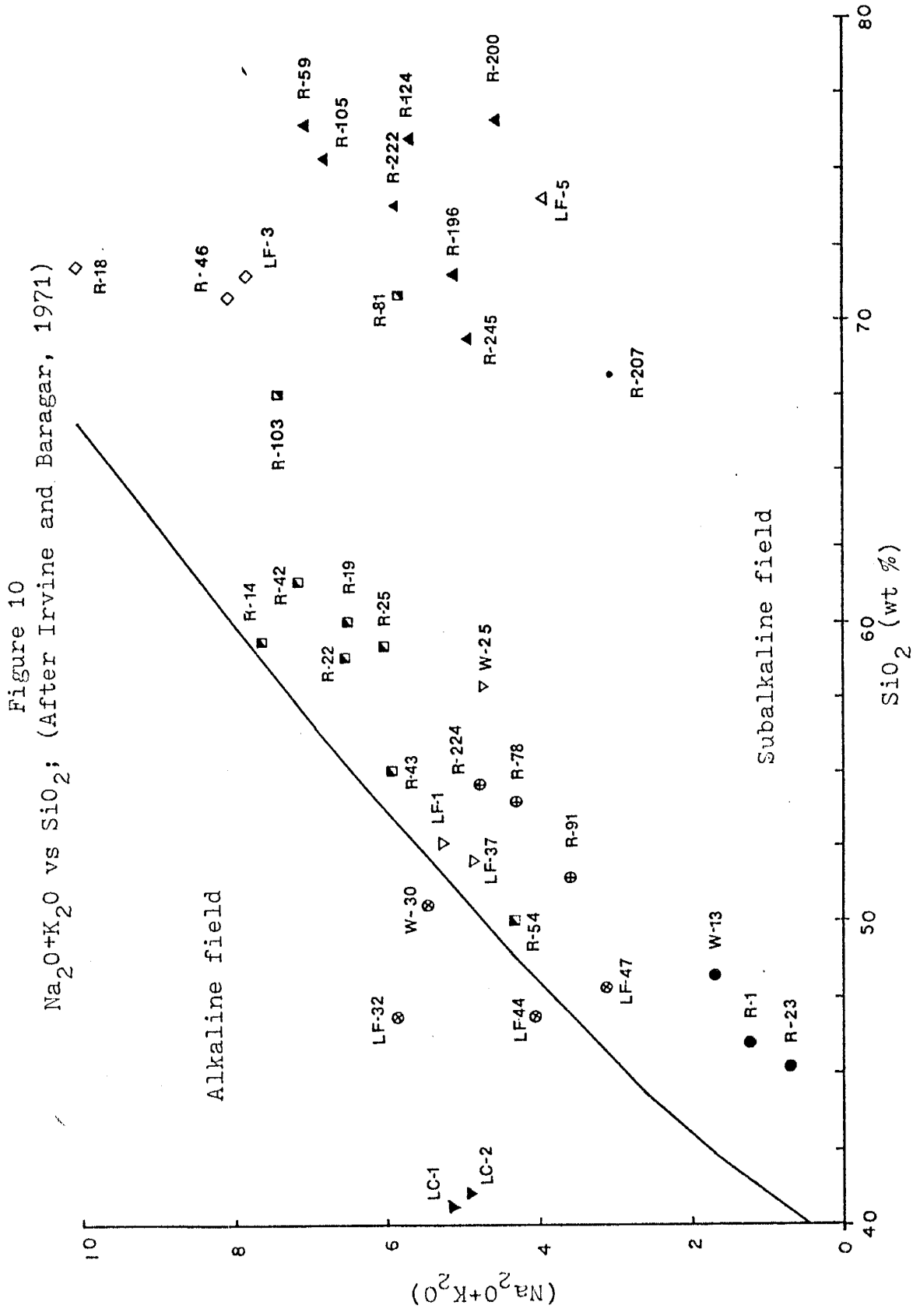

Figure 10
Na_2O+K_2O vs SiO_2; (After Irvine and Baragar, 1971)

Figure 11.
Al_2O_3 vs Normative Plagioclase
(After Irvine and Baragar, 1971)

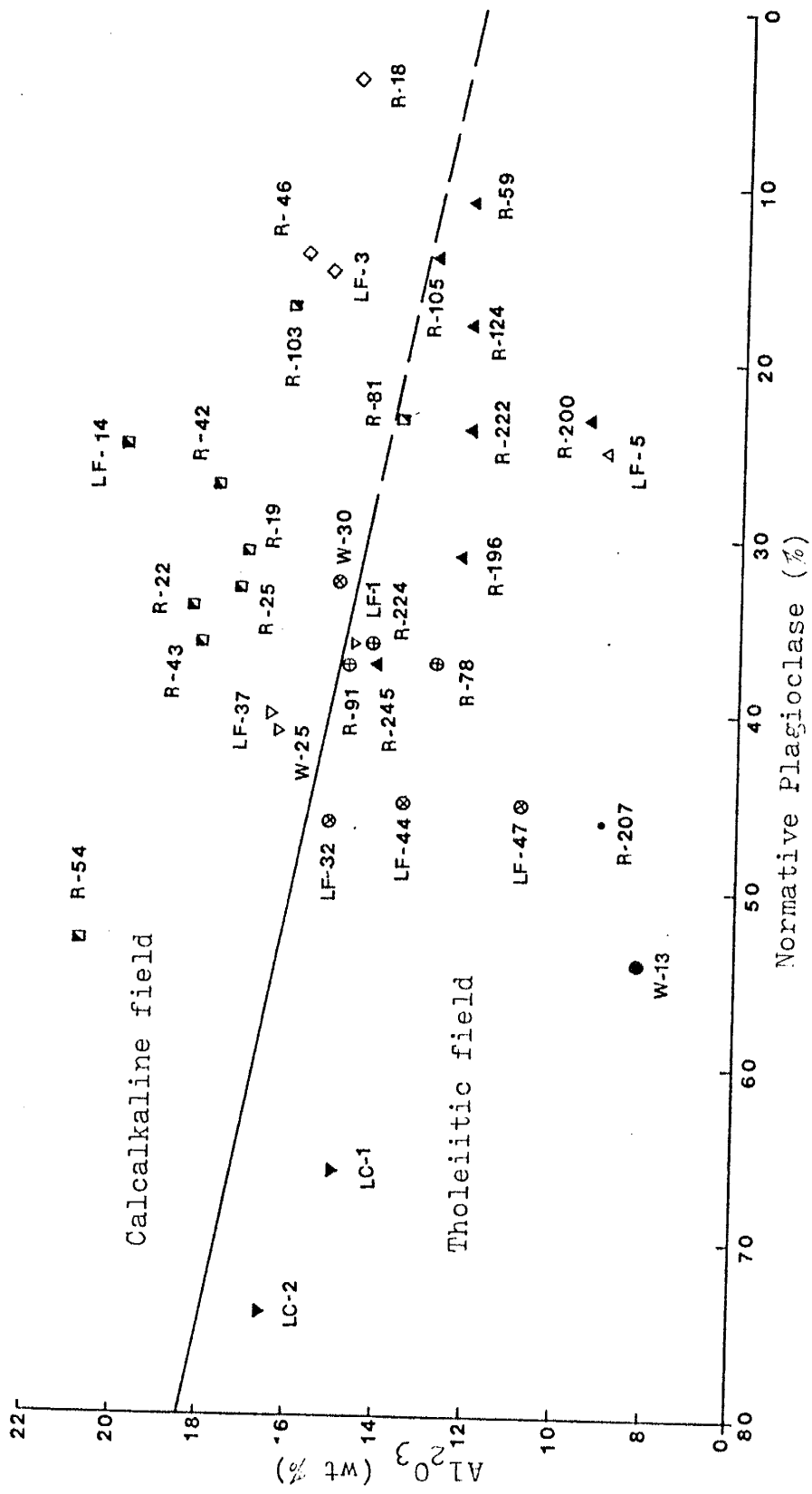

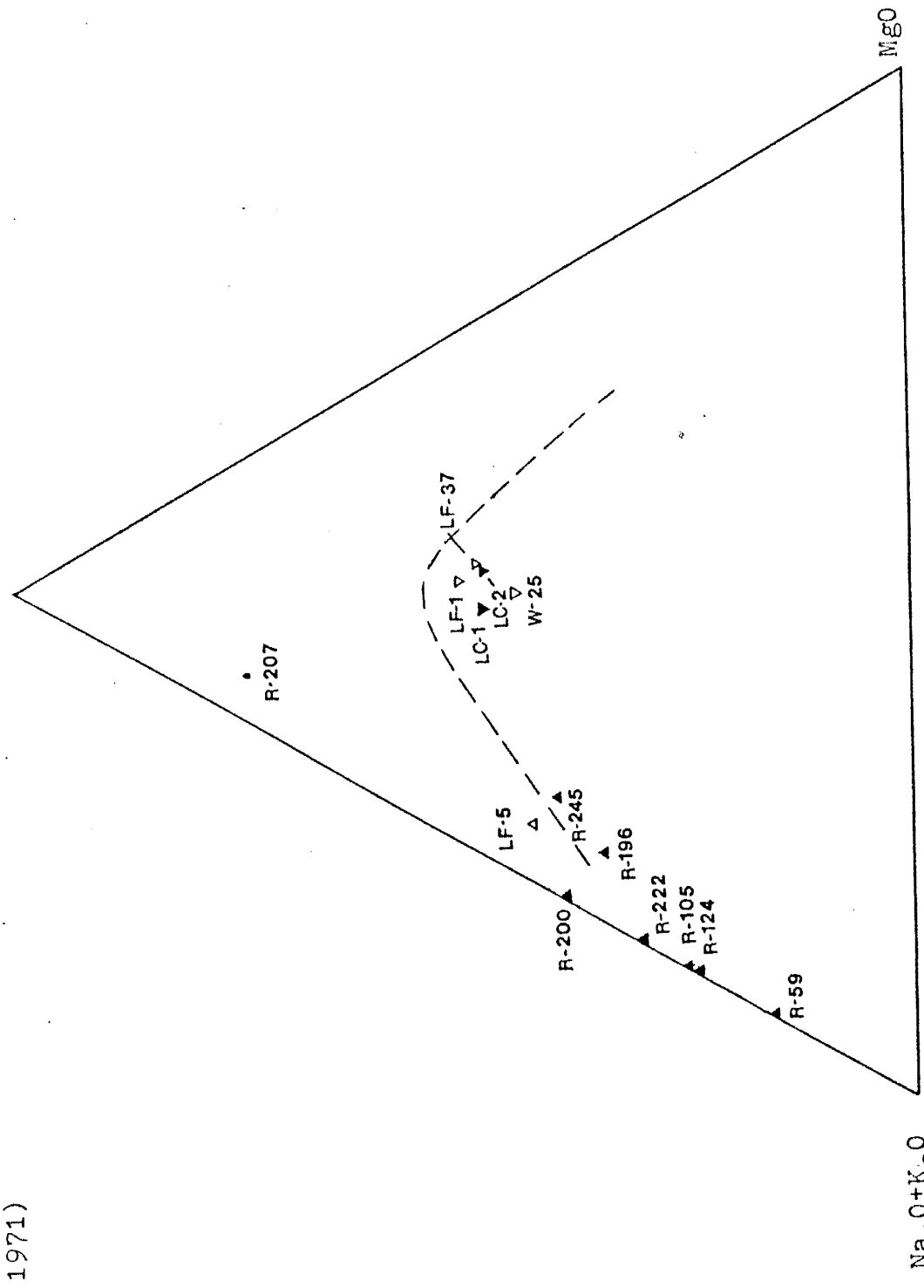

Figure 12A.

AFM Diagram for the Supracrustal Rocks. (After Irvine and Baragar, 1971)

Fe_2O_3 T

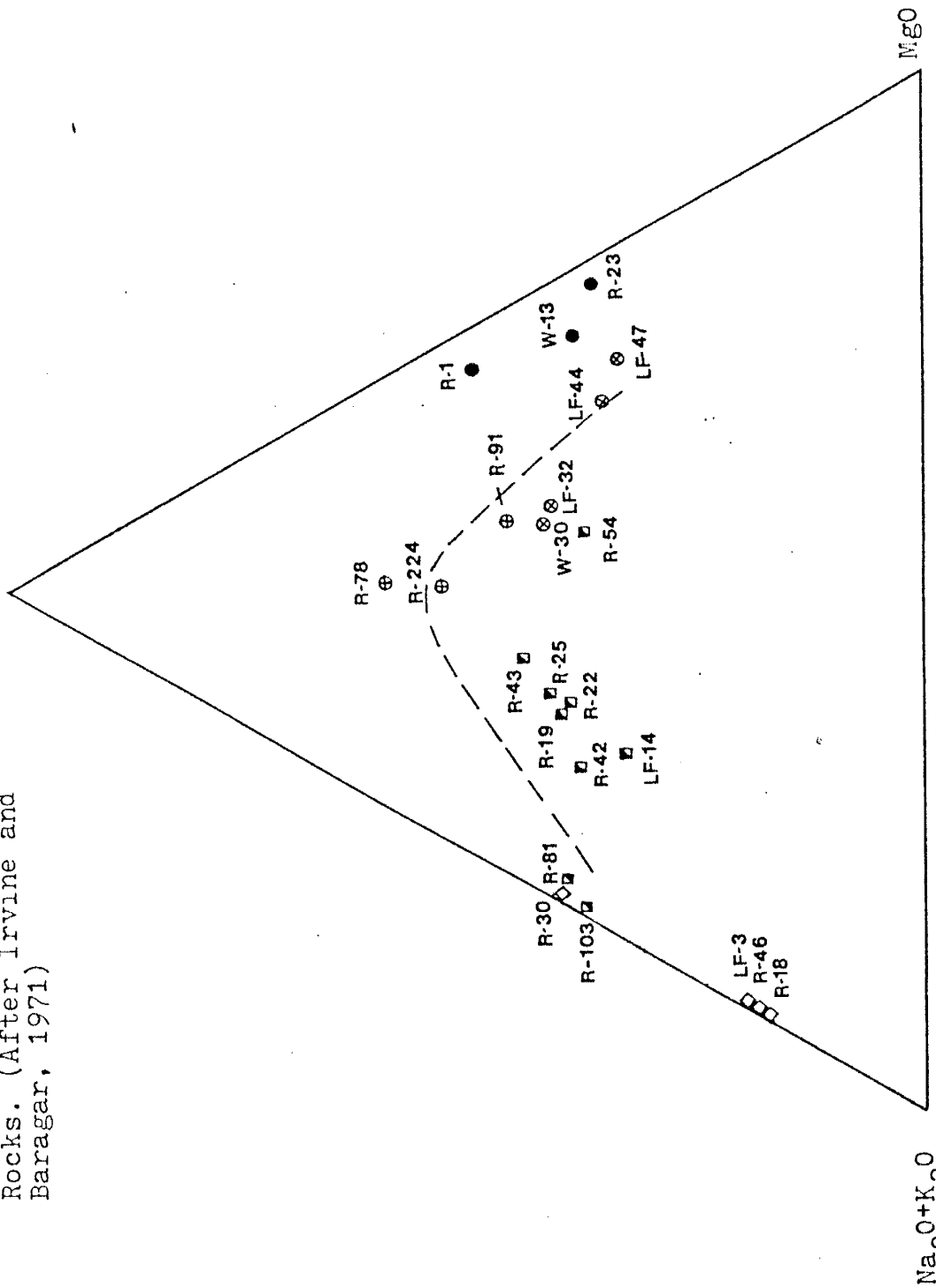

Figure 12B.
AFM Diagram for the Intrusive Rocks. (After Irvine and Baragar, 1971)

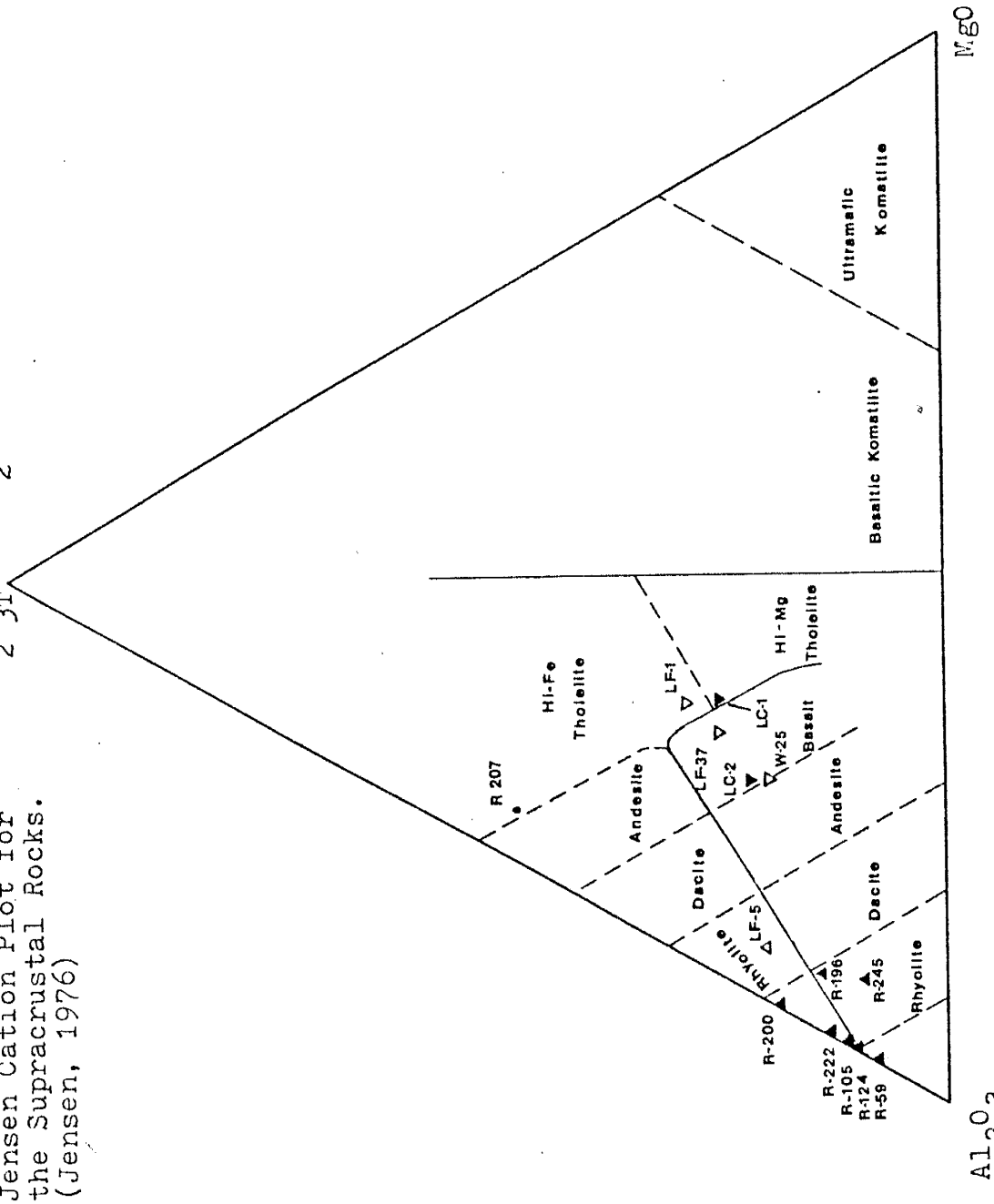

Figure 13A.
Jensen Cation Plot for the Supracrustal Rocks. (Jensen, 1976)

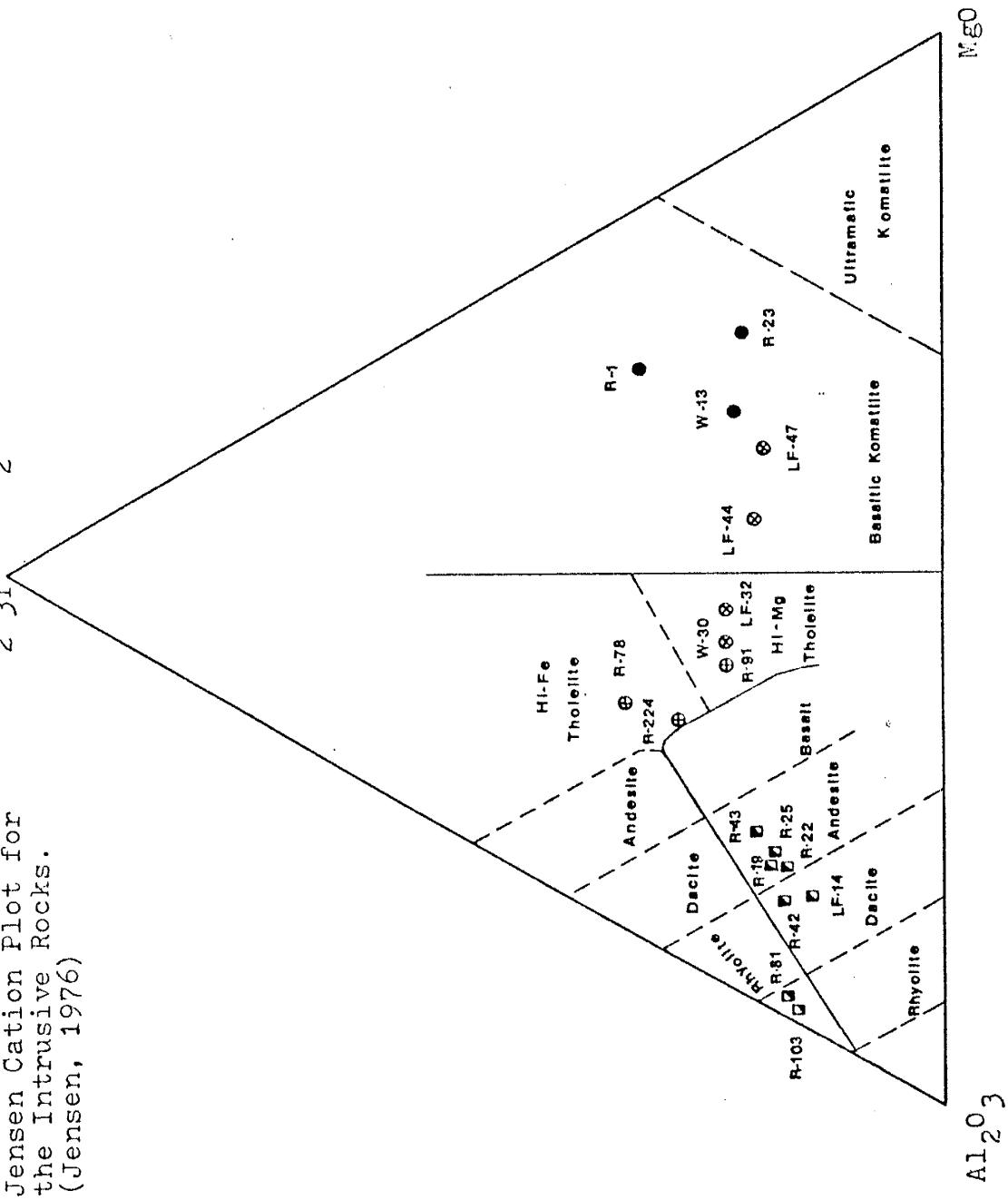

Figure 13B.
Jensen Cation Plot for the Intrusive Rocks.
(Jensen, 1976)

Figure 14.
$Fe_2O_{3T}+1/2(MgO+CaO)$ vs (Na_2O+K_2O) and (Al_2O_3/SiO_2); (Church, 1980)

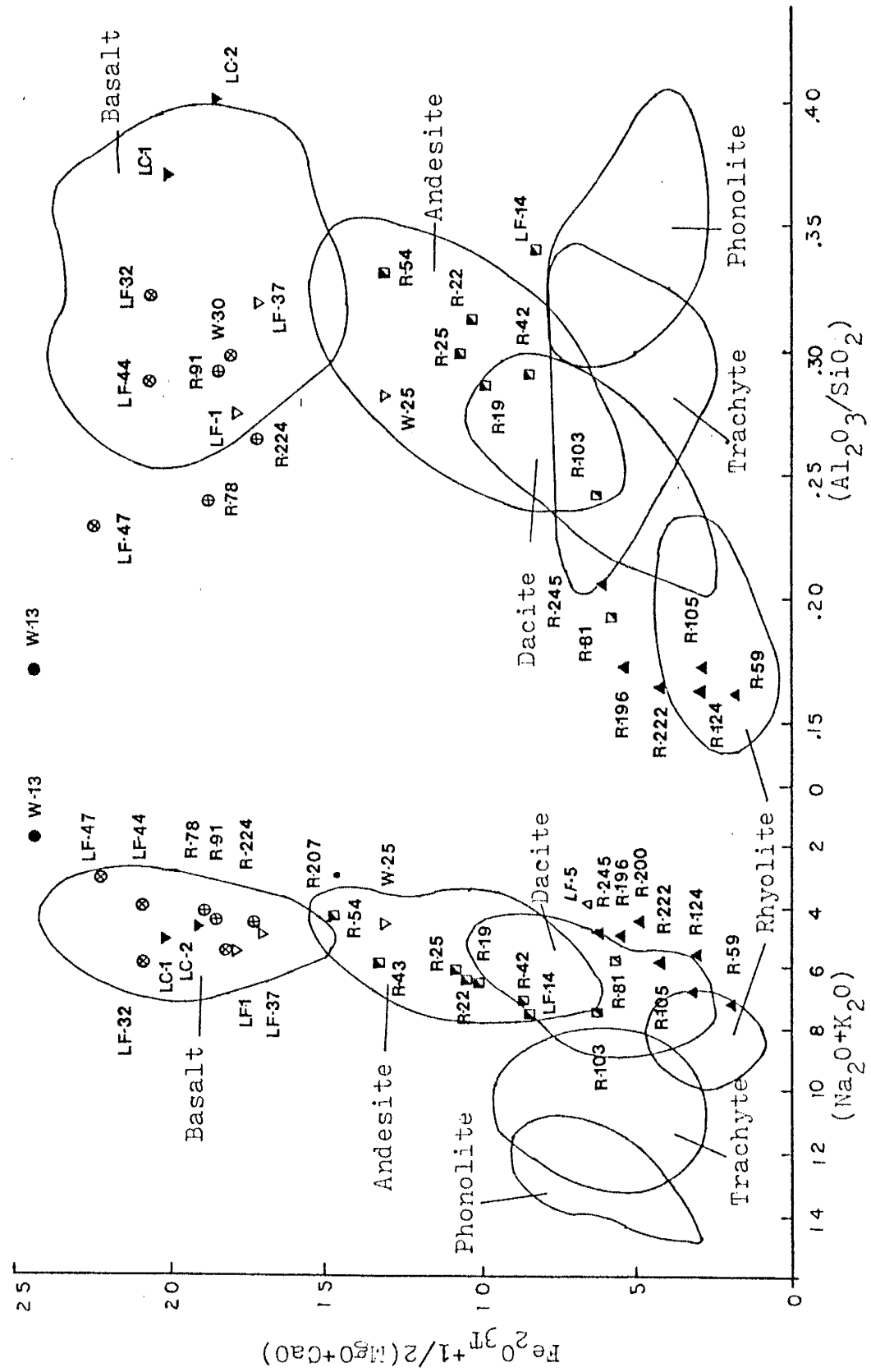

Figure 15.
SiO_2 vs Zr/TiO_2 (Winchester and Floyd, 1977)

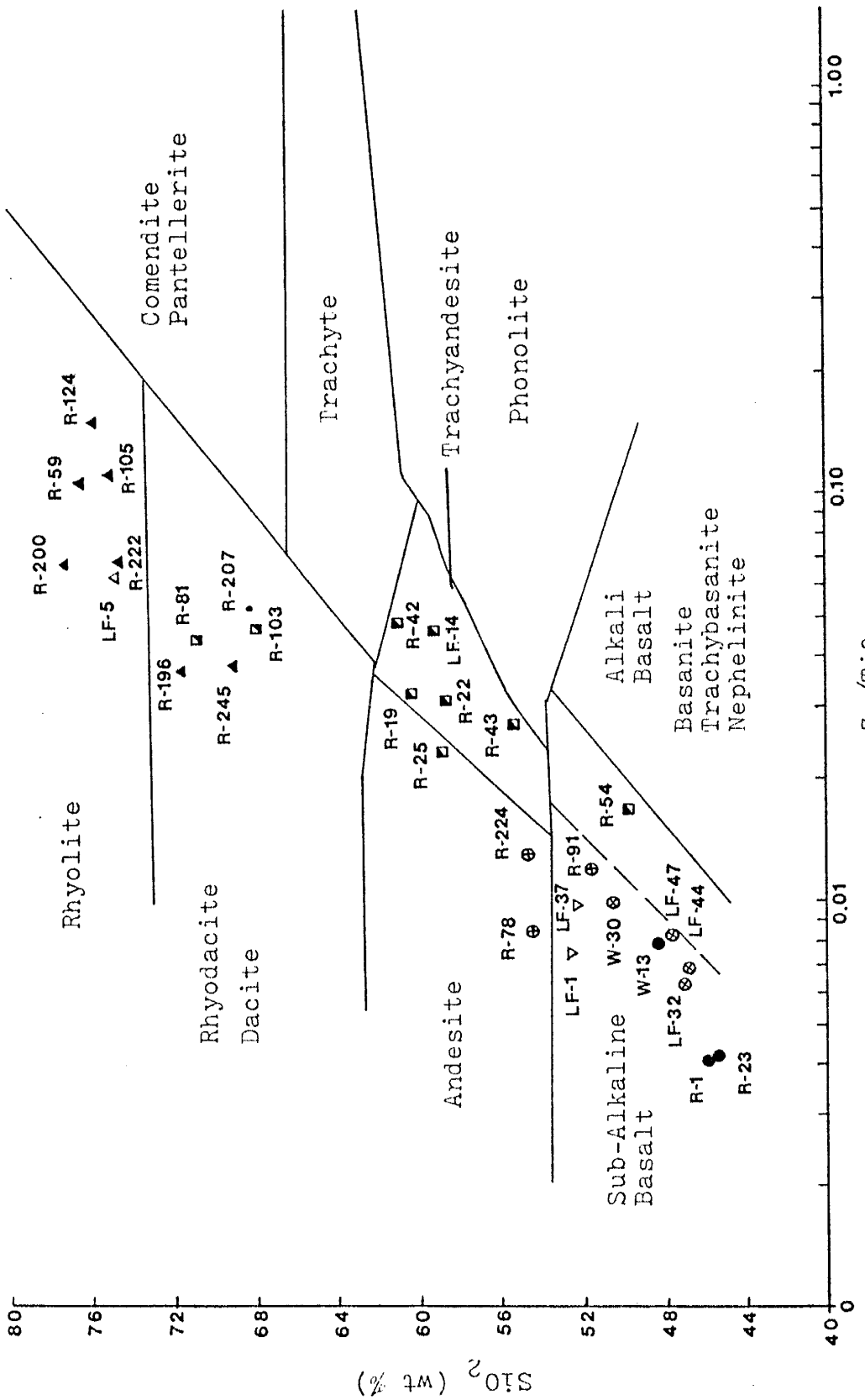

Figure 16.
Sc vs SiO_2

Figure 17.
TiO_2 vs Cr (Pearce,1975)

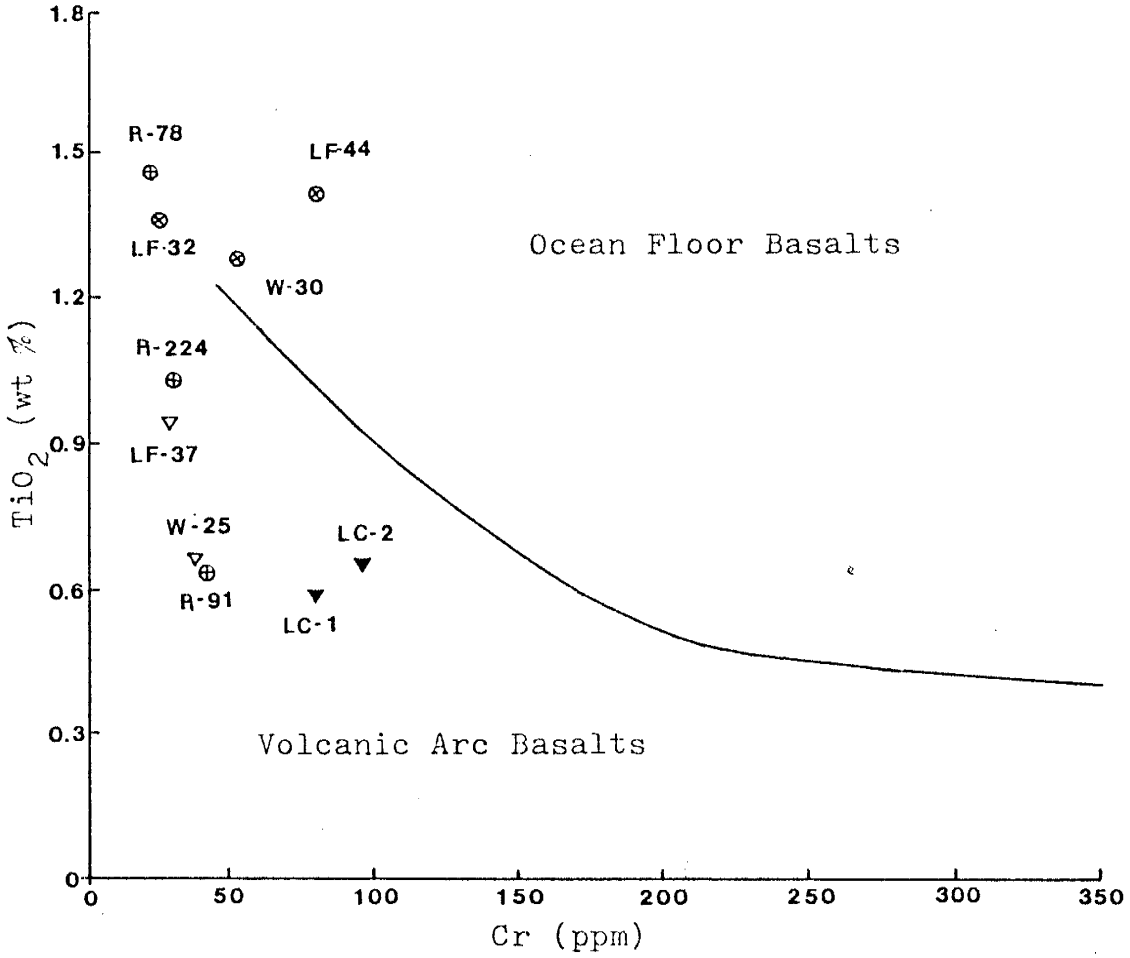

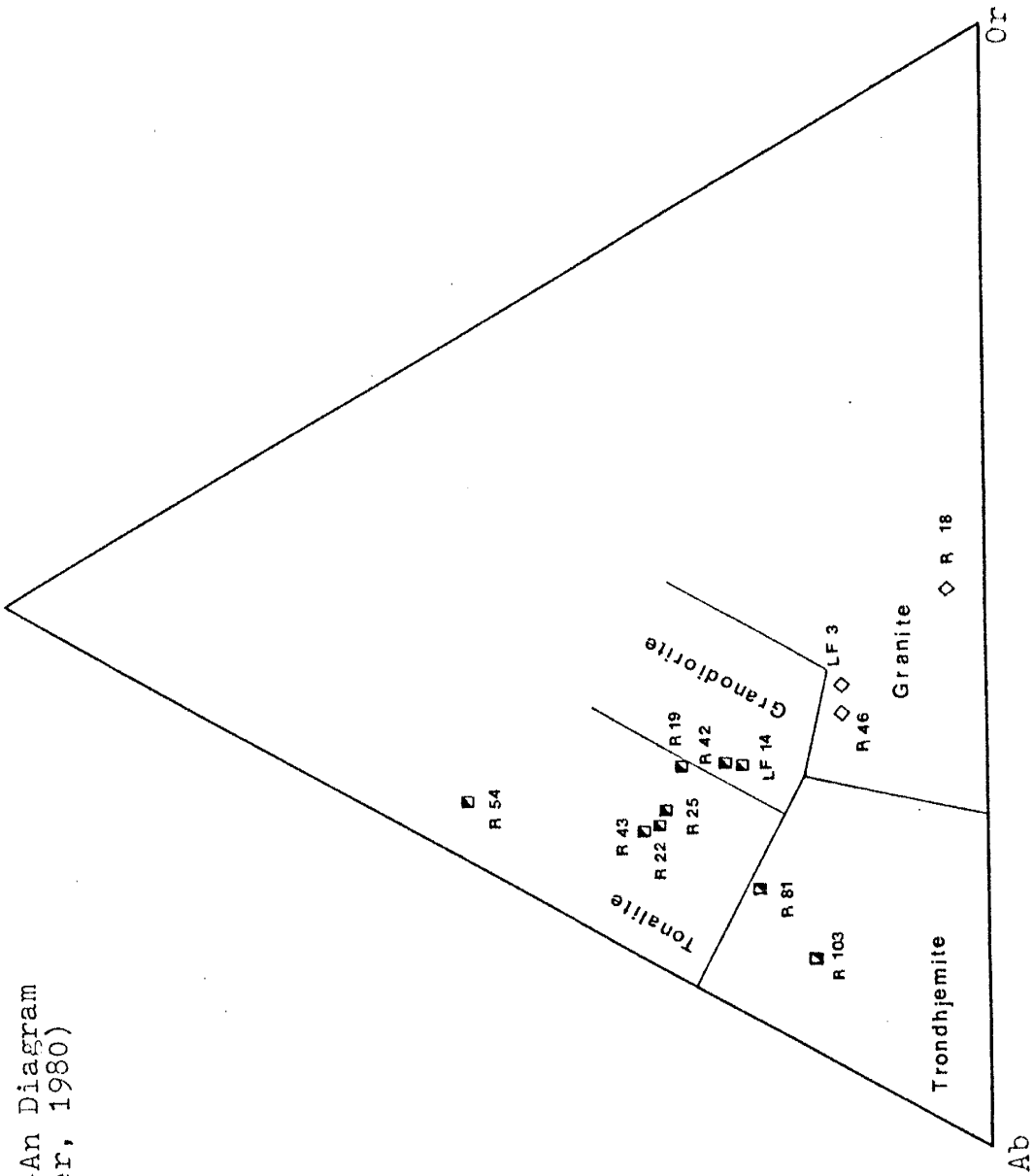

Figure 18.
Ab-Or-An Diagram
(Barker, 1980)

Figure 19.
REE Pattern for the
Felsic Volcanics

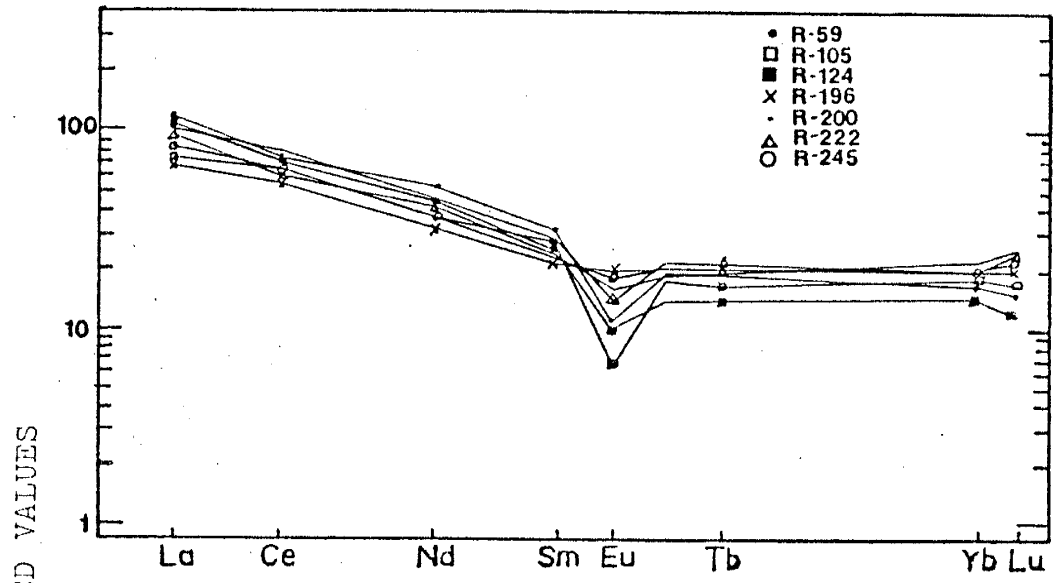

Figure 20.
REE Pattern for the
Mafic Schists

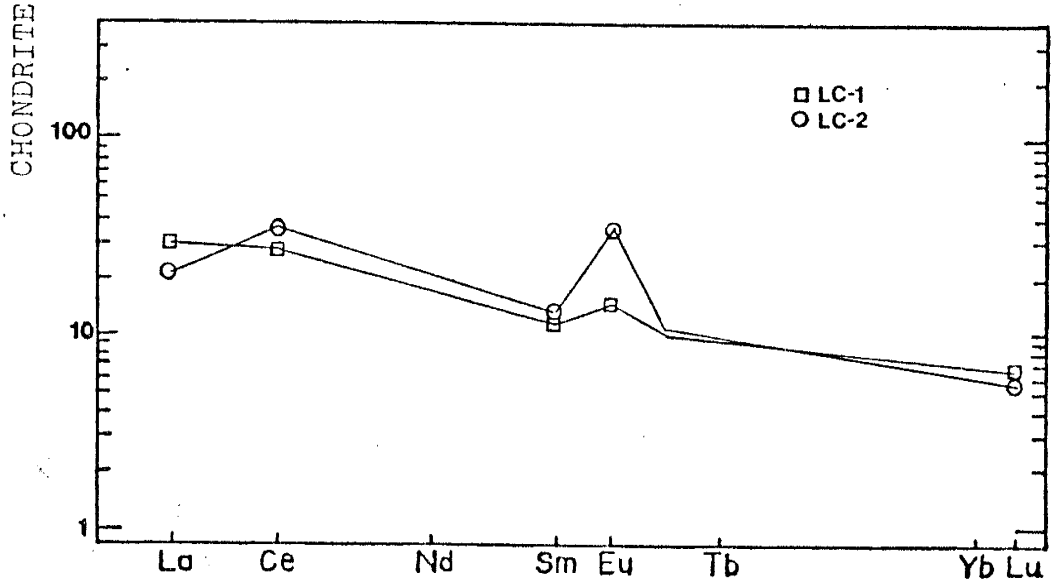

Figure 21.
REE Pattern for the
Layered Gneiss and Quartz-Sericite Schist

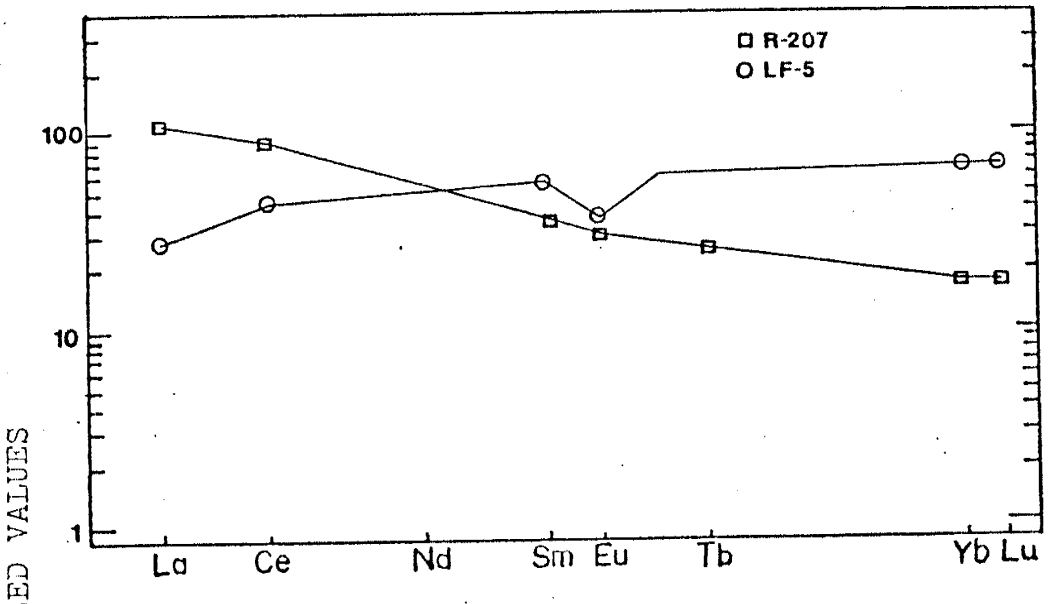

Figure 22.
REE Pattern for the
Hornblende-Biotite Gneiss

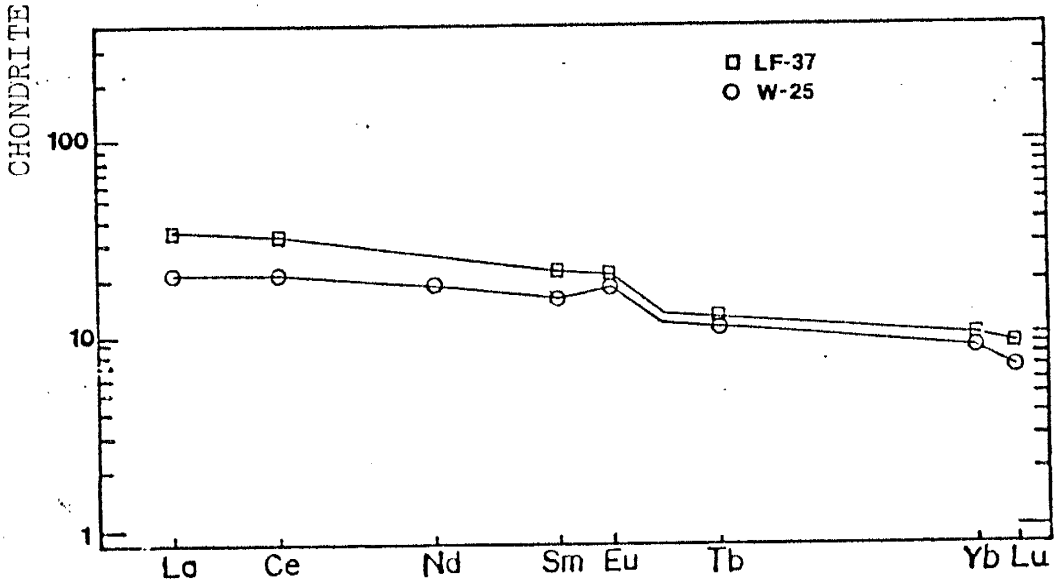

Figure 23.
REE Pattern for the
Gold Hill Amphibolites

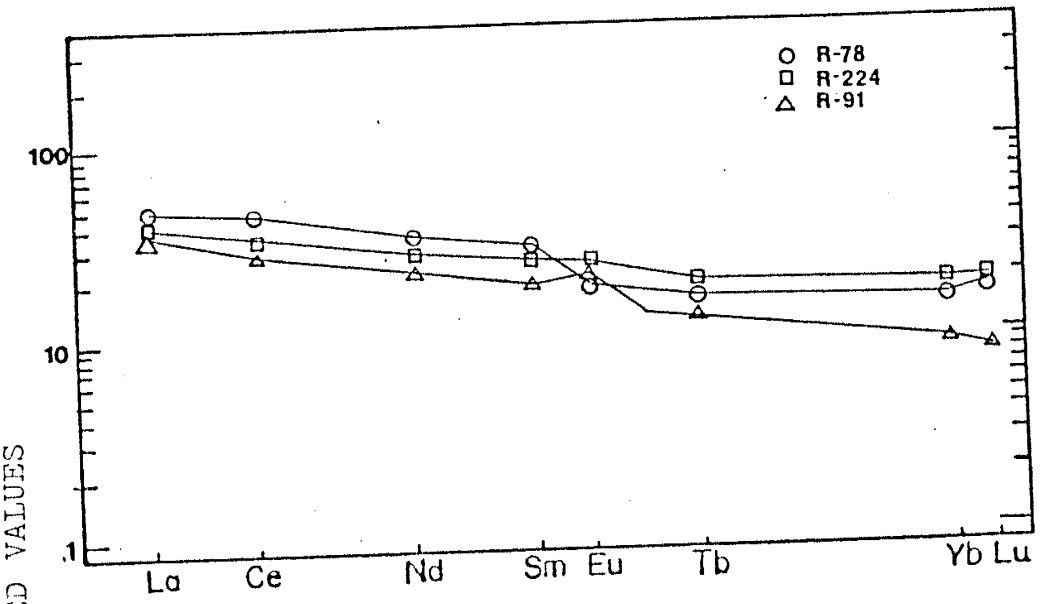

Figure 24.
REE Pattern for the
Wheeler Peak Amphibolites

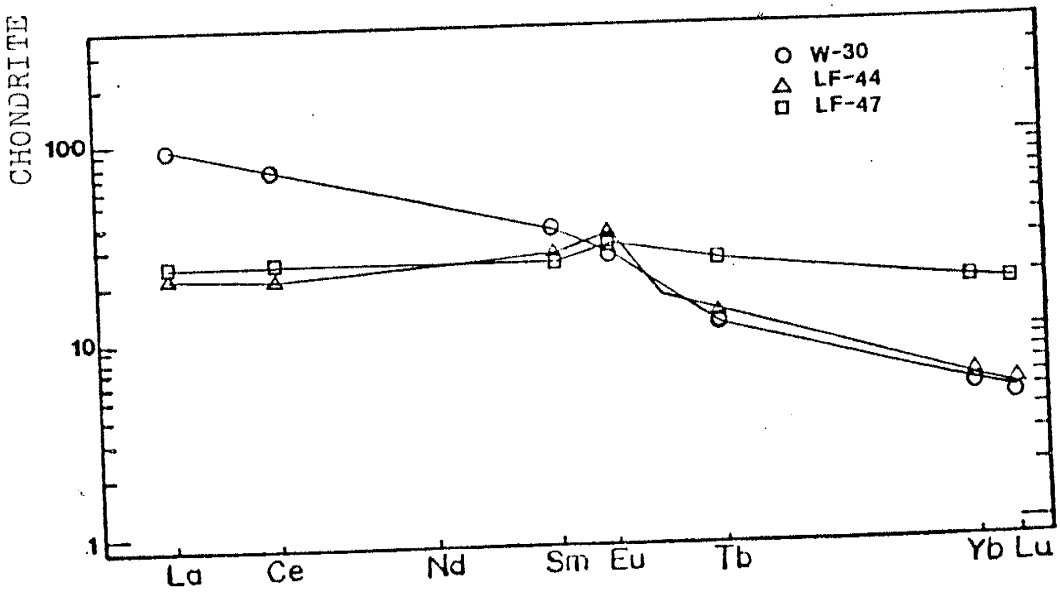

Figure 25.
REE Pattern for the
Hornblendites

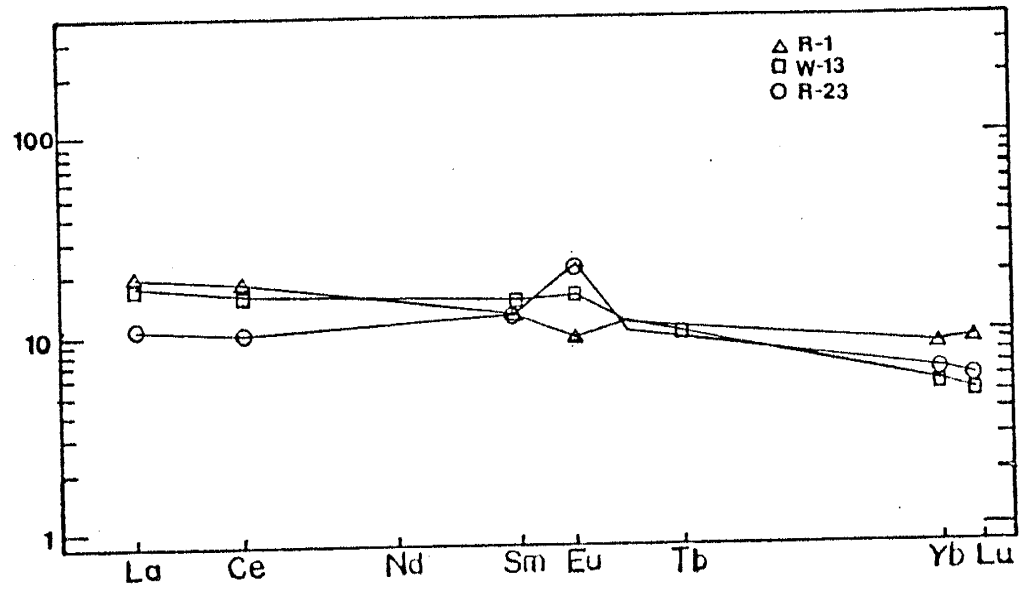

Figure 26.
REE Pattern for the
Granites

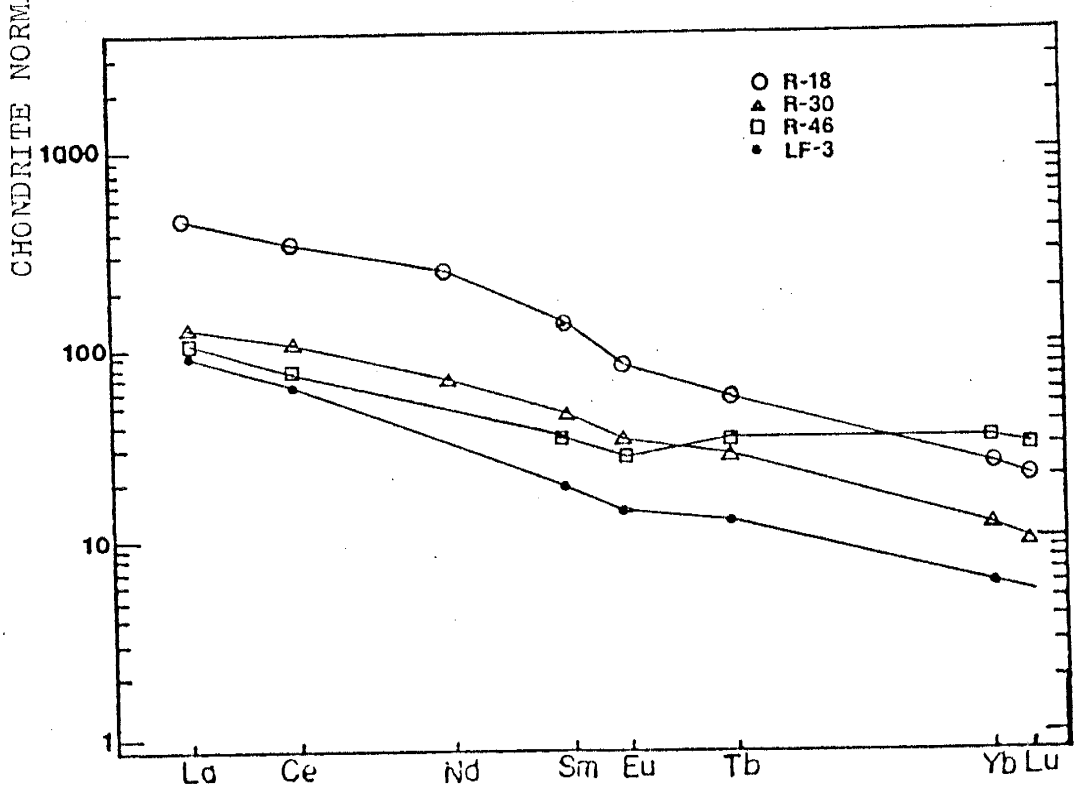

Figure 27.
REE Pattern for the
Type 1 Tonalites

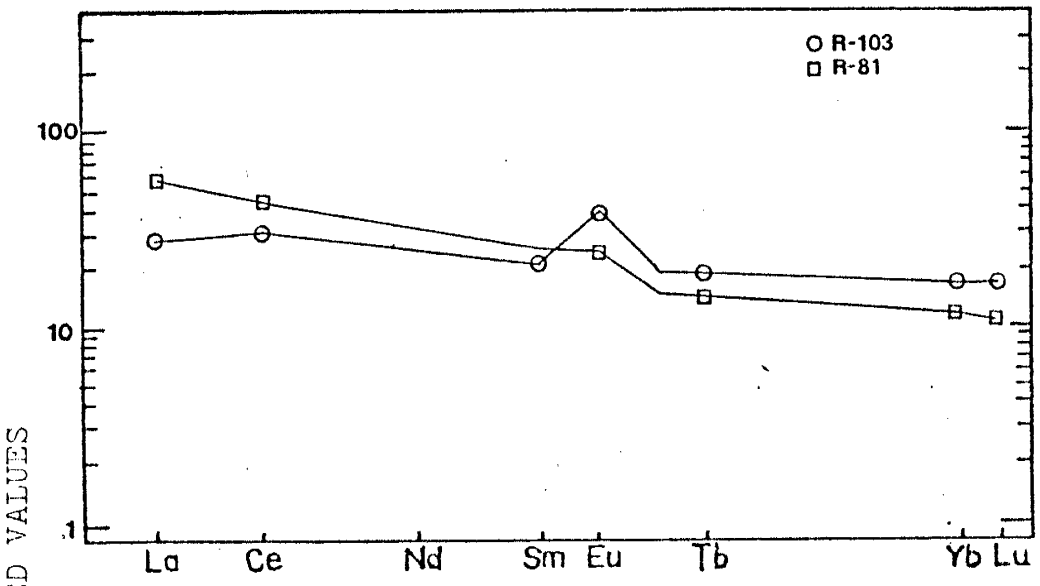

Figure 28.
REE Pattern for the
Type 2 Tonalites

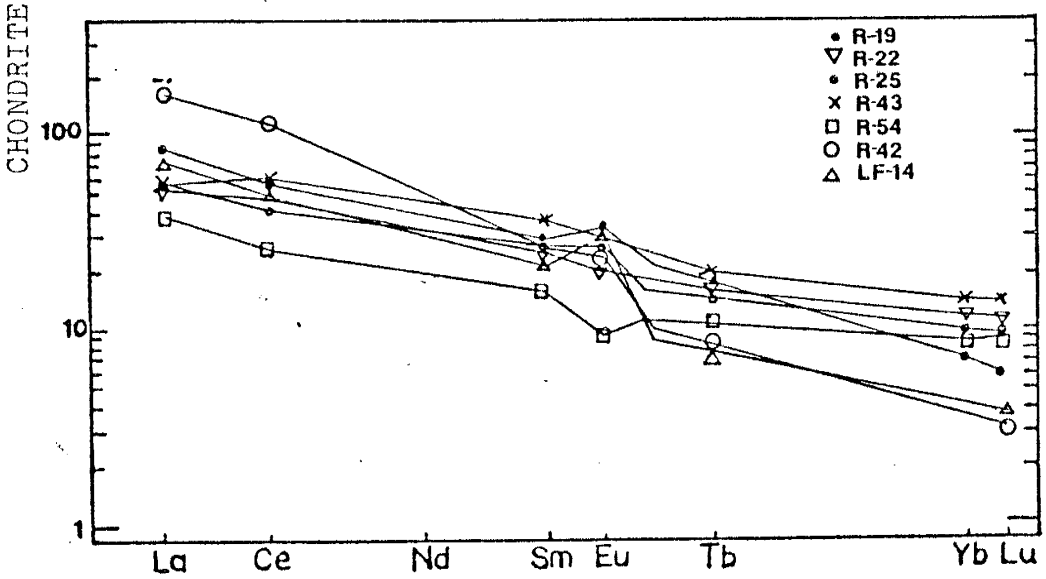

TECTONIC SETTING

A tentative comparison with Phanerozoic-type tectonic environment can be made, bearing in mind that the style of tectonics in the Proterozoic may have been somewhat different. The bimodal volcanics and volcaniclastic sediments of the Gold Hill section, in conjunction with numerous diabase dikes and sills, are indicative of an extensional environment (Martin and Piwinskii, 1972).

This extensional environment was at least partially covered by shallow seas as evidenced by the presence of ironstone. The sediments in the Taos Range (quartzites, arkoses and shales) also suggest a marine to fluvial environment. In the Rinconada Formation of the Picuris Mountains, Barrett and Kirschner (1979) have recognized fluvial, tidal flat, and shallow marine facies of quartzite and shale based on paleocurrent data. These authors, and others working in the Truchas Peak area (Grambling, 1979), recognize deepening basins to the south. Robertson and Moench (1979) have speculated that the volcanic and sedimentary rocks of the Pecos greenstone belt accumulated in a marine fault-bounded basin, either within or adjacent to a rifted continent. A continental rift system, aulacogen, or back arc basin environment can explain the bimodal volcanics, diabase dikes, and sediments found in the supracrustal successions.

No basement to the Proterozoic supracrustal rocks has been found in northern New Mexico and southern Colorado. Existing Sr isotope data suggest that if the supracrustal volcanics were deposited on pre-existing sialic basement, such basement must be less than or equal to 200 m.y. older than the volcanism (Condie and Budding, 1979). Perhaps this suggests a back-arc basin developed on oceanic crust which has since been subducted. However, If the supracrustal successions were deposited on typical oceanic crust, one would expect the presence of ophiolites, although none have been reported. On the other hand, no ophiolites are known to occur prior to 1,000 m.y. (Baer, 1977). This problem has yet to be resolved.

Following this proposed extensional environment, the supracrustal rocks underwent a strong compressional deformation accompanied by syntectonic plutonism. In the Taos Range, these plutons (type 2 tonalites) are of intermediate composition and show calc-alkaline trends. This is consistent with orogenic belts of the Phanerozoic (Martin and Piwinskii, 1972). Nowhere in the Proterozoic of northern New Mexico are volcanic rocks of intermediate composition found. This suggests that these plutons never reached the surface.

Two mechanisms can be used to explain the early tensional and later compressional environments in terms of recent tectonic regimes. The first mechanism is a back arc

basin which evolves into an island arc system. The second is a continental rift system which is later compressed due to lithospheric pressure. The first mechanism can explain the bimodal volcanics, the shallow marine environment, the syntectonic plutonism, and possibly the absence of previous oceanic crust (it may have been subducted). It cannot explain the lack of intermediate volcanics or the presence of mature clastic sediments (quartzites). The second mechanism, the continental rift model, can explain the bimodal volcanics, the mature clastic sediments, and possibly, the shallow marine environment and syntectonic plutonism. It fails to explain the absence of previous crust, which is necessary to rift in the first place, and what brought about the compression to close it up afterward. It is not known at this time what role, if any, the late syntectonic to post-tectonic granites played in either scheme.

In summary, it is suggested that the supracrustal and syntectonic plutonic rocks of the Taos Range can possibly be explained by comparisons with Phanerozoic plate tectonics. The supracrustal rocks were apparently deposted in an extensional environment, either a back arc basin or a continental rift, which later evolved into a compressional (orogenic) environment, either an island arc system or a compressed continental rift.

SUMMARY OF THE GEOLOGIC HISTORY OF THE PROTEROZOIC IN THE TAOS RANGE

(1) Eruption and deposition of basaltic? (mafic schists) and rhyolitic (felsic volcanics) volcaniclastic and volcanic rocks in the Gold Hill section, and mafic sediments of volcanic provenance in the Wheeler Peak sections. This appears to have taken place in a shallow marine environment and the chemical precipitation of ironstones occurred during periods of quiescence between volcanic eruptions. There is some local evidence to indicate that the rocks in the Gold Hill section are younger toward the north. However, folding and metamorphism have largely obscured age relationships in the volcanic rocks, and therefore, these rocks must be considered more or less contemporaneous in this study.

(2) Deposition of quartzites, arkoses and shales, which are also found in the Taos Range but not encountered in the measured sections of this study. The exact relationship between the volcanic rocks and these sediments is not known in the Taos Range. However, other studies suggest a simultaneous or slightly later deposition (Robertson and Moench, 1979; Grambling, 1979).

(3) Intrusion of one and possibly two sets of diabase dikes and sills in the Gold Hill section (intrusive amphibolite of the Gold Hill section).

(4) Intrusion of pyroxenite ultrabasic (hornblendite) dikes throughout the Taos Range. These dikes are most

abundant in the Wheeler Peak sections.

(5) Intrusion of a tonalite pluton into and west of the Gold Hill section. Geochemical data suggest that this tonalite may be a hypabyssal equivalent of the felsic volcanic rocks. However, this would require that the diabase and pyroxenite intruded the system early, since the tonalite is found to cut both of these other rock types.

(6) Onset of a metamorphic/deformational event which produced a strong NE-SW foliation and local isoclinal folding. Evidence for polyphase deformation, although present, is scarce in the measured sections. However, previous studies of the Taos Range and nearby Picuris Range indicate at least two, and possibly four folding events have occurred (Condie, 1980; Nielsen and Scott, 1979). Related regional metamorphism was to the lower amphibolite facies.

(7) Intrusion of syntectonic type 2 tonalite (diorite) plutons throughout the Taos Range, and intrusion of coarse amphibolite in the Wheeler Peak sections.

(8) Intrusion of late syntectonic to post tectonic granite plutons and dikes. These granites have not been dated at this time. However, they can possibly be assigned a similar age as other Precambrian granites in northern New Mexico. These occur at 1,673 m.y. (Embudo Granite, Fullagar and Shiver, 1973) and 1,650 m.y. (Tres Piedras Granite, Maxon, 1976). Long (1974) however, criticizes the single age by Fullagar and Shiver for the Embudo Granite and

suggests a spread in ages from more than 1,600 m.y. to possibly 1,400 m.y. for the Embudo Granite suite. This problem is still unresolved. Granite samples in this study show metamorphic textures. This fact suggests that regional compressive forces persisted during at least part of the intrusive event.

(9) Intrusion of quartz veins, pegmatite, and metasomatism dated at 1,425 m.y. (Gresens, 1975).

(10) A thermal event +/- local deformation dated at 1,350 m.y. (Gresens, 1975). This event probably represents minor heating of older metamorphic rocks (Long, 1972).

(11) A late deformational and thermal event dated at 1250 m.y. (Gresens, 1975).

BIBLIOGRAPHY

ıderson, C.A., and Silver, L.T., 1976, Yavapi Series: a greenstone belt: Arizona Geol. Society Digest, v.10, p. 13-26.

ıer, A.J., 1977, Speculations on the evolution of the lithosphere: Precambrian Research, v. 5, no. 3, p. 247-260.

ırker, F., 1969, Precambrian geology of the Needles Mountains southwestern Colorado: U.S. Geol. Survey Prof. Paper 644-A, 32p.

arker, F., Arth, J.G., Peterman, Z.E., and Friedman, I., 1976, The 1.7-1.8 b.y. tonalite-trondhjemites of southwestern Colorado and northern New Mexico: geochemistry and depth of genesis: Geol. Soc. America Bull., v. 87, p. 189-198.

ıarker, F., 1979, Trondhjemite: definition, environment and hypothesis of origin: in F. Barker (ed.) Trondhjemites, Dacites and related rocks, Elsevier, New York, p. 1-12.

ıarrett, M.E., and Kirschner, C.E., 1979, Depositional systems in the Rinconada Formation (Precambrian), Taos County, New Mexico: New Mexico Geol. Soc. Guidebook 30, p. 121-126.

ıoardman, S.J., 1976, Geology of the Precambrian metamorphic rocks of the Salida area, Chaffee County, Colorado: The Mountain Geologist, v. 13, no. 3, p. 89-100.

Braddock, W.A., 1966, Precambrian geology of the east flank of the Front Range near Fort Collins, Colorado (abstract): Geol. Soc. America Spec. Paper 87, p. 277.

Brown, E.H., Babcock, R.S., Clark, M.D., and Livingston, D.E., 1979, Geology of the older Precambrian rocks of the Grand Canyon Part I: petrology and structure of the Vishnu Complex: Precambrian Research, v. 8, p. 219-241.

Callender, J.F, Robertson, J.M., and Brookins, D.G., 1976, Summary of Precambrian geology and geochronology of northeastern New Mexico: New Mexico Geol. Soc. Guidebook 27, p. 129-135.

Carmichael, I.S., Turner, F.J., and Verhoogen, J., 1974, Igneous Petrology: Mcgraw-Hill, New York, 739p.

ırch, B.N., 1975, Quantitative classification and chemical comparison of common volcanic rocks: Geol. Soc. America Bull., v. 86, p. 257-263.

ark, K.F., and Read, C.B., 1972, Geology and ore deposits of the Eagle Nest Area, New Mexico: New Mexico Bureau of Mines and Mineral Resources, Bull. 94, 152p.

ark, M.D., 1979, Geology of the older Precambrian rocks of the Grand Canyon, Part III: petrology of mafic schists and amphibolites: Precambrian Research, v. 8, p. 277-302.

ndie, K.C., Viljoen, M.J., and Kable, E.J.D., 1977, Effects of alteration on element distributions in Archean tholeiites from the Barberton greenstone belt, South Africa: Contrib. Mineral. Petrol., v. 64, p. 75-89.

ndie, K.C., 1979, Precambrian rocks of the Taos Range and vicinity, northern New Mexico: New Mexico Geol. Soc. Guidebook 30, p. 107-111.

ndie, K.C., and Budding, A.J., 1979, Geology and geochemistry of Precambrian rocks, central and south-central New Mexico: New Mexico Bureau of Mines and Mineral Resources, Memoir 35, 58p.

ndie, K.C., 1980, Precambrian rocks of the Red River-Wheeler Peak area in northern New Mexico: New Mexico Bureau of Mines and Mineral Resources, Geologic Map 50.

ondie, K.C., and Nuter, J.A., 1981, Geochemistry of the Dubois greenstone succession: an early Proterozoic bimodal volcanic association in west-central Colorado: Precambrian Research, v. 15, p. 131-155.

ondie, K.C., 1981, A back-arc basin model for Proterozoic continental accretion in the Southwestern United States: Geology, in press.

wart, A., 1979, A review of the minerology and chemistry of Tertiary to recent dacitic, latitic, rhyolitic and related salic volcanic rocks, In: F. Barker (ed.), Trondhjemites, Dacites and Related Rocks, Elsevier, Amsterdam, p. 13-121.

ullagar, P.D., and Shiver, W.S., 1973, Geochronology and petrochemistry of the Embudo Granite, New Mexico: Geol. Soc. America Bull., v. 84, p. 2705-2712.

Gibson, T.R., 1981, Precambrian geology of the Burned Mountain-Hopewell Lake area, Rio Arriba County, New Mexico: M.S. Thesis, New Mexico Institute of Mining and Technology, 105p.

Gordon, G.E., Randle, K., Goles, G.G., Corliss, J.B., Beeson, M.H., and Oxley, S.S., 1968, Instrumental activation analysis of standard rocks with high resolution gamma-ray detectors: Geochim. Cosmochim. Acta, v. 32, p. 369-396.

Grambling, J.A., 1979, Precambrian geology of the Truchas Peaks Region, north-central New Mexico, and regional implications: New Mexico Geol. Soc. Guidebook 30, p. 135-143.

Gresens, R.L., 1975, Geochronology of Precambrian metamorphic rocks, north-central New Mexico: Geol. Soc. America Bull., v. 86, p. 1444-1448.

Gross, G.A., 1965, Geology of iron deposits of Canada: Canada Geol. Survey Econ. Geology Rept. 22, 181p.

Gruner, J.W., 1920, Geologic reconnaissance of the southern part of the Taos Range, New Mexico: Journal of Geology, v. 28, p. 731-742.

Hildreth, W., 1979, The Bishop Tuff: evidence for the origin of compositional zonation in silicic magma chambers: Geol. Soc. America Spec. Paper 180, p. 43-75.

Holdaway, M.J., 1978, Significance of chloritoid-bearing and staurolite-bearing rocks in the Picuris Range, New Mexico: Geol. Soc. America Bull., v. 89, p. 1404-1414.

Hynes, A., 1980, Carbonization and mobility of Ti, Y and Zr in Ascot Formation metabasalts, Southeast Quebec: Contrib. Mineral. Petrol., v. 75, p. 79-88.

Irvine, T.N., and Baragar, W.R.A., 1971, A guide to the classification of the common volcanic rocks: Canadian Jour. Earth Sci., v. 8, p. 523-549.

Jensen, L.S., 1976, A new cation plot for classifying subalkaline volcanic rocks: Ontario Div. Mines, MP 66, 22p.

Kent, S.C., 1980, Precambrian geology of the Tusas Mountain Area, Rio Arriba County, New Mexico: M.S. Thesis, New Mexico Institute of Mining and Technology, 151p.

Kimberly, M.M., 1978, Paleoenvironmental classification of

iron formations: Econ. Geol., v. 73, p. 215-229.

Leake, B.E., 1963, Origin of amphibolites from northwest Adirondaks, New York: Geol. Soc. America Bull., v. 74, p. 1193-1202.

Leake, B.E., 1964, The chemical distinction between ortho- and para-amphibolites: Jour. Petrology, v. 5, no. 2, p. 238-254.

Long, L.E., 1972, Rb-Sr chronology of Precambrian schist and pegmatite, La Madera quadrangle, northern New Mexico: Geol. Soc. America Bull., v. 83, p. 3425-3432.

Long, P.E., 1974, Contrasting types of Precambrian granitic rocks in the Dixon-Penasco area, northern New Mexico: New Mexico Geol. Soc. Guidebook 25, p. 101-108.

Martin, R.F., and Piwinskii, A.J., 1972, Magmatism and tectonic setting: Jour. Geoph. Research, V. 77, no. 26, p. 4966-4975.

Maxon, J.R., 1976, Age and implications of the Tres Piedras Granite, north-central New Mexico: Geol. Soc. America Abst. with Programs, v. 8, no. 5, p. 608.

McKinlay, P.F., 1956, Geology of the Costilla and Latir quadrangles, Taos County, New Mexico: New Mexico Bureau of Mines and Mineral Resources, Bull. 42, 32p.

McKinlay, P.F., 1957, Geology of the Questa quadrangle, Taos County, New Mexico: New Mexico Bureau of Mines and Mineral Resources, Bull. 53, 23p.

Miyashiro, A., 1973, Metamorphism and Metamorphic Belts: Wiley and Sons, New York, 492p.

Nielsen, K.C., and Scott, T.E., 1979, Precambrian deformational history of the Picuris Mountains, New Mexico: New Mexico Geol. Soc. Guidebook 30, p. 113-120.

Nockolds, S.R., 1954, Average chemical compositions of some igneous rocks: Geol. Soc. America Bull., v. 65, p. 1007-1032.

Nockolds, S.R., Knox, R.W.O'B., and Chinner, G.A., 1978, Petrology For Students: Cambridge Press, London, 435p.

Norrish, K., and Hutton, J.T., 1969, An accurate X-ray spectrographic method for the analtsis of a wide range of geological samples: Geochim. Cosmochim. Acta, v. 33, p. 431-453.

Pearce, J.A., 1975, Basalt geochemistry used to investigate past tectonic environments on Cyprus: Tectonophysics, v. 25, p. 41-67.

Robertson, J.M., and Moench, R.H., 1979, The Pecos greenstone belt: a Proterozoic volcano-sedimentary sequence in the southern Sangrè de Cristo Mountains, New Mexico: New Mexico Geol. Soc. Guidebook 30, p. 165-173.

Robertson, J.M., 1981, Bimodal volcanism in the early Proterozoic Pecos greenstone belt, southern Sange de Cristo Mountains, New Mexico: Geol. Soc. America Abst. with Programs, v. 13, no.2, p. 81, 103.

Reed, J.C., Robertson, J.M., and Lipman, P.W., 1981, Preliminary geologic map of the Wheeler Peak-Hondo Canyon area, Taos County, New Mexico: U.S.G.S Misc. Investigations Map no. 81-1077.

Schilling, J.H., 1960, Mineral resources of Taos County, New Mexico: New Mexico Bureau of Mines and Mineral Resources, Bull. 71, 124p.

Shaw, D.M., and Kudo, A.M., 1965, A test of the discriminant function in the amphibolite problem: Mineralogical Mag., v. 34, no. 268, p. 423-435.

Spry, A., 1969, Metamorphic Textures: Pergamon Press, Oxford, 350p.

Streckeisen, A.L., 1973, Plutonic rocks: classification and nomenclature recommended by the I.U.G.S. subcommission on the systematics of igneous rocks: Geotimes, v. 118, no. 10, p. 26-30.

Taylor, S.R., and Hallberg, J.A., 1977, Rare-earh elements in the Marda calc-alkaline suite: an Archean geochemical analogue of Andean-type volcanism: Geochim. Cosmochim. Acta, v. 41, p. 1125-1129.

Travis, R.B., 1955, Classification of rocks: Quaterly of the Colorado School of Mines, v. 50, no. 1, 98p.

Turner, F.J., 1981, Metamorphic Petrology: McGraw-Hill, New York, 524p.

Winchester, J.A., and Floyd, P.A., 1977, Geochemical discrimination of different magma series and their differentiation products using immobile elements: Chemical Geology, v. 20, p. 325-343.

APPENDIX A

PHOTOGRAPHIC PLATES

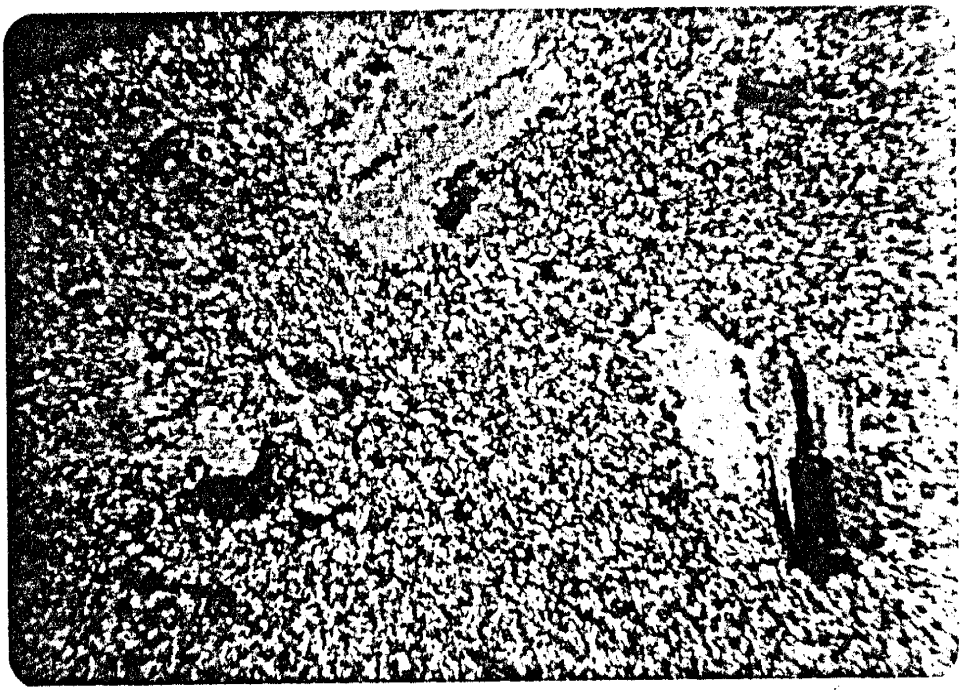

Plate 1. Plagioclase phenocrysts in the Felsic Volcanics. Note the relict zoning in the broken phenocryst in the lower left of the photograph. X-polars

1mm

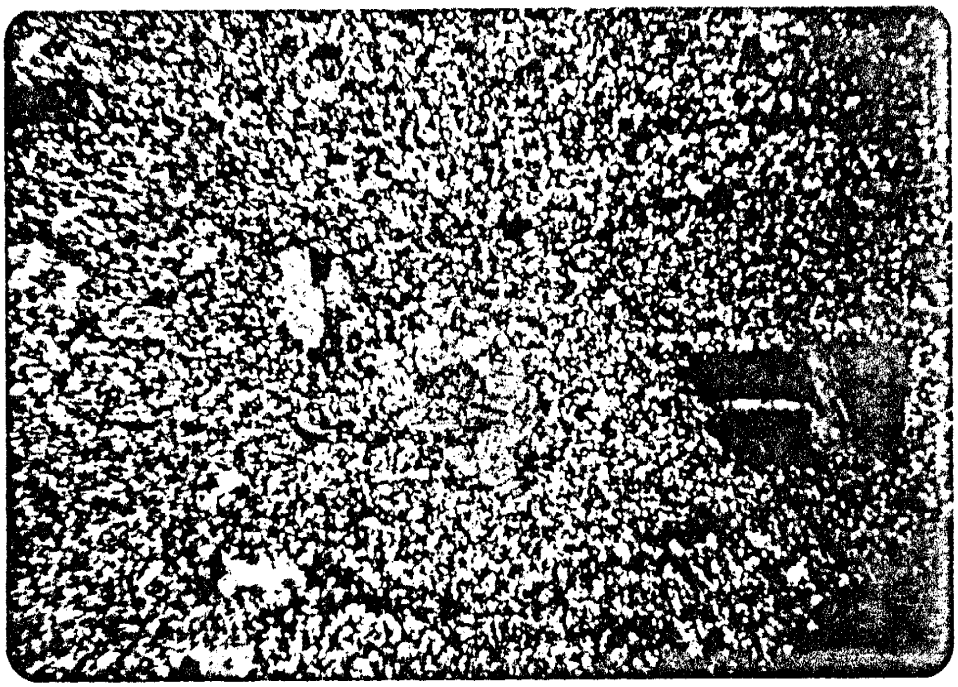

Plate 2. Plagioclase phenocrysts in the Felsic Volcanics. X-polars

1mm

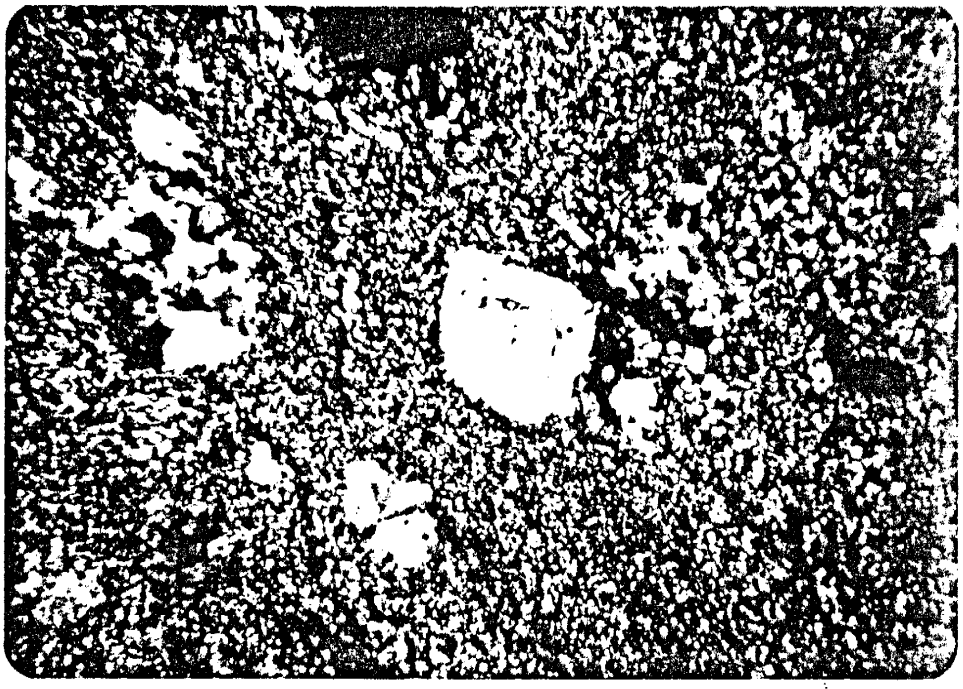

Plate 3. Subhedral and optically continuous quartz Phenocryst in the Felsic Volcanics. X-polars.

1 mm

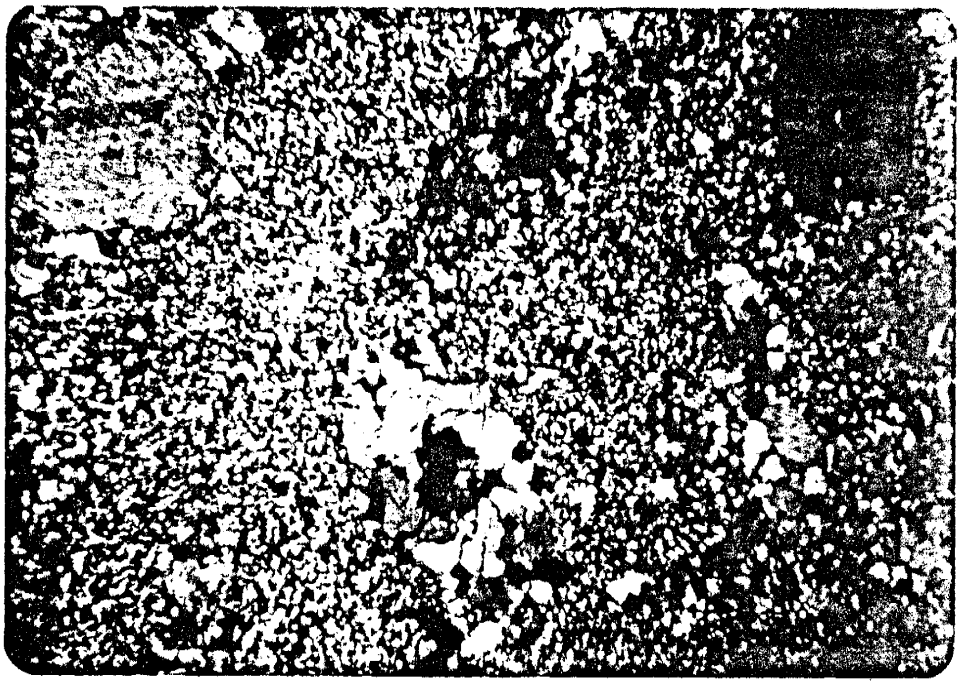

Plate 4. Plagioclase phenocrysts (Top left and right) and a quartz-muscovite grain (Center) in the Felsic Volcanics. X-polars.

1 mm

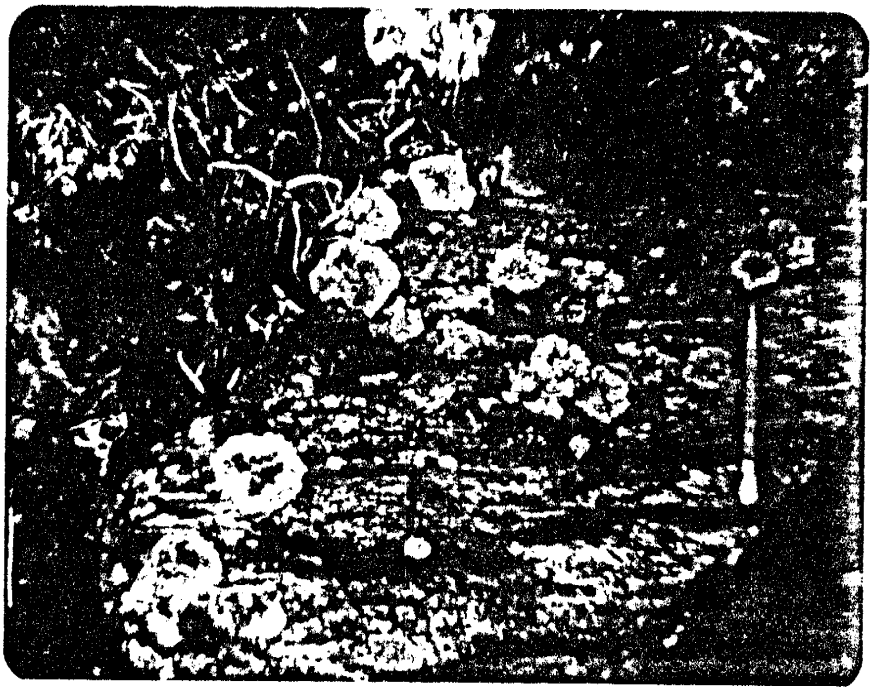

Plate 5. Biotite and muscovite-rich lenses in a phenocryst-rich Felsic Volcanic sample. Pencil length = 10cm.

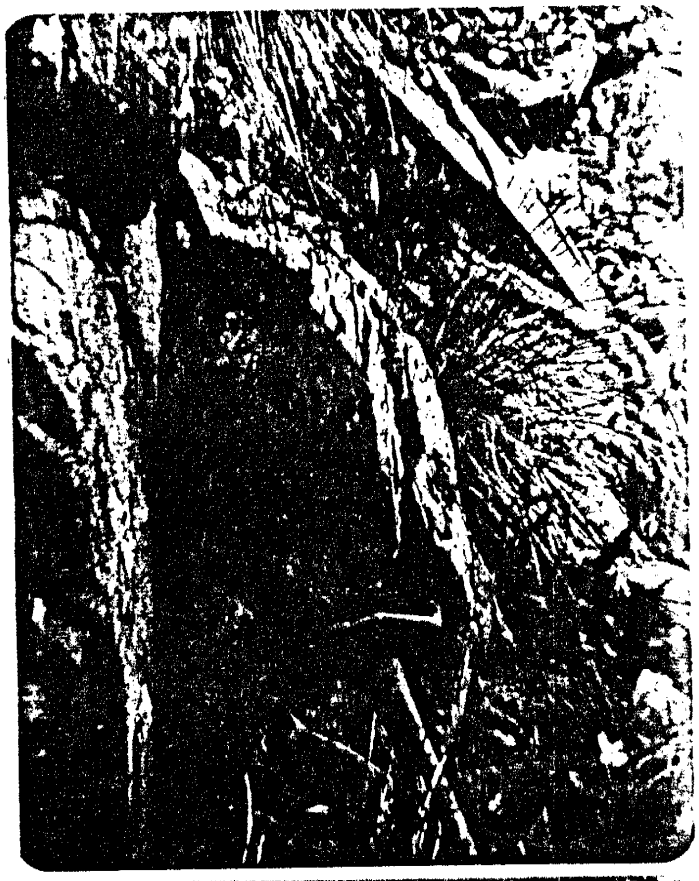

Plate 6.
Hammer Head = 12cm

Dark mafic fragments in the fine grained Mafic Schist.

Plate 7.
Pencil = 10cm

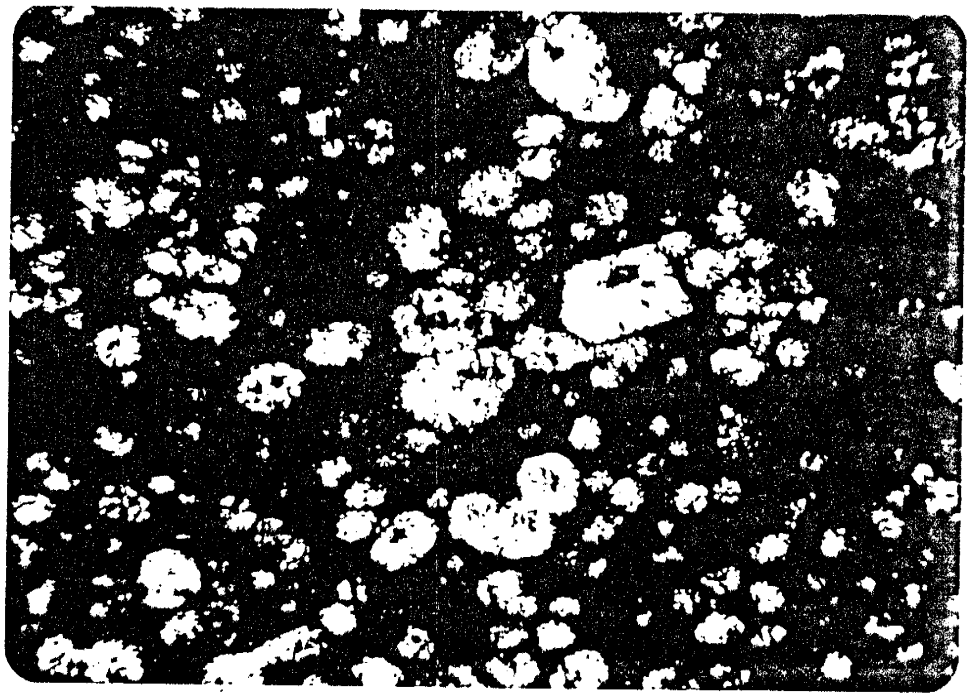

Plate 8. Photomicrograph of a mafic fragment from the Mafic Schist of the Gold Hill Section. Note the round to slightly elongate relict vesicles and the euhedral plagioclase phenocryst. X-polars.

1mm

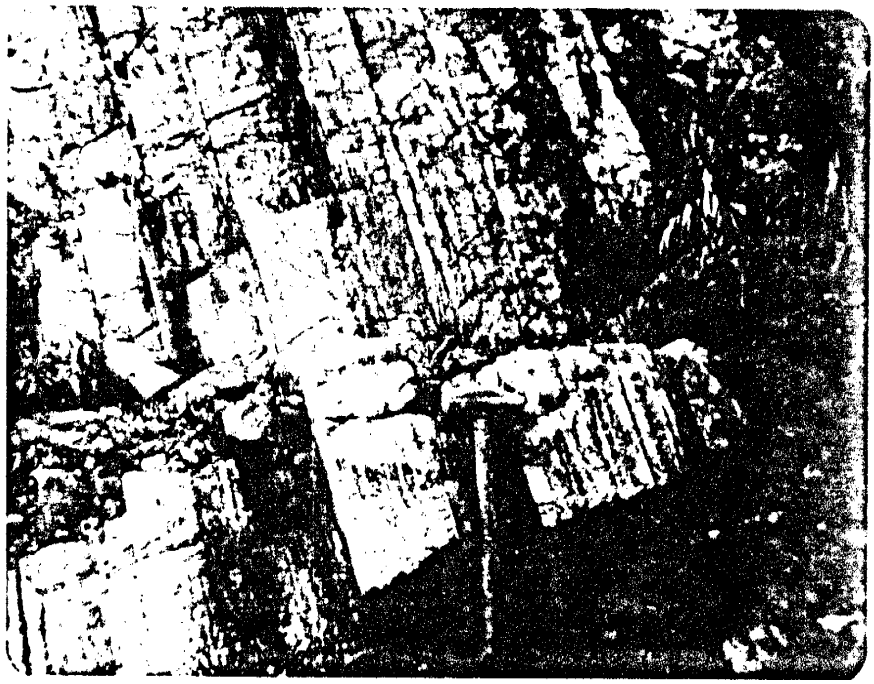

Plate 9. Layered Gneiss of the Gold Hill Section.
Hammer Head =12cm.

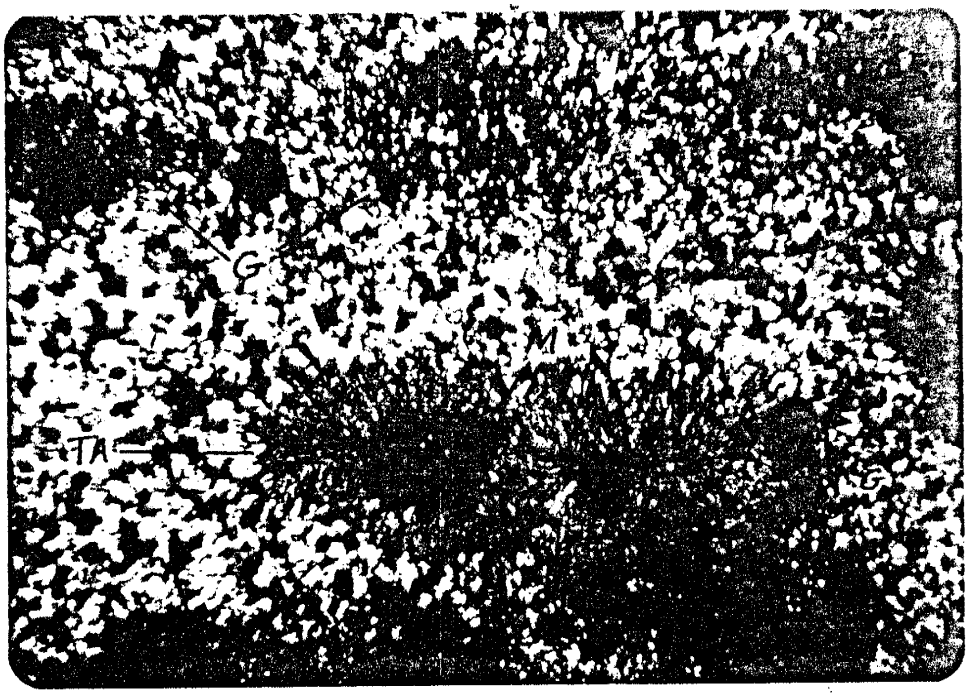

Plate 10. Photomicrograph of a garnet and magnetite-bearing unit in the Layered Gneiss. Garnet = G; Magnetite = M; Tremolite-Actinolite = TA. X-polars.

1 mm

Plate 11. Quartz layers in ironstone. X-polars.

1 mm

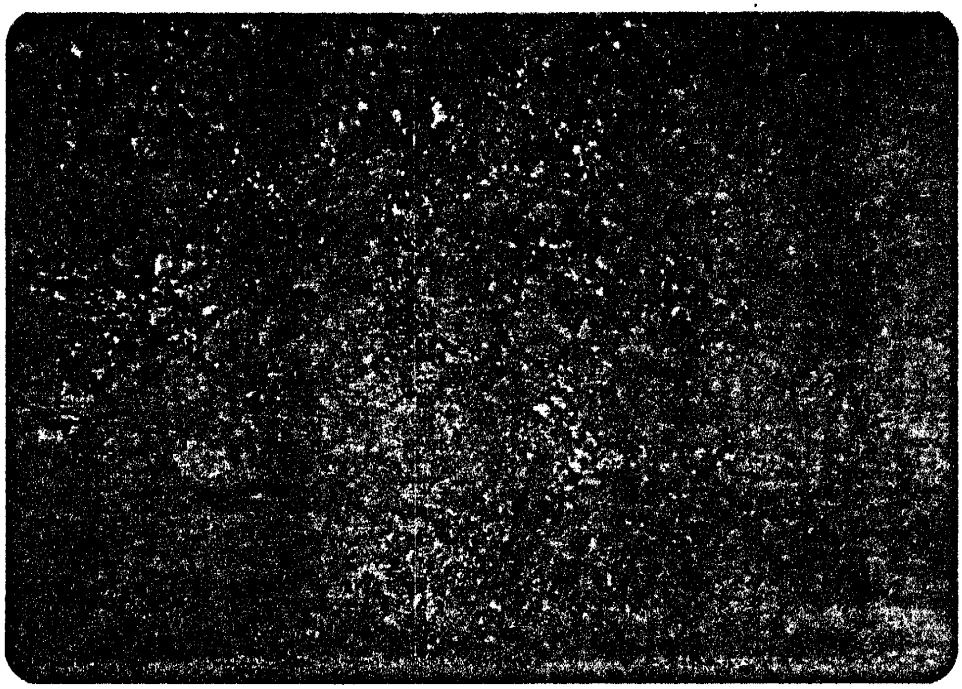

Plate 12. Amphibolite of the Gold Hill Section. Dark green hornblende surrounds hornblende pseudomorphs after pyroxene. Uncrossed polars.

1 mm

Plate 13 and 14 (Below). Coarse Amphibolite of the Wheeler Peak sections. Dark mineral is cumulus hornblende; light mineral is intercumulus plagioclase. Uncrossed polars.

1mm

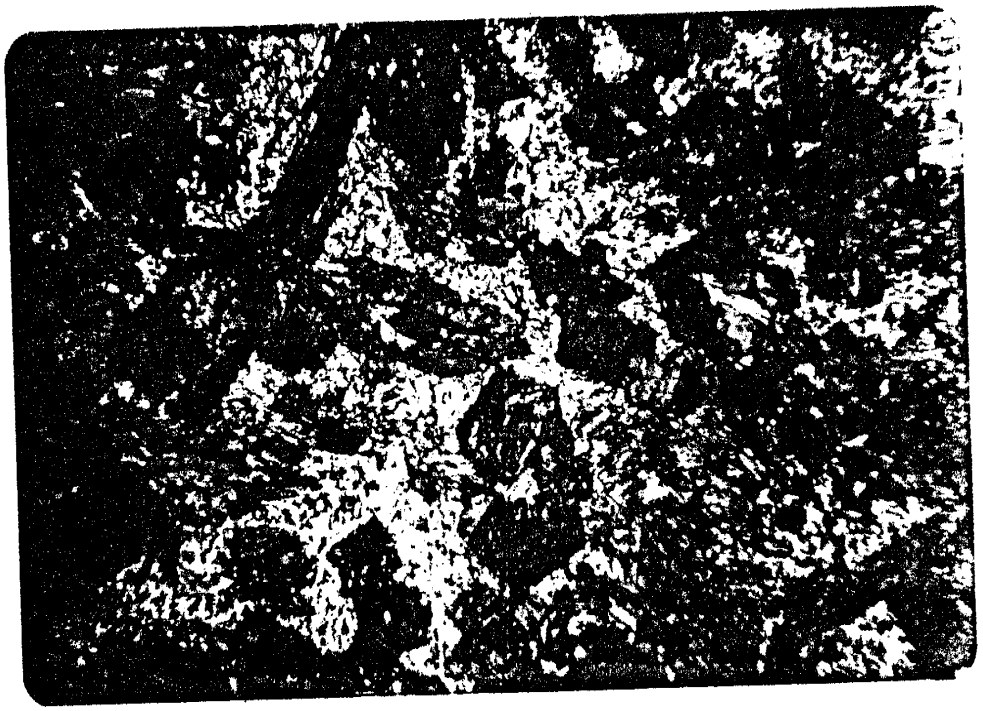

Plate 15A.

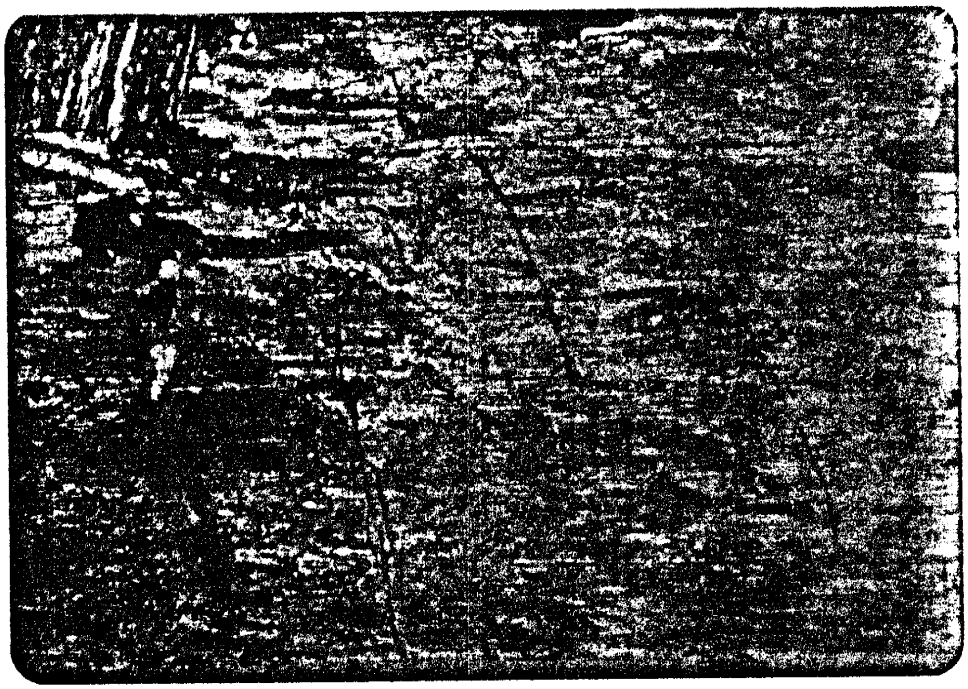

Plate 15B. A single hornblende crystal in hornblendite. Fine streaky hematite may represent relict schiller structure of original pyroxene.

0.1 mm

Plate 15A - Uncrossed polars
Plate 15B - X-polars

Plate 15A.

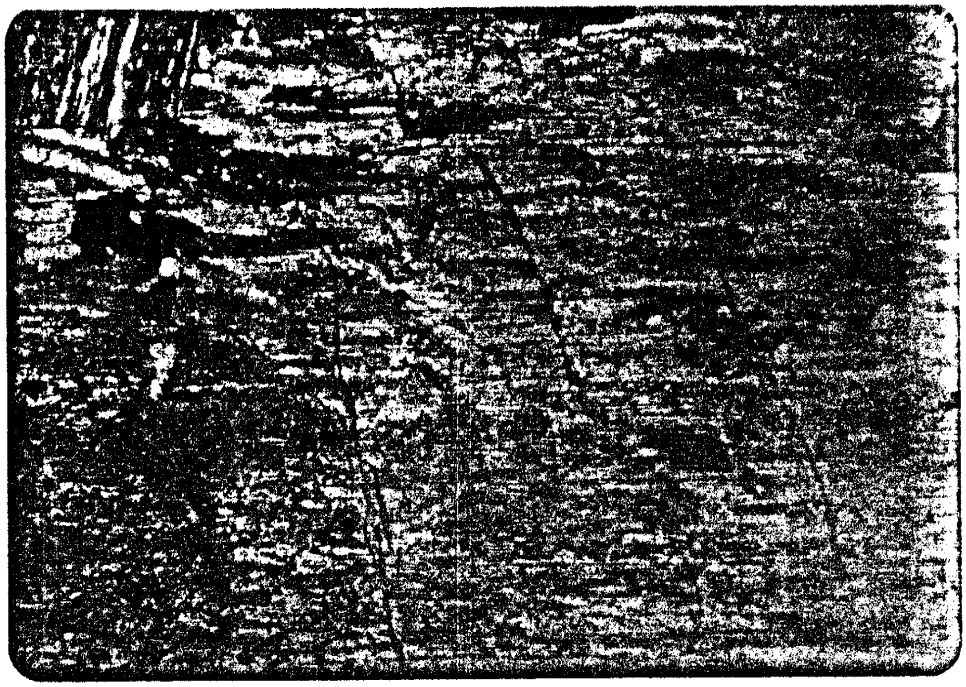

Plate 15B. A single hornblende crystal in hornblendite. Fine streaky hematite may represent relict schiller structure of original pyroxene.

0.1 mm

Plate 15A - Uncrossed polars
Plate 15B - X-polars

Plate 16. Small breccia zone in Hornblende-Biotite Gneiss of the Lake Fork Peak Section. Hammer Head = 12cm.

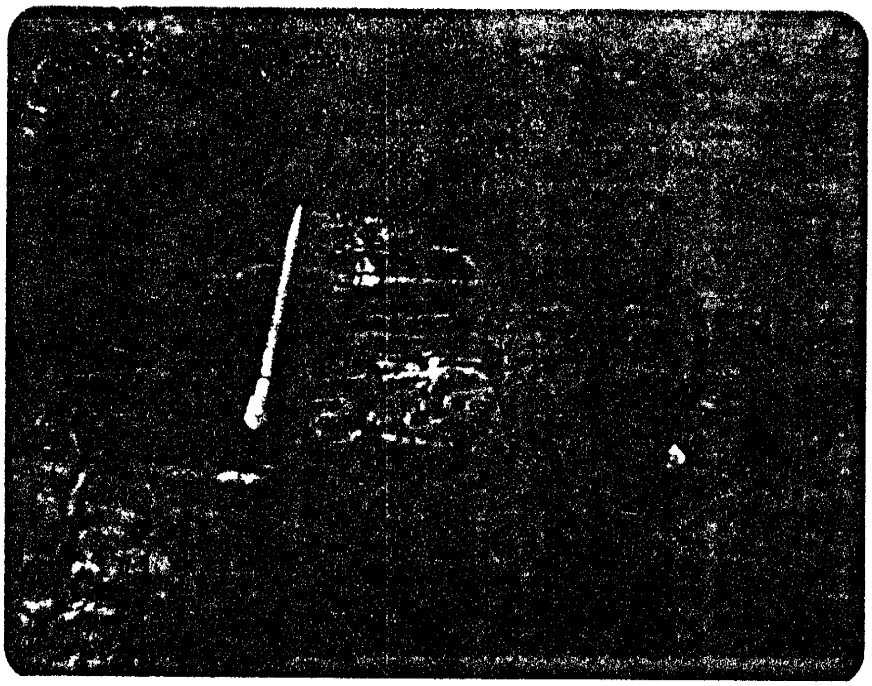

Plate 17. Intrabed folds in Layered Gneiss of the Gold Hill Section. Pencil = 10cm.

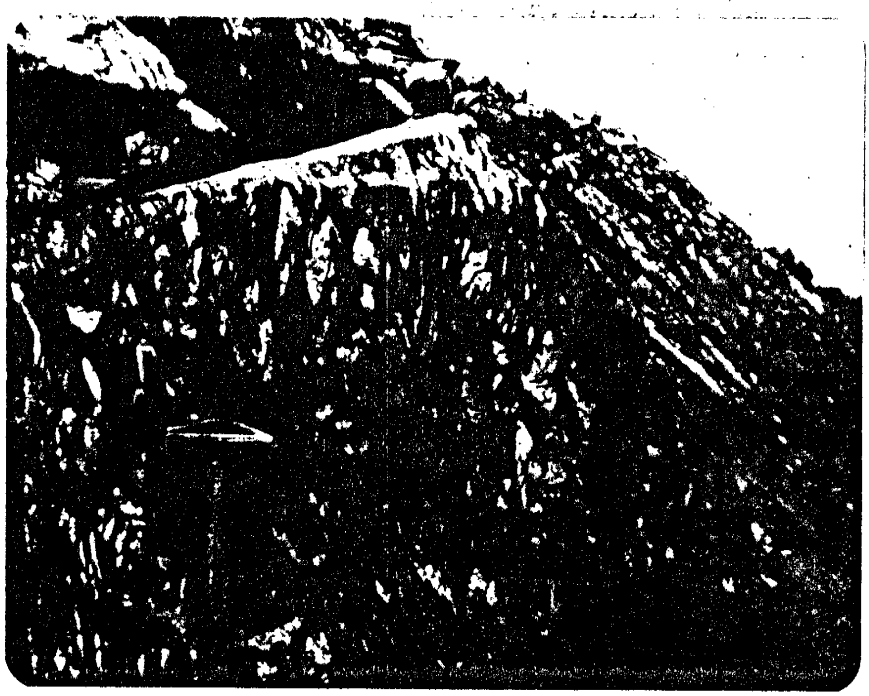

Plate 18. Sheared isoclinal fold noses in Hornblende-Biotite Gneiss of the Lake Fork Peak Section. Hammer Head = 12cm.

APPENDIX B

BRIEF PETROLOGIC DESCRIPTIONS OF THE ANALYZED SAMPLES

FELSIC VOLCANICS

R-59: Pale green, fine to medium grained, microporphyritic rock. Phenocrysts are composed of intergrown granoblastic quartz and muscovite (15-20% of rock; 1-4mm), optically continuous subhedral quartz (2-3%; 1-4mm), and highly sericitized, anhedral to subhedral microcline (5-7%; 2-4mm). Matrix minerals (~ 0.5mm in diameter) are mainly quartz and feldspar grains (Quartz + Plagioclase + K-feldspar ~ 60-65%), and subordinate biotite and sericite (3-5%). The texture of the matrix minerals is granoblastic. The biotite and sericite show parallel alignment, and some biotite is altered to chlorite.

R-105: Light brown to gray, fine to medium grained, microporphyritic rock. Phenocrysts composed of sericitized plagioclase (7-10%; 2-3mm), biotite and muscovite glomerophenocrysts (7-10%; 1-4mm), quartz (3-5%; 1-5mm), and highly sericitized microcline (3-5%; 2-3mm). Most phenocrysts are anhedral to subhedral, and the feldspars exhibit carlsbad, albite, and pericline twinning. Antiperthitic intergrowths are present in some feldspars. Matrix is composed of mostly quartz and feldspar (45-50%), aligned biotite (12-15%), and sericite (3-5%). Matrix minerals are all less than 0.5mm and the texture is granoblastic.

R-124: Pale green to dark gray, fine to medium grained, microporphyritic rock. Phenocrysts are composed of subhedral to euhedral plagioclase (20-25%; 2-5mm), and optically continuous round quartz (3-5%; 3-5mm). Plagioclase phenocrysts are slightly sericitized and show albite twinning. Broken crystals and relict occillatory zoning are sometimes preserved. Matrix material is composed of quartz and feldspar (60-63%), aligned biotite (3-5%), aligned sericite (1-2%), and minor microcline and hematite (less than or equal to 1%). Matrix minerals are between 0.25 and 0.5mm and granoblastic.

R-196: Light gray, fine to medium grained, microporphyritic rock in which black biotite and white feldspar gives a salt and pepper appearance. Phenocrysts are composed of carbonatized alkali feldspar (20-26%; 2-6mm), poikiloblastic chloritized biotite (10-15%; 2-3mm), and optically continuous anhedral quartz (3-4%; 2-3mm). Although alkali feldspar grain boundaries exhibit mortar texture, relict euhedral shape is observed in the staining for potassium. Some relict carlsbad twinning is poorly preserved. Matrix

is (0.1-0.5mm) composed of indistinguishable quartz and feldspar (25-30%), sericite (12-15%), and minor carbonate. The texture of the matrix minerals is granoblastic. This sample is cut by a small carbonate and biotite veinlet. Total carbonate in the rock, including the veinlet, matrix, and carbonatized alkali feldspar, is roughly 7-10%.

R-200: Pale green, fine to medium grained, microporphyritic rock with a distinct salt and pepper appearence due to well spaced biotite. Phenocrysts composed of untwinned, anhedral, and highly sericitized alkali feldspar (7-10%; 2-3mm), poikiloblastic anhedral biotite (10-15%; 1-3mm), and anhedral grains of granoblastic quartz (1-2%; 1-2mm). Matrix (0.5-1.0mm) is composed of quartz and feldspar (45-50%), aligned biotite (8-10%), aligned sericite (6-8%), and subhedral to euhedral epidote (3-5%). The texture of the matrix minerals is granoblastic. The epidote crystals are found as inclusions in the biotite and scattered through the matrix.

R-222: Pale green to gray, fine to medium grained, microporphyritic rock. Phenocrysts composed of alkali feldspar (15-18%; 1-5mm), and round to augen shaped, optically continuous quartz (1-2%; 1mm). Alkali feldspar shows relict carlsbad twinning, relict occillatory zoning, and locally perthitic intergrowths. Although grain boundaries exhibit mortar texture, subhedral to euhedral shapes are preserved in the staining for potassium. Matrix (0.1-0.5mm) composed of quartz and feldspar (45-50%), sericite (18-20%), and biotite (3-5%). The texture of the matrix minerals is granoblastic. Carbonization has affected roughly 5% of the rock.

R-245: Fine grained, pale green, aphanitic rock. This rock composed primarily of sericite (55-60%; less than or equal to 0.1mm), and poikiloblastic biotite (15-20%; <0.1-0,5mm). All minerals are anhedral and the micaceous minerals are strongly aligned. All minerals have a fresh appearence and are believed to be completely recrystallized.

MAFIC SCHISTS

LC-1: Light to medium dark green, fine grained , aphanitic rock. Strong foliation imparted by the parallel alignment of biotite. Major minerals are biotite (25-30%; 0.5-1.0mm), secondary carbonate (18-20%; 0.2-2.0mm), fresh albite (10-15%; 0.1-2.0mm), and a fine grained (less than or equal to 0.1mm), granoblastic quartz and feldspar matrix (25-30%). All minerals are anhedral and none exceed 2mm in maximum dimension. The centers of some carbonitized areas contain secondary untwinned feldspar. This sample is extremely carbonitized.

LC-2: Light to dark green, fine grained, mafic fragment bearing rock, with most of the fragments being blasto-amygdloidal. Minerals present are biotite (20-25%), secondary carbonate (20-25%), granoblastic quartz and feldspar (20-25%; less than or equal 0.1mm), fine grained bladed amphibole (12-15%), and epidote (7-10%). All minerals are less than 2mm and most are roughly 1mm or less. The fragments are composed of the fine grained bladed amphibole which is believed to be ferro-actinolite, a conclusion based mainly on extinction angles. Relict vesicles (0.5-3.0mm in diameter) are filled with epidote, carbonate, and granular quartz and feldspar. Some untwinned euhedral feldspar phenocrysts (2-3mm) are also found in the fragments.

LAYERED GNEISS

R-207: Dark gray, fine to coarse grained, porphyroblastic rock showing a fine layering. Porphyroblasts of red, poikilitic garnet are usually associated with the most mafic layers and are elongate along these layers. Garnets comprise 25-30% of the rock, and are 1-7mm long. Granoblastic, 0.5-1.0mm quartz grains comprise 50-55% of the rock and quartz grains are the inclusions in the garnets. The remaining minerals are poikiloblastic anhedral hornblende (5-7%; 0.5-1.5mm), chloritized biotite (3-5%; 0.5-1.0mm), and sericite (2-3%; 0.5-1.0mm).

HORNBLENDE-BIOTITE GNEISS

LF-1: Dark green to black, very fine grained, aphanitic and massive rock. Major minerals are poikiloblastic biotite (35-40%), quartz and plagioclase (30-35%), and subhedral secondary epidote (20-25%). All minerals are between 0.01 and 0.5mm and the texture is granoblastic.

W-25: Medium dark green to light gray, fine grained aphanitic rock which exhibits fine layering on weathered surfaces. Major minerals are blue-green to green needles of hornblende (30-35%), fresh plagioclase (35-40%; An 42-50), quartz (5-7%), biotite (7-10%), pyrite inclusions in hornblende (1-2%), epidote (3-5%), and sericite (1%). All minerals are anhedral and the rock texture is granoblastic. Grain sizes range from 0.1 to 0.5mm. Plagioclase is only locally sericitized and locally shows carlsbad and albite twinning.

LF-37: Dark gray to greenish black, fine grained, aphanitic rock. Major minerals are green to blue-green poikiloblastic hornblende (25-30%), albite twinned plagioclase (35-40%), aligned biotite (7-10%), quartz (12-15%), epidote (2-3%),

and pyrite (1-2%). All minerals are 0.05 to 0.5mm and anhedral, except for epidote and pyrite which are subhedral.

QUARTZ-SERICITE SCHIST

LF-5: Pale green, extremely fine grained, well foliated aphanitic rock. Minerals are quartz (50-55%; 0.01-0.05mm), sericite (20-25%; 0.01-0.05mm), epidote (15-18%; 0.05-0.5mm), and carbonate (1-2%; 0.05-0.1mm). Quartz is found as granoblastic trains and stringers with very fine, aligned sericite, carbonate, and epidote between them.

INTRUSIVE ROCKS

AMPHIBOLITE OF GOLD HILL

R-78: Dark greenish gray to black, fine grained, aphanitic rock. Major minerals are blue-green to green twinned hornblende (35-40%; 0.75-1.0mm), saussuritized plagioclase (30-35%; 0.5-1.0mm), quartz (12-15%; 0.5-0.75mm), and biotite (3-5%; 0.25-0.5%). Minor minerals are epidote, sphene, and hematite. All minerals are anhedral and the texture is granoblastic. Feldspars show carlsbad and albite twinning and often contain minor epidote.

R-91: Dark greenish gray to black, very fine grained, aphanitic rock. Major minerals are green to blue-green hornblende (45-50%), granular plagioclase (25-30%), granular quartz (5-8%), biotite (5-7%), and epidote (3-5%). Hematite occurs in trace amounts. Hornblende typically shows stronger pleochroism toward the outer edges and higher birefringence towards the center. Minerals are anhedral and are between 0.1 and 0.5mm. Tiny epidotes are associated with the granular plagioclase.

R-224: Dark gray to black, fine to medium grained, aphanitic rock. Major minerals are twinned green to blue-green hornblende (40-45%; 0.5-1.0mm), saussuritized plagioclase (35-38%; 0.1-1.0mm; An47-58), quartz (3-5%; 0.1-0.75mm), biotite (7-10%; 0.1-0.5mm), and hematite (1-2%). Trace amounts of epidote and sphene are also found. Hornblende is poikiloblastic and some of the plagioclase has poorly preserved carlsbad and albite twinning. The overall texture is granoblastic.

AMPHIBOLITES OF THE WHEELER PEAK SECTION

W-30: Dark green to black, medium grained rock. Major minerals are poikiloblastic hornblende (25-30%; 2-7mm), partially saussuritized plagioclase (30-35%; 0.5-6.0mm), biotite (20-25%; 1-3mm), quartz (2-5%; 0.1-0.5mm), and euhedral epidote (2-5%; 0.1-1.0mm). Trace amounts of

sphene, chalcopyrite, and apatite are also found. Inclusions in the green to blue-green hornblende are biotite, apatite, epidote, and sphene. Plagioclase shows poorly preserved and deformed albite and carldbad twinning, and perthitic intergrowths. All minerals are anhedral and the texture is granoblastic.

LF-32: Dark green to black medium grained rock. Major minerals are subhedral to euhedral hornblende (35-40%; 2-7mm), saussuritized plagioclase (25-30%; 0.1-2.0mm), large subhedral epidote (18-20%; 1-5mm), biotite (7-10%; 1-3mm), and trace amounts of hematite, apatite, and sphene. Green to blue-green hornblende typically forms in clusters with felsic material. Felsic material is found as areas of highly saussuritized plagioclase. Apatite, sphene, and biotite are associated with the hornblende.

LF-44: Dark green, coarse grained rock, which exhibits a mesocumulus texture in hand specimen. Major minerals are subhedral to euhedral hornblende (65-70%; 2-8mm), saussuritized plagioclase (7-10%; 2-6mm), epidote (10-15%; 0.5-2.0mm), sphene (2-3%; 0.5-1.0mm), and apatite (1-2%; 0.1-1.5mm). Only trace amounts of biotite occur in this rock. Green to locally blue-green hornblende is subhedral to euhedral and contains large clusters of apatite. Highly saussuritized plagioclase forms intercumulus material. Sphene is locally altered to perovskite.

LF-47: Dark gray to black, medium to coarse grained rock. Major minerals are anhedral to subhedral hornblende (65-70%; 1-5mm), sericitized and saussuritized plagioclase (12-15%; 2-6mm; An69), epidote (5-8%; 1-3mm), biotite (3-5%; 2-3mm), sphene (~1%; 0.5-1.0mm), and apatite (~1%; 0.1-0.5mm). Plagioclase shows albite twinning which is locally deformed. Biotite is partially chloritized. Some hornblende crystals show pale green cores with higher birefringence.

HORNBLENDITE

R-1: Dark green, medium to coarse grained rock. This sample is composed entirely of intergrown, green to blue-green hornblende crystals (90-95%; 3-6mm) which contain variable amounts of fine hematite (3-5%) and crystals of apatite (1-2%; 0.1-0.5mm). The hematite occurs in thin lines along cleavage planes and as thinner lines which greatly resemble schiller structure in pyroxene.

R-23: Dark green, medium to coarse grained rock which locally shows mesocumulus textures. Major minerals are intergrown hornblende (70-75%; 3-6mm), highly saussuritized and sericitized plagioclase (7-10%; 0.5-2.0mm), and epidote (12-15%; 0.1-0.8mm). Trace amounts of sphene and apatite

are associated with the hornblende. Plagioclase forms intercumulus material between green to blue-green hornblende crystals.

W-13: Dark green, fine to coarse grained, porphyroblastic rock. Major minerals are green to blue-green hornblende (75-80%), highly saussuritized and sericitized plagioclase (7-10%; 0.5-1.5mm), and epidote (10-11%; 0.1-0.5mm). Hornblende occurs as subhedral porphyroblasts (2-7mm) and as well foliated, subhedral to euhedral crystals in the matrix (0.5-1.5mm). Plagioclase and epidote occur with the fine hornblende in the matrix.

TYPE 1 TONALITE

R-81 AND R-103: Light to medium gray, fined to medium grained, porphyroblastic rock characterized by blue quartz porphyroblasts. Major minerals are anhedral quartz (30-35%; 2-4mm), anhedral plagioclase (45-50%; 3-7mm; An61), partially chloritized biotite (12-15%; 1-3mm), and trace amounts of epidote. Porphyroblasts of quartz and plagioclase are surrounded by biotite and show mortar texture. Sutured grain boundaries are found between some quartz grains. Some carlsbad and albite twinning is preserved in the highly sericitized plagioclase.

TYPE 2 TONALITE

R-19: Medium to dark gray, coarse grained, foliated rock. Major minerals are anhedral to subhedral plagioclase (40-43%; 4-7mm), biotite (25-30; 0.1-0.5mm), quartz (12-15%; 1-5mm), alkali feldspar (5-7%; 4-7mm), and epidote (3-5%; 0.1mm). Trace minerals are hematite, sphene and chlorite. Some poorly preserved carlsbad and albite twinning is found in plagioclase. Alkali feldspar only found near small veinlets composed of alkali feldspar, carbonate and quartz, and believed to be a metasomatic effect. The overall texture is granoblastic.

R-22, R-25, R-43: Medium to dark gray, medium to coarse grained, weakly to moderately well foliated rock. Major minerals are sericitized plagioclase (40-55%; 0.1-4.0mm; An56), subhedral hornblende (15-30%; 1-5mm), biotite (10-15%; 0.2-3.0mm), quartz (5-10%; 0.5-4.0mm), epidote (2-6%; 0.3-0.5mm), subhedral to euhedral sphene (1-3%; 0.5-2.0mm), apatite (1-2%; 0.1-0.5mm), and trace amounts of opaque minerals. Plagioclase typically shows carlabad and albite twinning, and some of the twin lamellae are bent due to metamorphic strain. Hornblende crystals are often twinned and contain inclusions of apatite, sphene and opaque minerals. Most of the larger minerals show mortar texture.

R-42,LF-14: Medium to dark gray, medium grained, strongly foliated and porphyroblastic rock. Major minerals are subhedral plagioclase (45-50%; 1-4mm), biotite (20-25%; 0.1-1.0mm), quartz (10-20%; 1-3mm), epidote (4-6%; 0.1-0.3mm), microcline (2-4%; 1-3mm), euhedral allanite (2-3%; 0.1-0.5mm), sphene (1-2%; 0.2-1.0mm), apatite (1-3%; 0.2mm), and trace amounts of hematite. Plagioclase crystals have highly sericitized cores, carlsbad and albite twins, and contain blebs of microcline. Quartz occurs as stringers and trains and both quartz and feldspar are surrounded by biotite.

R-54: Medium to dark gray, medium to coarse grained, weakly foliated rock. Major minerals are subhedral hornblende (35-40%; 1-3mm), fine grained granular plagioclase (25-30%; 0.1-1.0mm), granular quartz and plagioclase (20-25%; 0.1-1.0mm), chloritized biotite (3-5%; 0.5-2.0mm), and a brown isotropic unidentifiable mineral (<1%; ~0.5mm). Some relict twinning is poorly preserved in the granulated plagioclase and the original crystals appear to have originally been between 2 and 4mm across. The texture of the felsic material is granoblastic. The high mafic content and unidentified mineral is attributed to the local assimilation of mafic country rock and is supported by the presence of large (1X3 meters) xenoliths found near where this sample was taken.

GRANITE

R-18: Salmon pink, coarse grained, unfoliated rock. Major minerals are subhedral alkali feldspar (50-55%; 5-12mm), round quartz (12-15%; 3-5mm), anhedral plagioclase (7-10%; 3-7mm), chloritized biotite (7-10%; 0.5-3.0mm), sphene (3-5%; 0.5-1.0mm), opaque minerals (2-3%; 0.5-1.0mm), and epidote (1-2%; 0.5-1.0mm). Alkali feldspar shows perthitic, antiperthitic and myrmikitic intergrowths. Plagioclase shows albite twins and sericitization. Quartz grains show granoblastic to sutured boundaries and all minerals show varying degrees of mortar texture.

R-46: Salmon pink, coarse grained, unfoliated rock. Major minerals are anhedral alkali feldspar (25-30%; 4-7mm), suhedral plagioclase (20-25%; 1-5mm), granoblastic quartz (20-25%; 0.5-3.0mm), chloritized biotite (12-15%; 0.5-22.0mm), sphene (2-4%; 0.5-1.0mm), hematite (1-2%; 0.5-1.0mm), and epidote (1-2%; 0.1-0.5mm). Alkali feldspar is composed of perthitic microcline and plagioclase typically shows albite twinning and zoning. The feldspars exhibit mortar texture and quartz has granoblastic to sutured grain boundaries.

'-3: Light gray to light pinkish gray, fine to coarse
ained, strongly foliated and porphyritic rock. Major
nerals are round alkali feldspar porphyroblasts (25-30%;
·6mm), quartz (20-25%; 0.5-1.0mm), biotite (18-20%;
1-0.5mm), plagioclase (10-14%; 0.5-1.0mm), and epidote
'-10%; 0.3-0.5mm). Alkali feldspar porphyroblasts are
)stly perthitic microcline but also contain blebs of
.agioclase and quartz. The remaining minerals are
:retched and strongly aligned along the foliation. Quartz
ıd plagioclase form stringers and trains which are
ırrounded by biotite and epidote. Tiny allanite crystals
:e dispersed evenly through the biotite and epidote.

APPENDIX C

SAMPLING AND SAMPLE PREPARATION

Over 400 samples were collected from the three measured sections of this study. Most samples were collected in triplicate so that a thin section, geochemical sample and hand specimen would be available for analysis. All the major supracrustal and intrusive rock units were sampled as were any textural and/or compositional variations encountered within units. Back in Socorro, thirty seven samples were chosen for detailed petrography and geochemical analysis. The samples were chosen on the basis of the lack of obvious alteration and so that all rock types were represented. A sample location map for the majority of the thirty seven samples is given in Figure 26A and 26B. Those not shown were collected from outside the study areas and are from the following areas: samples R-18 and R-19 from the East Fork of the Red River near Ditch Cabin; R-22 and R-25 from the top of the Taos Ski Area along Bambi Trail; samples R-42 and R-43 from the ridge on the west side of La Cal Basin.

The samples chosen for geochemistry were initially broken down from hand specimen size to 1 to 4cm size with a sledge hammer. These 1 to 4cm pieces were then sent through a series of jaw crushers resulting in approximately 0.5 to a maximum of 2.0cm chips. Throughout the above crushing methods, all fine powder and any pieces containing

altered rock were removed.

The next phase involved sending the small chips through a high speed rotory grinder. Both the chips, which average 2mm, and powder were kept from this stage. The final step was to grind the samples in a RETCH MICROJET-5 high speed mortar and pestal. The final grain size was in the 10 mu range.

Samples of the powder were pressed into pellets for XRF analysis using a borax backing, distilled H2O (to aid in the removal of air), and 20 tons of pressure. For INAA, roughly 0.5 grams of powdered sample were placed in small polyurethane vials and wieghed to the nearest ten thousanth of a gram. The vials were then taken to the Sandia National Laboratory nuclear reactor to be irradiated.

APPENDIX D

X-RAY FLUORESCENCE ANALYSIS

The major elements Si, Ti, Al, Fe, Mg, Ca, and K, and the trace elements Rb, Sr, and Zr were determined by XRF analysis using a wavelength dispersive Philips Universal vacuum spectrometer. The analyte peaks measured were K-alpha peaks for all of the above elements and the X-ray path was a vacuum for the major elements and air for Rb, Sr, and Zr. The other important instrumental conditions are tabulated in Table 9.

Fifteen rock standards were measured for major elements along with the unknown samples and these standards were used to construct calibration curves. The standards used were AGV-1, BCR-1, BLCR, BR, F3, GA, GSP-1, G-12, G-25, HI-31, JB-1, JG-1, LOSP, PCC-1, and SY-1. Of these all but BLCR, HI-31, and LOSP are USGS rock standards. These latter three are intralab standards used at New Mexico Tech and their analyses are given in Table 11. Seven standards were analyzed along with the trace element analysis for the unknowns. These were AGV-1, BCR-1, GA, GH, GSP-1, G-2, and JB-1.

Instrumental variations in the counting process were compensated for by the ratio or drift pellet method. In this method a ratio is calculated from the average of the counts relative to a drift pellet. For the major elements the drift pellet used was the USGS standard JB-1. For the

TABLE 9
X-RAY FLUORESCENCE INSTRUMENT SETTINGS
AND ERROR CALCULATIONS

ELEMENT	KV/MA	TUBE	COLLIMATOR	DETECTOR	CRYSTAL	RMS%ERROR
Si	50/45	Cr	Coarse	FPC	Gypsum	0.85858
Ti	50/45	Cr	Fine	FPC	Quartz	0.26035
Al	50/45	Cr	Coarse	FPC	Gypsum	0.40241
Fe	50/45	Cr	Fine	FPC	Quartz	0.19376
Mg	50/45	Cr	Coarse	FPC	Gypsum	0.35370
Ca	50/45	Cr	Fine	FPC	Quartz	0.16907
K	50/45	Cr	Fine	FPC	Quartz	0.12200
Rb	50/45	Mo	Fine	Scin	LiF(200)	3.01880
Sr	50/45	Mo	Fine	Scin	LiF(200)	3.71504
Zr	45/40	W	Fine	Scin	LiF(200)	8.17735

FPC = Flow Proportional Counter
Scin = Scintillation Counter

trace elements the USGS standard AGV-1 was used. Counting error was kept below 1% by accumulating in excess of 10,000 total counts. This was done by long counting times, several repetitions, or both.

The raw counting data were processed through an Altair microcomputer. Matrix effects for the major element anaylsis were removed by multiple linear regressions of the standards used to construct the calibration curves. In the case of the trace elements the computer was used to calculate mass absorption coefficients for each sample at the specific wavelength for each element. The remaining correction and concentration calculations for the trace elements were done using a pocket calculator. The correlation coefficients for the corrected calibration curves were 0.99 or better for all the elements.

The error of the calibration curve is a good measure of the total error associated with the analytical procedure. This error is calculated by evaluating the difference between concentrations of standards calculated from the curve and concentrations used to construct the curve. The relative error of the calibration curve is given by:

$$\text{REL ERROR} = \sqrt{\frac{\sum^{n} \left(\frac{C(i)-M(i)}{\quad}\right)^2}{n}}$$

where C(i) and M(i) are the calculated and measured concentrations of the i-th element and there are n standards. This error has been calculated for the major and trace elements and is given in Table 9.

APPENDIX E

INSTRUMENTAL NEUTRON ACTIVATION ANALYSIS

Roughly 0.5 grams of powdered material from each of the studied samples was irradiated at the Sandia National Laboratory reactor in Albuquerque, New Mexico. A Nuclear Data 6600 4,096 channel gamma-ray spectrometer with a high resolution Li-drifted germanium detector system was used for the analysis of Na and eighteen trace elements. The methods used for the determinations are described in detail by Gordon et al (1968) and the instrumental parameters are given in Table 10. Depending on the half-life of the analyzed radionuclide, counting for different elements was done after 4, 7 and 28 day cooling periods.

Four USGS rock standards (AGV-1, BCR-1, GSP-1, and G-2), and one intralab rock standard (HI31) were used in calculating concentrations for the unknown samples. The ND6600 system is equipped with a computer which is capable of calculating the unknown concentrations by comparing the peak area of a given element with that of the standard. The computer also corrects for errors associated with dead time, weight differences between samples and standards, and for the radioactive decay occurring between sample and standard counting times.

TABLE 10
NEUTRON ACTIVATION INSTRUMENT PARAMETERS

RADIONUCLIDE	PEAK ENERGY (KeV)	COOLING TIME (DAYS)	COUNTING TIME (SECS)
153-Sm	103.2	4	4000
239-Np(U)	277.6	4	4000
24-Na	1368.4	4	4000
140-La	1596.2	4	4000
177-Lu	208.36	7	4000
175-Yb	396.1	7	4000
131-Ba	496.3	7	4000
147-Nd	91.11	28	5000
141-Ce	145.5	28	5000
169-Yb	177.0	28	5000
233-Pa(Th)	311.9	28	5000
51-Cr	320.1	28	5000
181-Hf	482.2	28	5000
134-Cs	797.0	28	5000
58-Co(Ni)	811.1	28	5000
160-Tb	879.3	28	5000
46-Sc	889.3	28	5000
182-Ta	1121.2	28	5000
60-Co	1332.5	28	5000
152-Eu	1408.1	28	5000

TABLE 11
Revised Results For Intralab Rock Standards
At New Mexico Tech (1976)

	LOSP	BLCR	HI31
SiO2	75.9	53.5	58.8
TiO2	0.20	0.89	0.88
Al2O3	12.3	18.1	16.7
Fe2O3T	1.81	7.62	6.47
MgO	0.07	4.85	4.21
CaO	0.93	8.39	6.50
Na2O	3.49	3.57	3.11
K2O	4.83	1.32	2.88
Total	99.53	98.24	99.56
Sc	5.7	32	-
Co	0.6	30	13
Cr	2.7	130	34
Ni	-	100	-
Rb	179	37	59
Sr	41	234	684
Ba	960	370	772
Zr	256	188	-
Cs	2.0	2.5	0.5
Hf	11	4.3	-
Ta	1.9	0.5	-
Th	2.4	4.0	-
La	70	12	33
Ce	160	28	67
Nd	70	15	-
Sm	16.7	4.0	7.5
Eu	2.4	1.28	1.8
Tb	3.1	0.8	0.85
Yb	11	3.5	3.3
Lu	1.8	0.55	0.56

This thesis is accepted on behalf of the faculty of the Institute by the following committee:

Adviser

2/2/1952
Date

FIGURE 29A

SAMPLE LOCATION MAP FOR THE GOLD HILL SECTION

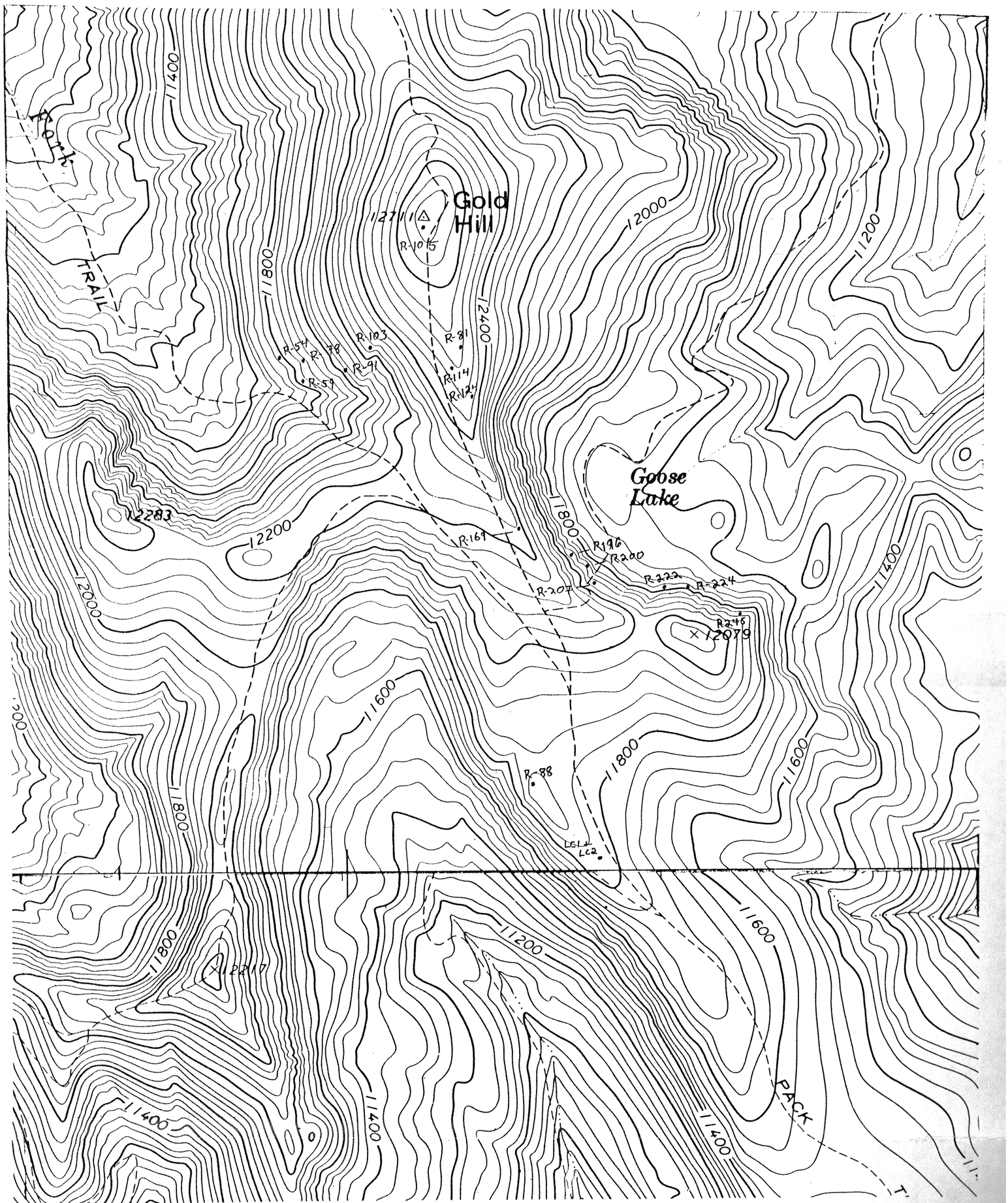

EXPLANATION OF THE GOLD HILL, LAKE FORK PEAK, AND WHEELER PEAK MEASURED SECTIONS

AGE RELATIONS

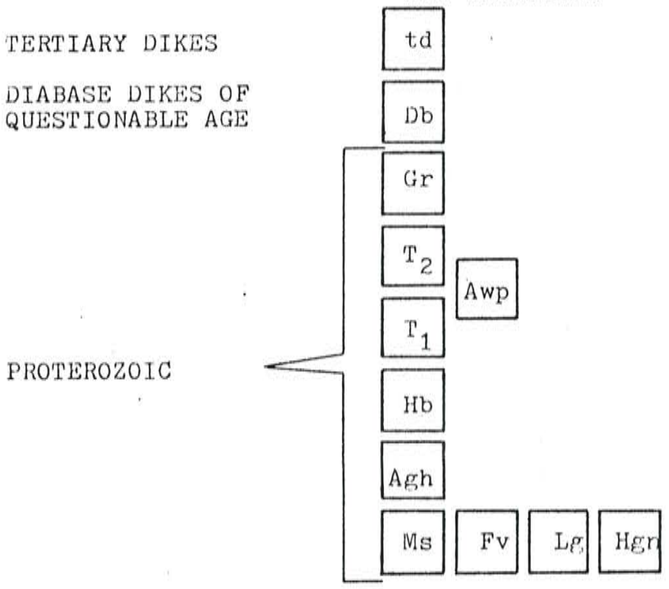

Granite Intrusives.

Type 2 Tonalite.

Type 1 Tonalite.

Intrusive Amphibolite of the Lake Fork Peak and Wheeler Peak Sections.

Hornblendite Intrusives.

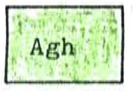

Intrusive Amphibolite of the Gold Hill Section.

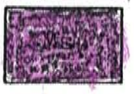

Mafic Schists of the Gold Hill Section.

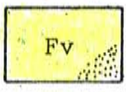

Felsic Volcanics of the Gold Hill Section. Dotted where highly silicified.

Layered Gneiss of the Gold Hill Section.

Hornblende-Biotite Gneiss of the Lake Fork Peak and Wheeler Peak Sections.

Agh units less than 10 meters thick

Furthest extent of traverse

Unit Contact

Fault with relative movement

Shear zone

⚒ Mine

70 Strike and Dip of Foliation

Vertical Strike and Dip

FIGURE 5A

GOLD HILL MEASURED SECTION

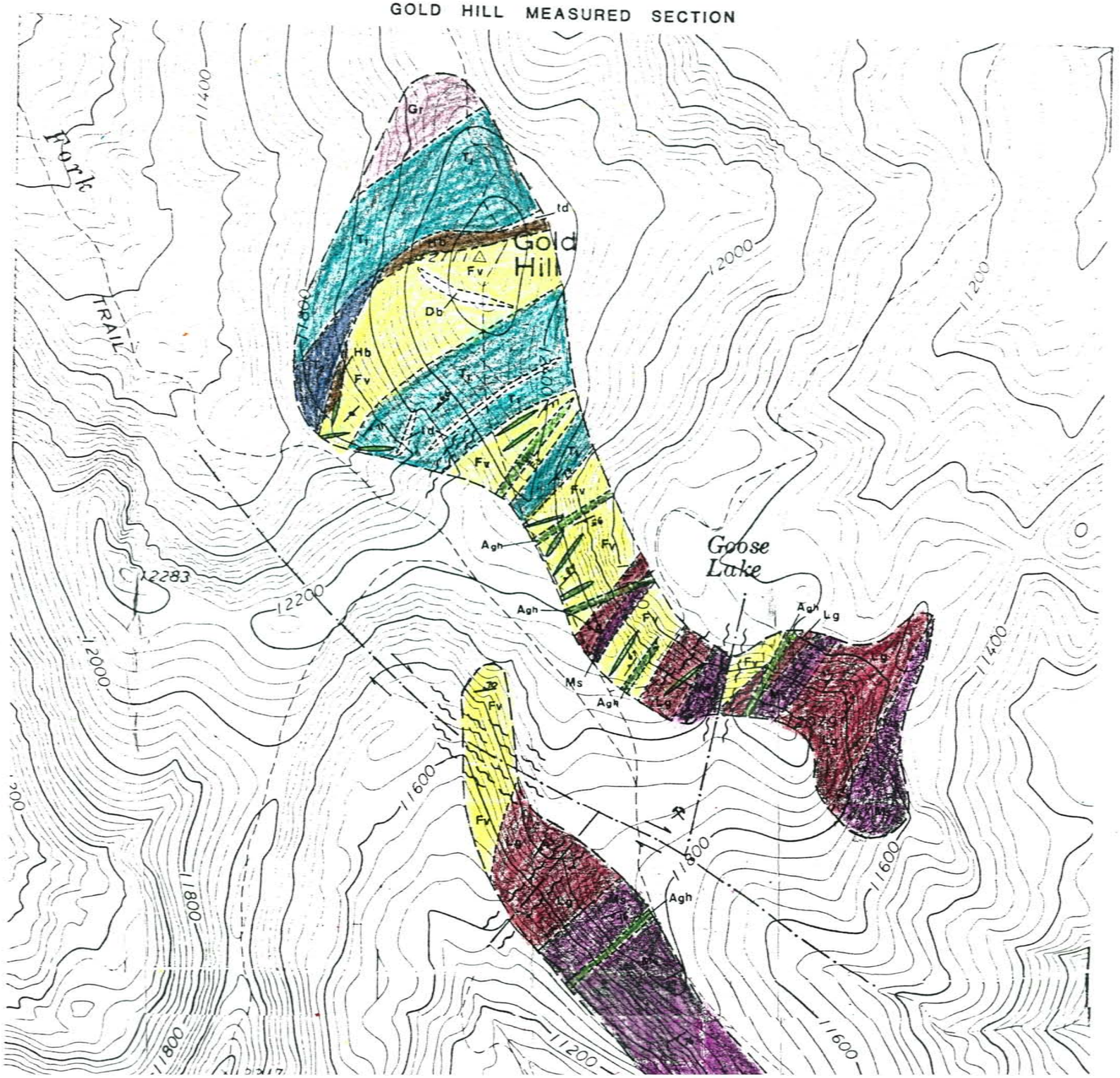

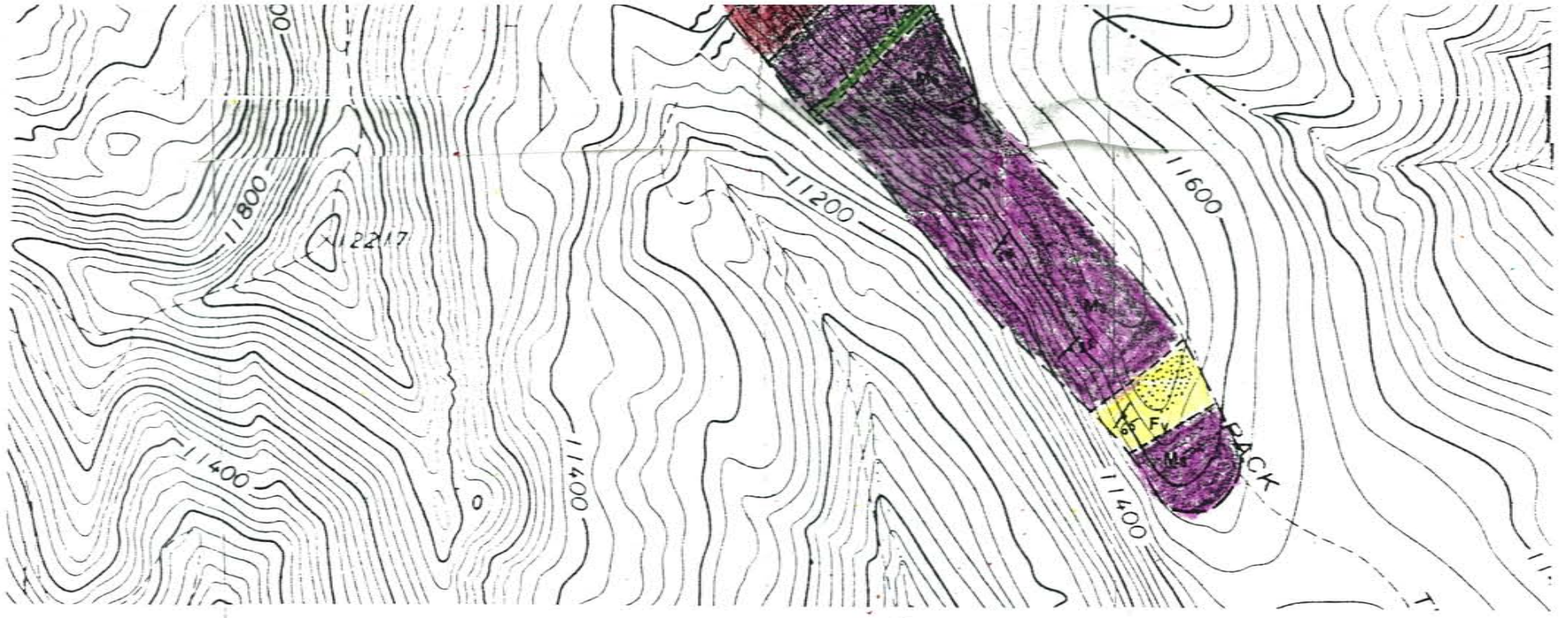

N

SCALE 1:12,000

0 1000 2000 3000 4000 5000 FEET

0 250 500 750 1000 METERS

FIGURE 5B

CONTOUR INTERVAL 40 FEET
BASE CONTOUR MAP FROM USGS 7.5 Min. QUADRANGLES

LAKE FORK PEAK MEASURED SECTION

WHEELER PEAK MEASURED SECTION

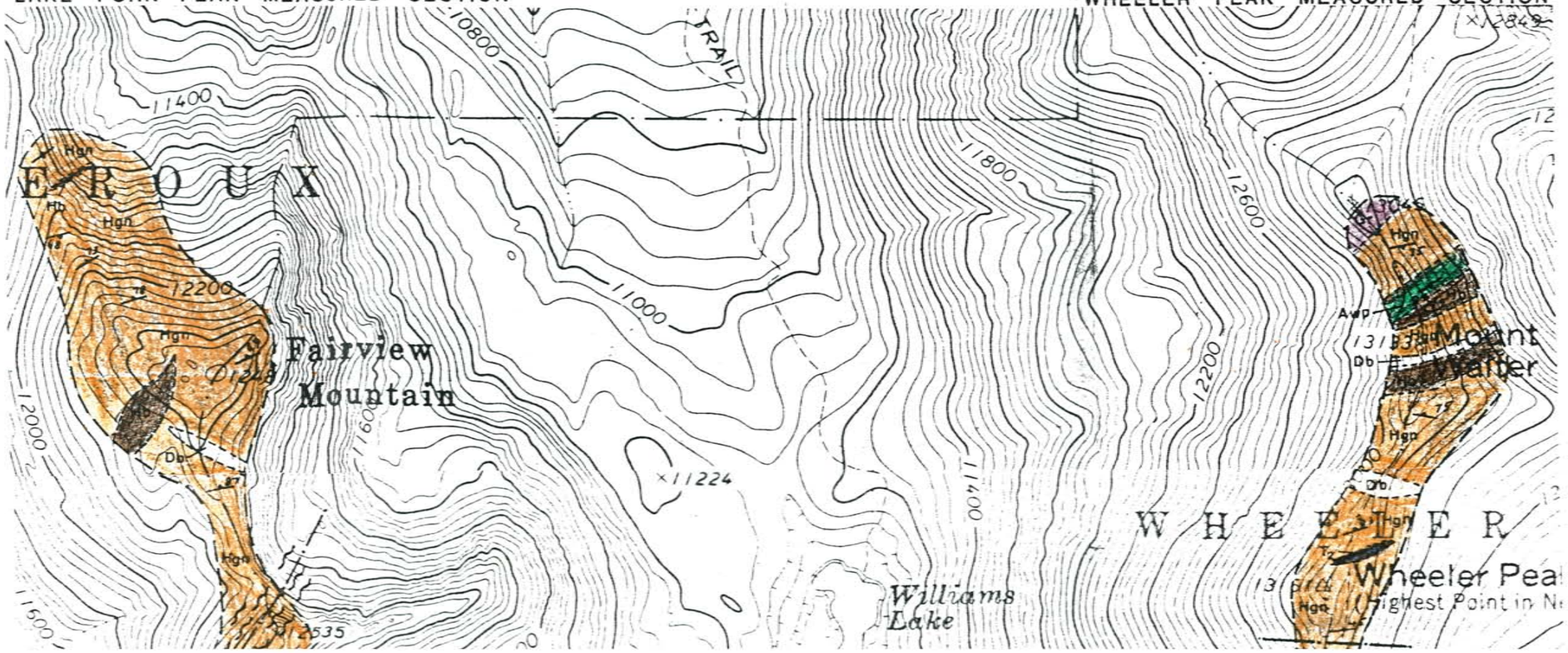

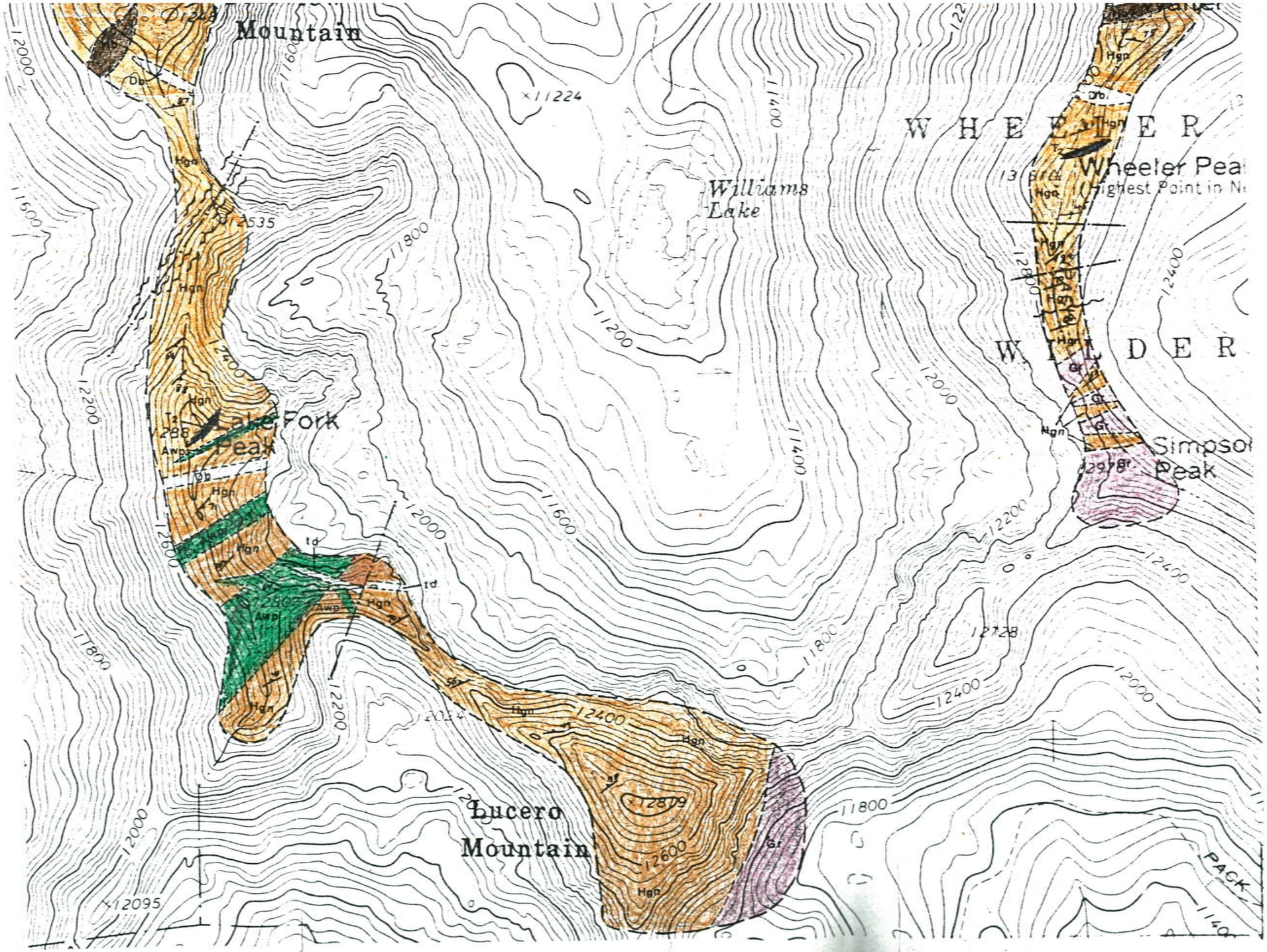
Mountain
Williams Lake
Lake Fork Peak
WHEELER
Wheeler Peak
Highest Point in N
Simpson Peak
Lucero Mountain
PACK
12000
11600
11800
12200
12400
11200
11400
×11224
×12095
12809
12728
12978
Hgn
Gr
Db
Awp
td

FIGURE 29B

SAMPLE LOCATION MAP FOR THE WHEELER PEAK AND LAKE FORK PEAK SECTIONS

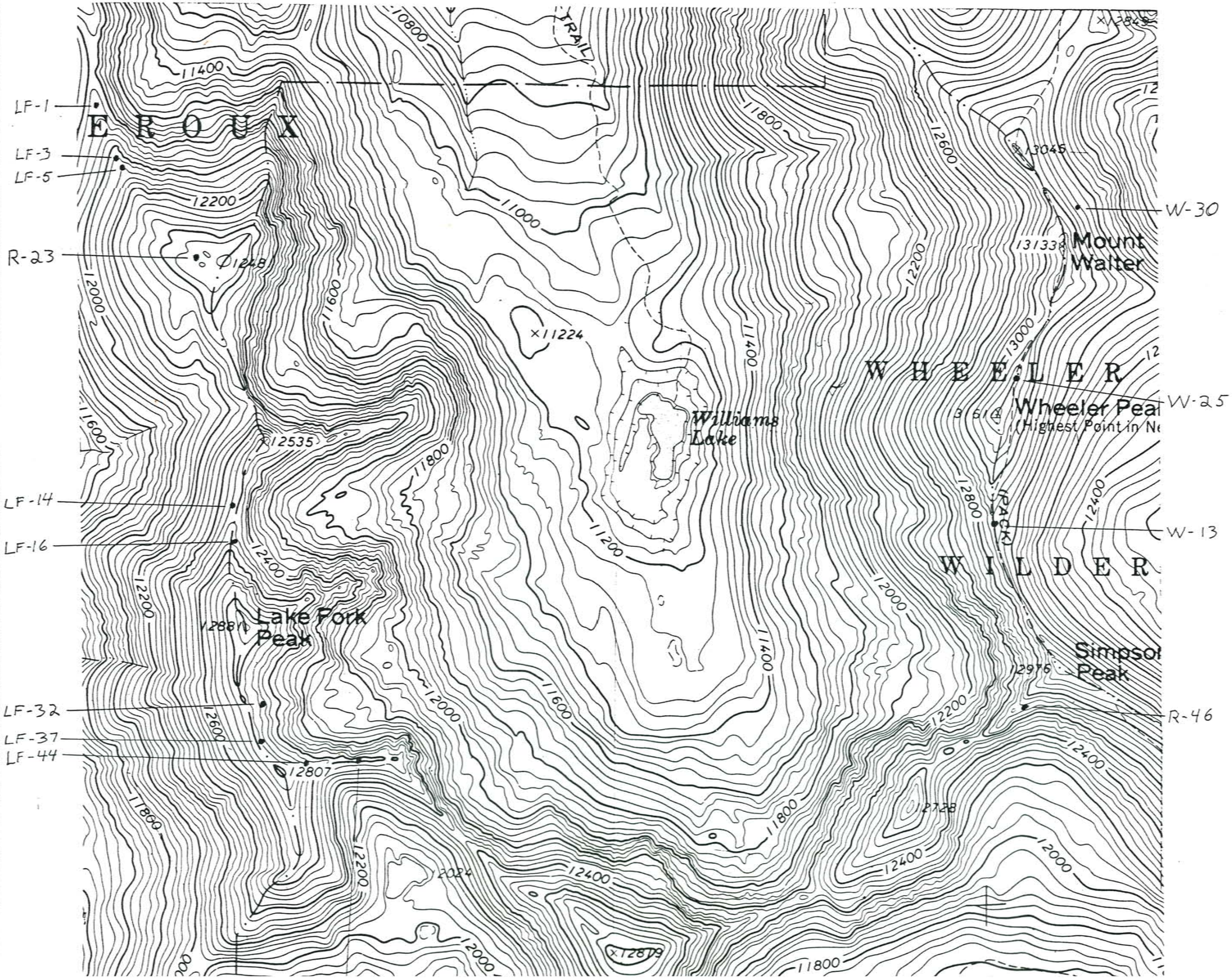

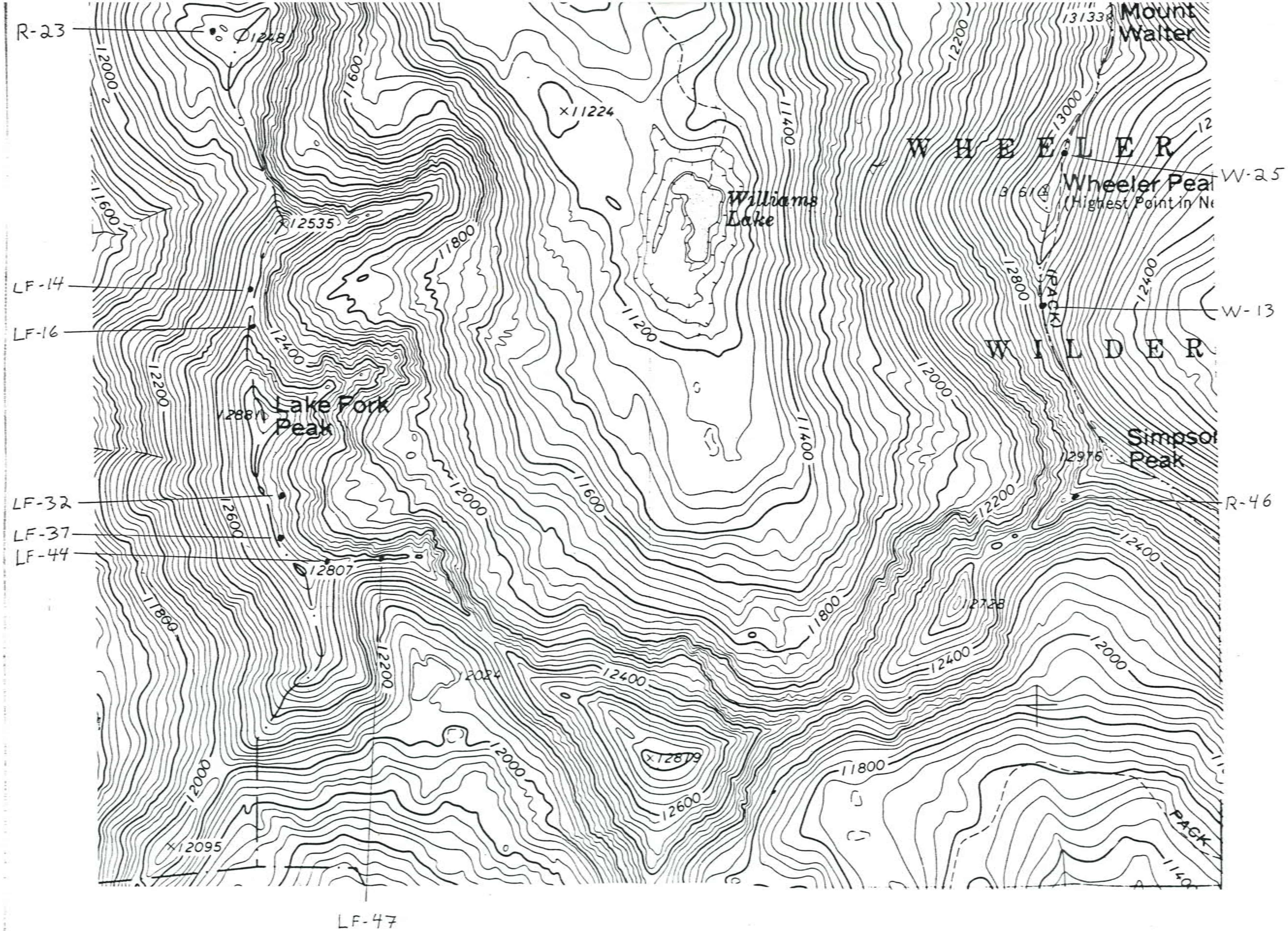

R-23
LF-14
LF-16
LF-32
LF-37
LF-44
LF-47
W-25
W-13
R-46
Mount Walter
13133
WHEELER
Wheeler Peak
(Highest Point in Ne
Williams Lake
WILDER
Lake Fork Peak
Simpson Peak
12976
12881
12807
12535
12728
12879
12095
12024
11224
PACK
(PACK)